THE EFFECT OF MISOPROSTOL ON NEURONAL STEM CELL MIGRATION AND DIFFERENTIATION

DENIS ADIGAMOV

A THESIS SUBMITTED TO
THE FACULTY OF GRADUATE STUDIES
IN PARTIAL FULFILLMENT OF THE REQUIREMENTS
FOR THE DEGREE OF
MASTER OF SCIENCE

GRADUATE PROGRAM IN BIOLOGY
YORK UNIVERSITY
TORONTO, ONTARIO

February 2020

Abstract

Misoprostol is a drug commonly used for medical termination of pregnancy, and improper use has been linked to neurodevelopmental disorders such as Moebius syndrome and Autism Spectrum Disorder (ASD). It is an analog of prostaglandin type E signalling lipids, like PGE_1 and PGE_2, and binds the same E-Prostanoid receptors, which regulate mechanisms of neurodevelopment. Previous research from the Crawford lab found that PGE_2 affected migration, differentiation, and expression of genes associated with ASD in NE-4C neuroectodermal stem cells, and neurite elongation in Neuro-2A neuroblastoma cells. The objective of this study was to determine if misoprostol alters the same cellular behaviors in NE-4C and Neuro-2A cells. Time-lapse microscopy was used to observe migration, neurosphere morphology, and neurite extension in the cell models. Misoprostol treatment decreased migration (speed and distance travelled) of NE-4C stem cells in a dose-dependent manner. Expression of stem cell marker *Oct4* and neuronal marker *MapT* demonstrated a misoprostol induced delay in NE-4C differentiation. This was associated with changes in neurosphere morphology and expression of adhesion molecule genes, *Cdh2* and *NCAM*. In differentiating Neuro-2A cells, chronic misoprostol exposure elongated primary neurites and branches, but decreased branch density. These results demonstrate the influence of misoprostol on cellular mechanisms of migration, differentiation, and neurite elongation, suggesting that prenatal exposure may alter these processes, resulting in abnormal neurodevelopment.

Dedication

I would like to dedicate this thesis to my family. To my parents Rustam and Ella Adigamov, for doing everything you could to support me in my goals. You have both sacrificed so much so that I would have everything I needed. If you had not immigrated to Canada those 20 odd years ago, I would never have had the opportunities that I do now. Most of all, I want to dedicate this work to my brother, Alexander Adigamov, you have always been my number one supporter. You are always the happiest to hear about my progress, and always there for me if I need something. You inspire me to work hard every day and remind me that I should never squander the opportunities that life may throw at me. To those mentioned above, thank you dearly. I will always be grateful for your undying faith in me, and work hard to make you proud. As such, I dedicate this work to you, in honour of your never-ending support.

Acknowledgements

I would like to acknowledge some of the wonderful people that have been so important in shaping my graduate experience. Thank you, Ashby Kissoondoyal, for introducing me to dungeons and dragons and mentoring me in cell culture procedures and western blot analysis. You have been a friend to me from the start and really helped guide and integrate me into the lab when I joined. Thank you, Christine Wong, for teaching me protein and RNA/DNA isolation, and being a role model of what I consider to be the ideal scientist. Thank you, Ravneet Rai-Bhogal, for demonstrating fierce work ethic and integrity. Thank you Eizaaz Ahmad for passing on the torch to me when I joined the lab. Thank you, Isabel Bestard-Lorigados, for teaching me quantitative PCR analyses, and hoarding all the dice. Thank you, Sarah Wheeler, for participating in intellectual discussions, and for being a compassionate friend when I needed it. Thank you to Stephen Anthony Rose, Harshill Patel, and Arshad Imrit for helping me learn Python and further my understanding of statistics. Thank you, Keenan Sterling and Sasha Udhesister, for your support in my final semesters. Thank you, Lily Solomon-Harris, for your love, care, and support in my final moments leading up to the defense. Thank you, Kyle Belozerov, for being a great friend and mentor throughout my studies since BIOL-4061. Thank you, Dorota Crawford, for guiding my growth as a scientist and adult throughout the program. Your belief and encouragement helped to push me when I needed it most. And thank you to anyone else that I may have missed for taking part in this journey. I have learned a lot and grown as an academic and scientific thinker. This experience will always be a part of me.

Table of Contents

Abstract ---------- *ii*

Dedication ---------- *iii*

Acknowledgements ---------- *iv*

Table of Contents ---------- *v*

List of Tables ---------- *vi*

List of Figures ---------- *vii*

List of abbreviations and definitions ---------- *viii*

1 - INTRODUCTION ---------- *1*

1.1 - Lipid Signalling in the brain ---------- **1**

1.2 - Prostaglandin E2 signalling ---------- **4**

1.3 - The Role of Prostaglandin E2 in the nervous system ---------- **7**

1.4 – Abnormalities in the PGE_2 signalling pathway and brain pathology ---------- **9**

1.5 - The role of the COX-2/PGE_2 signalling pathway in Autism – Molecular and behavioural evidence ---------- **11**

1.6 – Misoprostol ---------- **13**

1.7 - Experimental Model Systems ---------- **16**

1.8 - Objectives and Hypothesis ---------- **20**

Study 1: The role of misoprostol in the migration of undifferentiated neuroectodermal (NE-4C) stem cells ---------- 21

Study 2: Misoprostol increases the growth of NE-4C neurospheres and delays differentiation 22

Study 3: The effect of misoprostol on neurite length, CREB phosphorylation, and branch density in Neuro-2A cells ---------- 23

2 - METHODS ---------- *24*

2.1 - Cell Culture ---------- 24

2.2 - RNA and Protein Isolation ---------- 24

2.3 - Western Blot analyses ---------- 25

2.4 - Reverse Transcription and Polymerase Chain Reaction ---------- 26

2.5 - Quantitative Real-Time PCR ---------- 27

2.6 - NE-4C Migration Timelapses ---------- 30

2.7 - Differentiation of NE-4C cells and neurosphere induction ---------- 30

2.8 - Measuring neurospheres ---------- 31

2.9 - Differentiation of Neuro-2A cells and neurite analysis ---------- 31

2.10 - Statistical Analysis ---------- 32

3 - RESULTS ---------- *34*

3.1 - STUDY 1: The role of misoprostol in the migration of undifferentiated neuroectodermal (NE-4C) stem cells ---------- 34

3.1.1 - Dose dependent effect of Misoprostol on the migration of undifferentiated NE-4C stem cells ---------- 34

3.1.2 - Misoprostol decreased the expression of CREB protein in NE-4C stem cells ---------- 37

3.2 - STUDY 2: Misoprostol increases the growth of NE-4C neurospheres and delays differentiation ---------- 43

3.2.1 - Misoprostol slows the rate of differentiation ---------- 43

3.2.2 - Misoprostol's effect on the size of neurospheres ---------- 45

3.2.3 - Expression of cell adhesion molecules during differentiation ---------- 47

3.3 - STUDY 3: The effect of misoprostol on neurite length, CREB phosphorylation, and branch density in Neuro-2A cells ---------- 55

3.3.1 - Misoprostol affects the length of Neuro-2A neurites ---------- 55

3.3.2 – Misoprostol affects the density of neurite branches ---------- 57

3.3.4 - Misoprostol regulates CREB phosphorylation ---------- 58

4 - Discussion ---------- *65*

4.1 - Misoprostol reduces the migration ability of NE-4C stem cells ---------- 66

4.2 – Reduced motility delays early differentiation in misoprostol treated NE-4C stem cells --------- 69

4.3 – Misoprostol affects neurosphere morphology and delays differentiation of NE-4C cells by altering the expression of *Cdh2* and *NCAM* at different phases ---------- 70

4.3.1 - *Cdh2* expression is associated with decreased migration and delayed differentiation----- 71

4.3.2 - *NCAM* expression affects early neurosphere formation and commitment to neuronal differentiation.---------- 73

4.3.3 - Misoprostol affects neurosphere morphology by delaying differentiation ---------- 75

4.5 – Comparing the effects of misoprostol and other teratogens in the neurosphere model of development ---------- 77

4.6 - Misoprostol induces neurite elongation ---------- 80

4.7 - Misoprostol decreases the density of neurite branches in differentiating Neuro-2A cells ------ 83

4.8 – Limitations---------- 85

4.9 - Conclusion---------- 87

Bibliography* ----------*89

Appendix A: Copyright Permission ---------- 109

List of Tables

Table 1: Primers used for PCR amplification. 27

Table 2: Primers used for qRT-PCR. 29

List of Figures

Figure 1: Prostaglandin Synthesis 3

Figure 2: EP Receptor Signaling 6

Figure 3: NE-4C differentiation process 18

Figure 4: Illustration of the timeline for NE-4C cell tracking 39

Figure 5: Misoprostol decreased the migration of undifferentiated NE-4C cells. 40

Figure 6: Misoprostol affected the dispersion of undifferentiated NE-4C cells. 41

Figure 7: Misoprostol decreased total CREB protein level in NE-4C stem cells. 42

Figure 8: NE-4C neurospheres at different stages of differentiation. 50

Figure 9: Misoprostol increased neurosphere size during differentiation of NE-4C cells. 52

Figure 10: Misoprostol increased *Cdh2* expression of differentiated NE-4C cells. 53

Figure 11: Misoprostol altered *NCAM* expression of differentiating NE-4C cells. 54

Figure 12: Representative images of differentiating Neuro-2A cells and neurites 60

Figure 13: Growth of Neuro-2A neurites during differentiation 61

Figure 14: Length ratio of primary neurites compared to branches 62

Figure 15: Neurite branch formation and density in Neuro-2A cells treated with Vehicle or 30 µM Misoprostol. 63

Figure 16: Level of CREB and pCREB proteins in Neuro-2A cells after 3 days of differentiation 64

List of abbreviations and definitions

AA	Arachadonic Acid
AD	Alzheimer's Disease
ANOVA	ANalysis Of VAriance
APP	Amyloid Precursor Protein
ASD	Autism Spectrum Disorder
ATCC	American Type Culture Collection
ATP	Adenosine TriPhosphate
β-Catenin	A transcription co-factor for genes like PTGS2-2 and WNT
Ca^{2+}	Calcium
CAMKII	Calcium Calmodulin Kinase II
cAMP	Cyclic Adenosine MonoPhosphate
Cdh2	Cadherins 2 or N-Cadherin
cDNA	complimentary DNA
COX-1	Cyclo-oxygenase 1 Enzyme
COX-2	Cyclo-oxygenase 2 Enzyme
COXIB	Selective COX-2 inhibitor
CREB	cAMP Response Element Binding protein, a transcription factor for CREB mediated genes
pCREB	Ser-133 phosphorylated CREB protein, the active form of CREB which promotes gene transcription
cDNA	Complimentary DNA strand
Ct	Celsius Threshold value
D_	Day 1,2,3,4,6,8 of differentiation
DMSO	DiMethyl SulfOxide, the vehicle used in the control treatments
DNAse	DNase enzyme which digests DNA strands
dNTP	Deoxy riboNucleotide TriPhosphate
DRG	Dorsal Root Ganglia

E_	Embryonic Day _
ECL	Enhanced ChemiLuminescence
EDTA	EthyleneDiamineTetracetic Acid
EMT	Epithelial to Mesenchymal Transition
EP_	E-Prostanoid Receptor (1-4)
ESC	Embryonic Stem Cell
EUROCAT	European Registration of Congenital Anomalies and Twins
Fold Change	Protein quantity represented as a fold change relative to a control protein
GABA	gamma-aminobutyric acid - a neurotransmitter
Gapdh	Glyceraldehyde 3-phosphate dehydrogenase
Gfap	Glial fibrillary acidic protein, highly expressed in astrocytes
GI	GastroIntestinal system
CNS	Central Nervous System
GSK3β	Glycogen Synthase Kinase 3 Beta, negative regulator of WNT signalling
HPRT	Hypoxanthine PhosphoRibosyl Transferase
HSD	Honestly Significant Difference method of Tukey post-hoc analysis
hIPSC	Human Induced Pluripotent Stem Cells
IL-1β	Interleukin 1 Beta
iPSC	Induced Pluripotent Stem Cells
LTP	Long Term Potentiation
M-MuLV	Moloney Murine Leukemia Virus Reverse transcriptase
MapT	Microtubule – Associated Protein Tau, involved in microtubule stabilization, highly expressed in neurons
MEM	Minimal Essential Medium
MP	Misoprostol (dose is 30 μM unless otherwise referenced)
MP10	10 μM dose of Misoprostol
MP30	30 μM dose of Misoprostol
MW	Molecular Weight

Na^+	Sodium
NCAM	Neural Cell Adhesion Molecule
NE-4C	Neuro Ectodermal stem cell
Neuro-2A	Neuroblastoma cell line derived from the murine neural crest
NSAID	Non-Steroidal Anti-inflammatory Drug
Oct4	Octamer Binding Transcription Factor 4, undifferentiated embryonic stem cell gene
Oligo dT	deoxyThymine single strand for priming the poly(a) tail of messenger RNA
P_	Postnatal day _
p value	Probability of getting a specific outcome assuming the null hypothesis is true
PCR	Polymerase Chain Reaction
pCREB	Serine 133 phosphorylated CREB protein
PD	Parkinson's Disease
PGE_2	Prostaglandin E2
PGES	Prostaglandin E synthase
PGK1	PhosphoGlycerate Kinase 1
PI-3K	Phosphatydil Inositol-3-Kinase
PKA	Protein Kinase A
PKC	Protein Kinase C
PLA2	Phospholipase A2
Ptgs2	Prostaglandin-endoperoxide synthase gene, responsible for expression of COX-2
PSA	PolySialic Acid
PSA-NCAM	PolySialylated Neural Cell Adhesion Molecule
qPCR	quantitative PCR, which refers to qRT-PCR
qRT-PCR	quantitative Real Time Polymerase Chain Reaction

rDNase	recombinant DNase enzyme which digests contaminant DNA strands
RNA	RiboNucleic Acid
RNase	Rnase enzyme which digests contaminant RNA strands
RQ	Relative Quantity of gene expression compared to a reference
RT-PCR	Reverse Transcription Polymerase Chain Reaction
SDS	Sodium Dodecyl Sulfate
SEM	Standard Error of the Mean
TAE	Tris-Acetate-EDTA buffer
V	Vehicle
VPA	Valproic Acid
WNT	Wingless-related Integration site gene, responsible for expression of the WNT morphogen
WHO	World Health Organization

1 - INTRODUCTION

1.1 - Lipid Signalling in the brain

Fatty acids are critical for the proper maintenance and development of the human body. These lipids are then metabolized into many bioactive molecules. For example, linoleic acid is converted into arachidonic acid (AA), a polyunsaturated omega-6 fatty acid. AA is mainly present within cell membranes in the liver, muscles, and brain. Phospholipase A2 (PLA2) acts on cell membranes to release AA in response to various stimuli such as inflammation, illness, and stress [1,2] (**Fig 1**). AA is a common precursor to the majority of eicosanoids (such as prostaglandins, thromboxanes and leukotrienes) which are signalling molecules that have many physiological functions (primarily immunity, brain health, cell growth and pain perception). Prostaglandins and thromboxanes are synthesized from AA via the action of cyclooxygenase enzymes (COX-1 and COX-2) [1]. COX-1 is expressed constitutively throughout most of the body. COX-2 is inducible in peripheral tissues but is constitutively expressed in the central nervous system [3]. In the brain, COX-1 is expressed in microglia, astrocytes and neurons while COX-2 is expressed in glutamatergic neuronal cells [4]. Stimuli such as trauma and inflammation are able to induce COX-2 expression, which has been implicated with the pathological production of prostaglandins [5]. COX enzymes synthesize prostaglandin H2 which is further synthesized into prostaglandin E2 (PGE_2) via PGES (prostaglandin E-synthase). **(Fig 1).** Environmental factors and diet can affect the balance of the endogenous fatty acids which are required to produce these molecules. Many diseases

such as Alzheimer's Disease (AD), schizophrenia, and autism spectrum disorder (ASD), have been linked to altered fatty acid levels [6], signifying their importance for neurodevelopment.

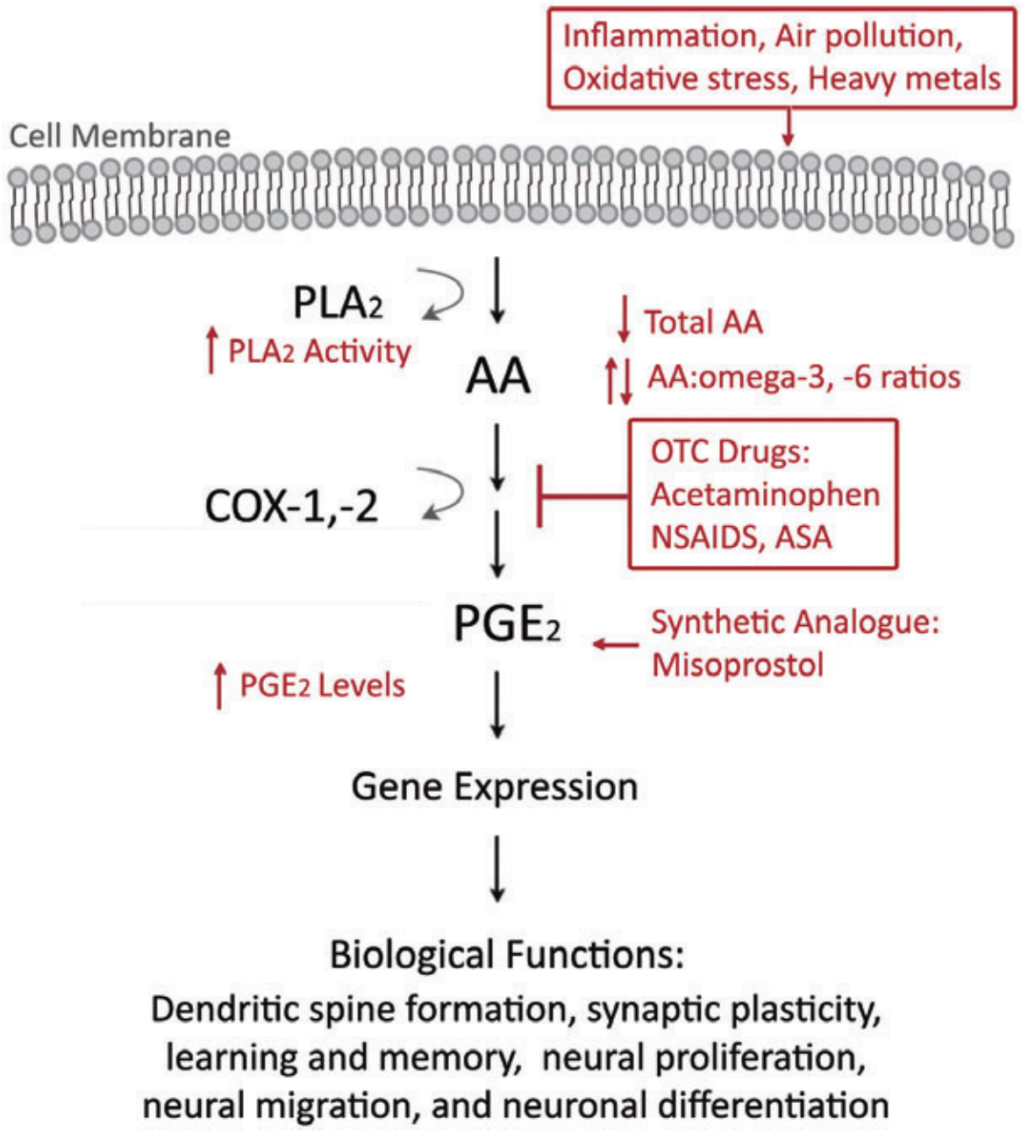

Figure 1: Prostaglandin Synthesis
Phospholipase A_2 replenishes the arachadonic acid supply from the plasma membrane. Arachadonic Acid (AA) precursor is then converted to PGE_2 by COX1/2 enzymes. Common drugs such as NSAID's inhibit COX activity. Environmental factors such as air pollution and heavy metal affect the supply of membrane phospholipids. The up and down arrows represent findings from ASD. PGE_2 goes on to bind any of the EP1-4 receptors leading to its physiological effects. Being an analogue, Misoprostol can also bind the EP1-4 receptors. Figure modified from[20].

1.2 - Prostaglandin E2 signalling

PGE_2 is the principle molecule responsible for physiological regulation in the prostaglandin system. PGE_2 acts on four E-Prostanoid (EP1-4) receptors with varying affinities (EP3>EP4>>EP2>EP1) [7]. EP receptors initiate signalling cascades through bound G proteins. EP4 and EP2 receptor binding activates adenylate cyclase which increases the concentration of cAMP signalling molecules that can activate Protein Kinase-A (PKA). Furthermore, both receptors can activate Phosphatydil Inositol-3-Kinase (PI-3K). EP1 binding increases intracellular [Ca^{2+}] levels which activate Protein Kinase-C (PKC). EP3 has three different splice variants which can increase or decrease cAMP and [Ca^{2+}] depending on which G protein subunit was bound. Elevations in [Ca^{2+}] increase Calcium Calmodulin Kinase II (CAMKII) activity, which has been shown to play a critical role in long term potentiation [8]. Enzymes like Protein Kinase C (PKC) and PLA-2 are also [Ca^{2+}] dependant and have been found to be regulated by PGE_2 signalling[4,9]. In an *in-vitro* neural stem cell model, EP4 and EP2 receptors were localized to the Golgi Apparatus and nuclear envelope respectively, while EP1 and EP3 were on the endoplasmic reticulum membrane and plasma membrane. PGE_2 signalling caused EP4 translocation to the plasma membrane in stem cells, and to the growth cones in differentiating neuronal cells. [10,11]. Prostaglandin signalling leads to the activation of downstream kinases which regulate gene transcription to control cell functions and regulatory responses such as proliferation, differentiation, and migration [12] **(Fig 2).** A major target of these kinases is the transcription factor CREB. In immature mouse cortical neurons, PKA and CAMKII induced Ser-133 CREB phosphorylation which resulted in decreased dendritic numbers and length, as well as decreased neuron

survival [13]. Another study found EP4 receptor dependent inhibition of CREB activation in HEK-293 cells via PGE_2 [14]. These are just some examples of the many effectors part of the prostaglandin E2 network. Disrupting the activity of any of these targets may have varied effects on neural development and behavior.

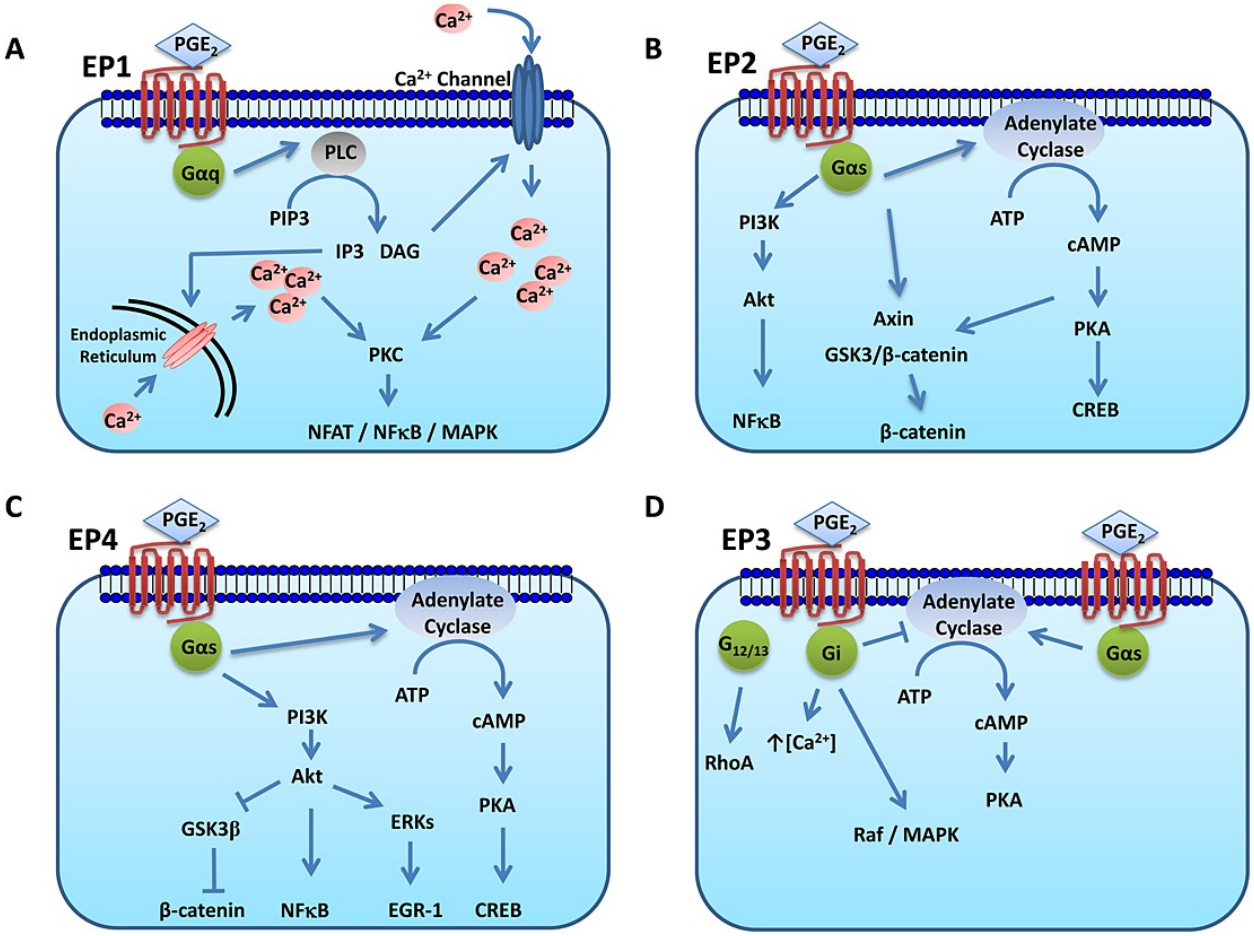

Figure 2: EP Receptor Signaling
A) EP1 receptor signaling activates PLC and increases intracellular [Ca^{2+}] which regulates PKC activity. **B)** EP2 receptor signalling increases cAMP which activates PKA and CREB. PI-3K is also activated. **C)** EP4 receptor also regulates CREB phosphorylation and PI-3K activity. **D)** EP3 receptor regulates cAMP and [Ca^{2+}] in either direction, depending on the splice variant. Figure taken from [8], refer to **Appendix A** for copyright permissions.

1.3 - The Role of Prostaglandin E2 in the nervous system

Prostaglandins are involved in a wide diversity of physiological functions which are mediated by COX activity. This includes pain perception, immune regulation, cardiovascular function, fertility, and neuronal development. During episodes of inflammation such as fever or trauma, cytokines like Interleukin 1-Beta (IL-1β) induce COX-2 expression [15]. This leads to an increase in PGE_2 which causes vasodilation and hyper-permeability at the site of inflammation[16]. The inflammation response also induces hyper-nociception in sensory neurons from rat Dorsal Root Ganglia (DRG) via EP4 receptor binding and PKA activation.

In the central nervous system, PGE_2 is the primary signalling lipid, regulated mostly by constitutively expressed COX-2. One of the primary functions of PGE_2 is to facilitate synaptic signalling, plasticity, and long term potentiation in brain regions such as the hippocampus[5]. COX-2/PGE_2 signaling in hippocampal and cortical neurons regulates formation of dendritic spines and facilitates activity dependant synaptic plasticity [17]. By regulating [Ca^{2+}] it can alter synapse activity through changes in gene expression [18]. Retrograde PGE_2 signalling at post synaptic terminals has been associated with Long Term Potentiation (LTP) via presynaptic EP2 receptor mediated activity [19]. Furthermore, research in ASD and AD have discovered neuroprotective roles for PGE_2 [4]. COX-2 activity can be induced in microglia, imparting neuroprotective anti-inflammatory effects through the activation of EP2 and EP4 receptors, increasing the expression of neurotrophins [4]. Research from the Crawford lab has found that altering COX and PGE_2 activity affects the expression of morphogens like WNT which can disrupt prenatal development and neuronal differentiation [10,20,21]. This is due to the role

of PGE_2 in regulating dendritic spine formation, neuronal migration, and cell fate [22–24]. Events such as brain trauma and ischemia lead to neuroinflammation which induces COX-2 activity and increases PGE_2. This increase was found to exacerbate neurodegeneration following ischemic strokes. The neurotoxic response is due to over excitation of glutamatergic neurons which can cause synaptic dysfunction and apoptosis[5]. Furthermore, EP1 activation was found to be neurotoxic by impairing the Na^+ Ca^{2+} exchange in overexcited neurons[25]. The neurotoxic and neuroprotective effects of prostaglandins maintain a fine balance which is mediated by COX-1 and COX-2 activity.[26] In the digestive system, constitutive COX-1 expression is required for the protection of epithelial cells that line the gastrointestinal tract [9,26,27]. In reproduction, PGE_2 promotes oocyte maturation, sperm penetration, and early embryonic development. The presence of a COX knockout renders mice infertile [28]. Perturbations in PGE_2 signalling during conception and pregnancy could affect embryogenesis and neurodevelopment with lasting behavioral changes after birth[20].

1.4 – Abnormalities in the PGE_2 signalling pathway and brain pathology

The functional importance and ubiquitous nature of prostaglandin signalling has made it a valuable target for chemical manipulation. Some of the most widespread analgesics used are Non-Steroidal Anti-Inflammatory Drugs (NSAIDs) or Coxib's (selective COX-2 inhibitors). Aspirin and ibuprofen are common NSAIDs that relieve pain, headaches, and inflammation. These drugs block the production of PGE_2 by the inducible COX-2 in the peripheral tissues [3]. However, COX-2 is constitutively expressed in the brain. As such, the action of these drugs during critical periods in pregnancy have been associated with increased likelihood of neurodevelopmental disorders [29] (**Fig 1**). Clinical studies in individuals with ASD show that disruption of PGE_2 signalling due to various genetic and environmental risk factors contributes to irregularities during embryonic neurodevelopment which leads to various autism related behavioral differences [20,21,30]. For example, it was found that individuals with autism had heightened levels of PGE_2 in their blood plasma [2]. Altered PGE_2 levels could disrupt the regulation of neurological functions such as synaptic plasticity, neuronal migration, and differentiation (**Fig 1**). Furthermore, children with ASD had reduced methylation capabilities and increased levels of harmful oxidative stress biomarkers like oxidized glutathione [31]. Neuroactive steroid hormones, such as androsterone and pregnenolone, were also elevated in ASD afflicted children [32]. Markers, like the ones mentioned above, can be examined to describe neurological damage or developmental irregularities. The differentiation and development of living organisms is highly regulated by molecules called morphogens. For example, the *WNT* gene, responsible for producing the WNT morphogen, has been shown to regulate cell fate, neuronal migration, and

organogenesis during embryonic development [24,33,34]. Many of these functions are similar to the ones listed for PGE_2 in **Figure 1**. Recent research from the Crawford lab has provided evidence that PGE_2 can affect the expression of *WNT* and related genes [10,20,21,24,30]. Therefore, alterations in PGE_2 signalling can be detrimental due to its effects on gene expression. It was found that people with autism have a neuronal signalling imbalance where there are more excitatory signals than inhibitory[35]. This is attributed to reduced GABA signalling in ASD afflicted individuals[36]. Research has shown that PGE_2 is able to regulate GABA by affecting $[Ca^{2+}]$ levels via EP1 and EP3 receptors [37,38] (**Fig 2**). In activated microglia, prostaglandin synthesis was found to be inhibited by a metabolite of acetaminophen [39]. There is a risk that pregnant mothers who take these medications may be affecting the neurodevelopment of their children. A cohort study associated prenatal acetaminophen use with the development of ASD and hyperkinetic symptoms[40]. Even perfumes and cosmetics have neuromodulating effects which can increase the risk of ASD symptoms [41]. The chemicals used in fragrances are poorly regulated and rarely disclosed. One study tested 91 perfumes and found that they all exhibited at least some degree of mutagenic activity on human neuroblastoma cells at concentrations expected to reach a fetal brain[41]. Therefore, from conception children are vulnerable to environmental factors which could alter neurodevelopment.

1.5 - The role of the COX-2/PGE_2 signalling pathway in Autism – Molecular and behavioural evidence

Research from the Crawford lab focuses on the neurodevelopmental effects of altered PGE_2 signalling, employing the use of murine cell models, like neuroblastomas (Neuro-2A) and neuroectodermal stem cells (NE-4C), and murine animal models. The *in-vitro* research with NE-4C cells has shown that higher levels of PGE_2 augments the proliferation and migration of stem cells, elongates neuronal extensions, elevates intracellular calcium levels, and expedites neuronal differentiation [10,18,24,42]. Dysregulation of these traits can have consequences in neuronal communication and signalling [12]. It was found that PGE_2 interacts with the WNT morphogen, which is responsible for body axis patterning, cell fate, cell proliferation, and cell migration [24,43]. Abnormal WNT signalling has been previously associated with ASD [34]. One study from the Crawford lab performed whole genome microarray analysis on COX-1 and COX-2 knockout mice at embryonic day 16 and 19 [21]. They found that only the E16 COX-2 knockout affected *WNT* gene expression[21]. This was associated with increased levels of active β-Catenin and an overall increase in the number of affected genes[21]. β-Catenin is a transcription co-factor that regulates the expression of genes including COX-2 (*ptgs2*) and *WNT* [44]. Further research observed the effect of maternal PGE_2 injections on the brains of embryonic and early postnatal murine offspring [30]. They found that PGE_2 increased the expression of two *WNT* target genes at each of the developmental stages [30]. This was associated with increased stability (not marked for degradation by GSK3β) and activation (PKA phosphorylation) of β-Catenin [30]. Moreover, offspring of PGE_2 injected mice displayed reduced cell density in the cerebellum and altered

neuronal migration in the neocortex [43]. The findings were age-dependant and sex-dependant, similar to ASD pathology in humans. The most recent research from the Crawford lab observed ASD related behaviors such as repetition, anxiety, and motor defects in COX-2 deficient mice [20] and maternal PGE_2 injected offspring [45]. These behaviours were more prominent in the male mice [20], suggesting a sex bias that is also found in human cases of ASD [46]. Moreover, COX-2 deficiency had a greater effect on ASD related gene expression in males than in females[20]. PGE_2 injection resulted in more pronounced anxiety and social behaviors, whereas COX-2 deficiency caused motor deficits not seen in PGE_2 injected offspring [45]. Maternal perturbations in COX-2/PGE_2 signalling was also shown to affect microglial cell density, morphology, and activity in P8 mice brains [47]. Evidence from the literature suggests that microglia play an essential role in regulating neurodevelopmental processes like migration, differentiation, and synaptic plasticity [48–50]. Overall, evidence from the Crawford lab has demonstrated that PGE_2 can affect neurodevelopment by disrupting cellular processes and altering ASD related gene expression, leading to behavioral defects postnatally.

1.6 – Misoprostol

The prostaglandin pathway has proven to be a very effective target for therapeutic manipulation. As mentioned earlier, prostaglandin function is determined by the activation of EP receptors. Therefore, agonists and antagonists against the majority of EP receptors have been manufactured for research and clinical use [7]. Additionally, many pharmaceutical drugs impart their effects by acting on the prostaglandin signalling pathway. Such medicines include NSAID's (Nonsteroidal anti-inflammatory drugs; general COX inhibitors), Coxibs (selective COX-2 inhibitors), corticosteroids (inhibit PLA_2), and misoprostol [51]. Misoprostol is a PGE_1 analogue that is commonly used to induce labor, treat stomach ulcers, and medically terminate pregnancy. Clinical studies have found that prenatal misoprostol exposure was linked to increased risk of birth defects such as Moebius syndrome, limb malformations, and ASD-like characteristics [52–56]. The prenatal brain undergoes rapid development and is susceptible to changes in lipid signalling brought on by diet or drugs. For medical termination of pregnancy, the World Health Organization (WHO) suggests 200 mg of oral mifepristone followed by 800 µg of misoprostol, repeating as necessary [57]. Mifepristone is a steroidal antiprogestogen medication which induces uterine contractions by inhibiting progesterone from binding EP receptors on the uterus [58]. It also primes the myometrium for prostaglandins, therefore enhancing uterine contractions when taken in combination with misoprostol [58]. Common side effects of misoprostol include nausea, diarrhea, heavy bleeding and in rare cases uterine rupture [57]. Misoprostol alone is about 75% effective for complete termination of pregnancy in the first trimester, compared to 95% when taken in conjunction with mifepristone [59–61]. A clinical study found that ongoing

pregnancy occurred in 16.6% of women assigned to misoprostol treatment alone [60]. In comparison, only 1.5% of women had ongoing pregnancy when given mifepristone with misoprostol [60]. Children born following misoprostol exposure are associated with a greater risk of birth defects. One of the largest clinical studies which looked at first trimester misoprostol exposure, in approximately 250 pregnant women, found that it was associated with an almost 2-fold increase in major congenital malformations, as defined by EUROCAT (European Registration of Congenital Anomalies and Twins) [54,62]. The majority of participants took the oral formulation with malformations arising from doses as low as 200 μg [54,56]. This resulted in symptoms like facial paralysis and club feet, which are consistent with Moebius syndrome and misoprostol exposure [52,53,63,64]. During the first gestational month an embryo has already formed the neural tube and begun to form the forebrain, midbrain, and hindbrain. Insults during this critical period can result in severe defects such as spina bifida[65]. Coincidentally, this is approximately the same time when mothers would take misoprostol which led to the aforementioned malformations [56,66]. In more conservative countries, such as those in Latin America, only 1 in 4 abortions are considered safe and many women resort to off-label illegal use of misoprostol [59,67,68]. The lack of proper training and available follow-up care greatly increases risk of adverse events. Furthermore, off-label misoprostol is most commonly available in oral formulation, while vaginal and sublingual routes are far more effective [66,69].

While the majority of research on misoprostol has been clinical, the Crawford lab has previously shown in differentiated neuroblastoma (Neuro-2A) cells that misoprostol decreases neurite length and increases intracellular [Ca^{2+}] levels via PKA [70,71]. One

study determined that neonatal misoprostol injections did not cause neurodevelopmental toxicity based on their evaluations of sensory and motor development in the mice [72]. However, the use of misoprostol in that study is analogous to the timing when women would use misoprostol to induce labour. The preceding clinical research was primarily from prenatal misoprostol exposure, in which women would use it to medically terminate a pregnancy or to treat their GI issues. Although the majority of research in the Crawford lab is focused on PGE_2, misoprostol binds the same EP receptors (EP3=EP4=EP2>>EP1) as PGE_2, at approximately a 10-100 fold decreased affinity [7]. This is due, in part, to their similar molecular structures. One of the ways natural prostanoids and EP receptor agonists differ from each other is based on their ring substructure [73]. PGE_2 has a hydroxyl group on its E-ring which directly interacts with the EP receptor to mediate activity [74]. However, this interaction does not occur with misoprostol, possibly contributing to its decreased receptor affinity [73]. Therefore, misoprostol is likely to act via similar mechanisms as PGE_2, by binding the same EP receptors. Currently there is a lack of molecular research on misoprostol's influence on neuronal development. **In this thesis, I aim to describe the effect of misoprostol on neuronal stem cells and their differentiation.**

1.7 - Experimental Model Systems

Two well established neuronal cell models were chosen for this research, neuroectodermal (NE-4C) stem cells and neuroblastoma (Neuro-2A) cells.

NE-4C stem cells are an *in-vitro* model system commonly used to study embryonic brain development because they can be induced to differentiate, following similar processes that occur during neurodevelopment [10,11,18,24,75]. NE-4C cells are derived from the brains of embryonic day 9 (E9) mice, which is analogous to the period when women would take misoprostol to terminate pregnancy. This corresponds to a gestational age of 5 weeks in humans, when somites would begin to form along the body axis to signal migrating neuronal precursors in the developing nervous system [76]**.** By lacking functional *p53* genes, the cells are immortalized. Through established methodology, the cells can reliably be induced to differentiate into astrocytes or neurons, or they can be maintained in their undifferentiated state [75]. Therefore, this model system allows the study of two different stages of brain development.

Development of the nervous system relies on specific environmental niches which promote proper migration, differentiation, and communication of cells. Neurosphere assays are often used as an *in-vitro* model system which resembles some of these processes [24,77–80]. When induced to differentiate, NE-4C cells cluster together and form sphere shaped aggregates [81]. The formation of the spheres and the progress of differentiation is outlined in **Figure 3**. This characteristic progression was previously confirmed in the Crawford lab for NE-4C cells [24]. Neurospheres provide a microenvironment for neurogenesis to occur, in which cells are constantly proliferating and differentiating. Morphological characteristics, such as size, are indicative of their

proliferation [77] and differentiation capabilities [79]**.** Furthermore, cell-cell communication and adhesion are greatly regulated for neurogenesis within these microenvironments. One of the ways in which these cells communicate with each other is through Notch signalling. Notch and WNT/β-catenin are known to regulate each other transcriptionally, and post-transcriptionally [82].

The adhesion of neighboring cells and the communications between them are regulated via cadherins, integrins, laminins, and cell adhesion molecules. Examples like N-Cadherins (Cdh2) or Neural cell adhesion molecule (NCAM) are widely expressed during embryonic development, and specifically during neuronal differentiation [83,84]. Cdh2 is a type I classical cadherin that is regulated by [Ca^{2+}]. The transmembrane protein has been shown to interact with β-catenin as an effector [85]. In cultured rodent cortical neurons, Cdh2 promoted cellular aggregation, neurite branching, and synaptic differentiation [86]. One of the main functions of NCAM is to regulate the migration and differentiation of neuronal precursors [87]. Prenatally, it's enzymatic activity is often modified by the addition of polysialic acid (PSA) to become PSA-NCAM [84,88].

Previous research has already shown that PGE_2 effects neurosphere morphology and *Cdh2* expression [24]. It is likely that prenatal exposure to drugs which alter prostaglandin signalling, would affect neurodevelopment through the previously mentioned mechanisms.

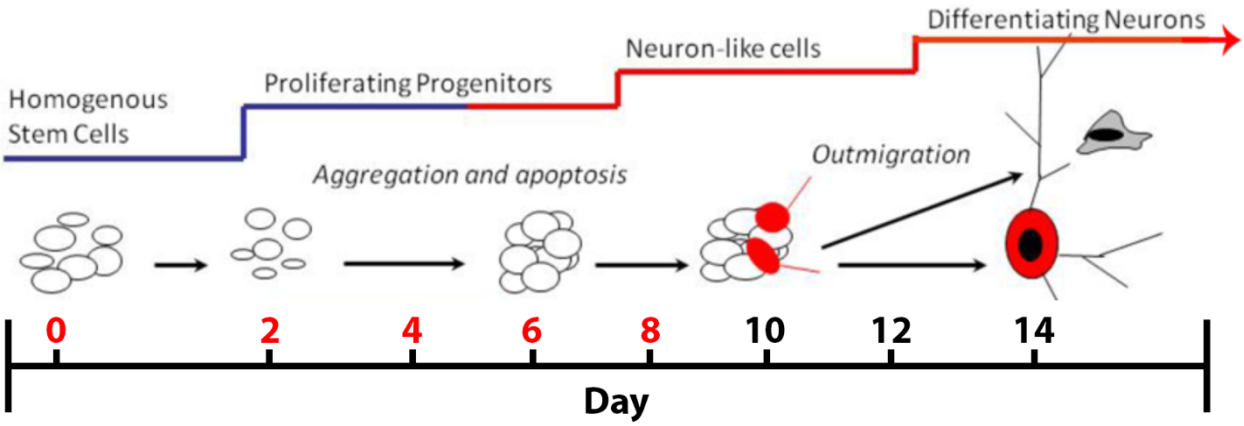

Figure 3: NE-4C differentiation process
The process of differentiation for NE-4C cells. Aggregation occurs around day 2, and neurospheres are formed around day 6. Following growth, committed neuronal progenitors migrate outwards around day 10. Adapted from [117].

The second cell model used here is Neuro-2A cells derived from the murine neural crest. This cell line is commonly used to study synaptic signalling, neuronal differentiation, actin mechanics, and dendritic arborization. For example, one study found that Dock4, a gene associated with ASD [89], regulates neurite formation in differentiated Neuro-2A cells through actin and Rac1 activity. It concluded that healthy Dock4 expression was needed for proper neuronal network formation in the developing brain[90]. In Neuro-2A cells, axons and dendrites are indistinguishable from each other. However, many processes which regulate neurite extensions are also shared between axons and dendrites [91,92]. Previous research in the Crawford lab has shown that acute treatment with PGE_2 or misoprostol increased intracellular [Ca^{2+}] levels and decreased the length of neurites in Neuro-2A cells [70,71]. These cells can be induced to differentiate, which can be observed by neuritogenesis and extension length. This cell model enabled research on chronic misoprostol exposure during differentiation and neurite formation. The results may reflect the development of prenatal neuronal networks in the misoprostol exposed fetus.

1.8 - Objectives and Hypothesis

The literature has demonstrated that prostaglandin E2 signalling plays a vital role for proper functioning and development. Altered signalling has been implicated in many neurodevelopmental pathologies such as ASD, AD, Parkinson's Disease (PD), etc. [2,4,5,12,20,55,63]. Diet, medicine, and other external factors such as perfumes have been shown to affect PGE_2 production and contribute to these disorders [93,94]. In many countries, using misoprostol alone is still recommended as a safe choice for medical termination of pregnancies [59,66–69]. However, little is known about misoprostol's adverse effect on prenatal neurodevelopment. There have been many published case studies where the misuse of misoprostol for terminating pregnancy during the critical period led to the development of Moebius syndrome and ASD [52,54,56,63]. Previous studies from the Crawford lab have demonstrated that in mice a single injection of the endogenous PGE_2 during the first trimester can result in abnormal expression of ASD genes and autism-related behaviours [20,30]. Previously in NE-4C cells, PGE_2 affected stem cell migration, the rate of differentiation, neurosphere morphology, and gene expression [10,24]. Misoprostol exposure on differentiated Neuro-2A cells was shown to cause neurite retraction and altered CREB signalling [70,71]. In this study I examined the effect of misoprostol exposure on neuronal stem cells and their differentiation.

The main **goal** of this research is to uncover the molecular mechanisms by which misoprostol affects neuronal development and whether the effect is dose dependent.

I **hypothesize** that misoprostol will elicit similar effects (differentiation, migration, extension) in neuronal cells as PGE_2, based on previously published research from the Crawford lab [10,18,24,71,95].

The research outlined in this thesis has been separated into three studies, each focusing on specific aspects of neuronal development:

Study 1: The role of misoprostol in the migration of undifferentiated neuroectodermal (NE-4C) stem cells

The **first study** investigated the effect of misoprostol on cellular migration in undifferentiated neuroectodermal NE-4C stem cells. The **main goal** of this study is to determine the effect of misoprostol on traits of motility in undifferentiated NE-4C cells. Time-lapse videos of the cell cultures were made under a 10x inverted phase contrast Nikon Eclipse TI-E microscope every ten minutes for a total of 24 hours in order to record individual cell tracking. Cells were then tracked and analyzed using NIS Elements software (Nikon). This method has previously been used to show the effect of PGE_2 on migration in NE-4C cells[10]. CREB activity, a common downstream transcription factor, was determined through western blot analyses. Previous research with Neuro-2A cells showed that PGE_2 and misoprostol both affect CREB phosphorylation, which regulates gene transcription, via EP receptor signalling [95].

I **hypothesize** that misoprostol will affect the distance travelled, displacement, and overall speed of movement in NE-4C stem cells, through pathways that result in altered CREB activity.

Study 2: Misoprostol increases the growth of NE-4C neurospheres and delays differentiation

The **second study** determines misoprostol's influence on aggregation and clustering of differentiating NE-4C cells in neurospheres. The **main goal** of this study is to determine the effect of misoprostol on the rate of differentiation of NE-4C cells. Using the same software and microscope as described in study 1, the morphology of differentiating neurospheres was analyzed based on area, perimeter, and roundness over an 8 day period. The expression of specific genetic markers was analyzed via PCR to describe the progress of differentiation in the cells. This method has previously been used to show that PGE_2 increases the rate of differentiation and the size of neurospheres in NE-4C cells [24]. They also found that *Cdh2* expression, a gene involved in cell adhesion, was affected by PGE_2 exposure.[24]. Therefore, I used quantitative real-time PCR (qRT-PCR) to measure the expression of adhesion molecule genes *Cdh2* and *NCAM*.

I **hypothesize** that misoprostol will affect the morphology of neurospheres, the rate of differentiation, and the expression of adhesion molecules, in differentiating NE-4C cells.

Study 3: The effect of misoprostol on neurite length, CREB phosphorylation, and branch density in Neuro-2A cells

The **third study** looks at chronic misoprostol exposure in differentiating neuroblastoma Neuro-2A cells. The **main goal** of this study is to determine the effect of misoprostol on neurite extensions. Cells were recorded using the same microscope as described above in study 1 over a 3 day period. Neurite extensions were analyzed using the Fiji distribution of ImageJ with the Simple Neurite Tracer plugin [96–98]. The Crawford lab has previously found that PGE_2 and misoprostol induced neurite retraction in differentiated Neuro-2A cells [70]. This study differs by exposing Neuro-2A cells to misoprostol chronically from the start of differentiation. It was previously shown that acute PGE_2 and misoprostol exposure affects CREB phosphorylation in Neuro-2A cells [95]. Therefore, in this study I used western blots to examine CREB activity for differentiated Neuro-2A cells under chronic misoprostol treatment.

I **hypothesize** that misoprostol will affect neurite formation, elongation, and CREB expression in differentiating Neuro-2A cells.

2 - METHODS

2.1 - Cell Culture

Murine NE-4C cells or Neuro-2A cells (ATCC) were kept in an incubator at 5% CO_2 and 95% humidity at 37 ^oC. Cells were grown in growth media on culture plates coated with 0.01% Poly-L-Lysine (Sigma, 70,000-150,000 MW). Growth media consisted of Minimum Essential Medium (MEM, Gibco) supplemented with 2mM L-Glutamine (Sigma), 100 U/mL Penicillin/Streptomycin (Invitrogen), and 10% Fetal Bovine Serum (Gibco). Cells were regularly subcultured at a 10:1 ratio and growth medium was changed every 2 days.

2.2 - RNA and Protein Isolation

Isolation of protein and RNA was done following the Nucleospin RNA/Protein protocol with the required reagents included in the kit (Macherey Nagel). Briefly, culture plates were aspirated and treated with a lysis buffer (inactivating RNases, proteases, etc.) prior to manual collection with a cell scraper (SPL Life Sciences). Lysates were treated with 70% ethanol to prime the nucleic acids to bind to the silica membrane. A filtration step bound the RNA to the silica membrane, while the flow-through contained protein for later isolation. A recombinant DNA nuclease (rDNase) reaction mixture was applied to the bound silica membrane to remove contaminating DNA. After several washes to purify the solution, RNA was eluted with RNase free water. Isolation was performed with RNase free labware and sterile practices. Protein was precipitated by treating the flow-through with Protein Precipitator buffer and 50% ethanol. After drying,

the protein pellet was dissolved in a 1% SDS solution containing protease inhibitors (β-glycerophosphate and sodium orthovandate). All samples were kept at -20 ^{o}C prior to further analyses.

2.3 - Western Blot analyses

Misoprostol's influence on CREB phosphorylation was determined by quantifying the protein expression of CREB and pCREB (Serine 133 phospho-CREB*)* in the cell cultures. Samples were prepared by treating 25ug of protein with 1x Laemmli loading buffer (BioRad) before being loaded on 10% SDS-polyacrylamide gels for electrophoresis and subsequent transfer onto 0.2µm nitrocellulose membranes (BioRad). Membranes were incubated overnight with rabbit monoclonal primary anti-CREB (Cell Signalling #9197) or rabbit monoclonal primary anti-pCREB (Cell Signalling #9198) at a 1:1000 dilution in 5% Bovine Serum Albumin (BioShop), followed by goat anti-rabbit horseradish peroxidase-conjugated secondary antibody (Abcam #ab6721). Membranes were treated with ECL enhanced chemiluminescence substrate (BioRad) prior to visualization with the Geliance 600 Imaging System (Perkin Elmer). Band intensities were quantified using Genetools software (SynGene). Relative quantities for CREB and pCREB were determined against the expression of *Gapdh (Glyceraldehyde 3-phosphate dehydrogenase)* housekeeping gene (1:10,000, Abcam #ab8245; goat anti-mouse horseradish peroxidase-conjugated secondary antibody, Abcam #ab97040). Fold change values were calculated relative to the vehicle control samples. All results were obtained from 3 biological replicates.

2.4 - Reverse Transcription and Polymerase Chain Reaction

Gene expression was analyzed by Reverse Transcription Polymerase Chain (RT-PCR) Reaction. Isolated RNA (3ug) samples were treated with 1x DNAse I buffer (New England Biolabs (NEB)) for 10 minutes at 37^{o}C to remove any DNA contaminants. Ethylenediaminetetraacetic acid (5mM EDTA, Sigma) was then added for 10 minutes at 75^{o}C to inactivate DNAse I. The treated RNA samples were subsequently incubated with 200 µM dNTP (NEB) and 4.6 µM Oligo$(dT)_{18}$ (NEB) for 5 minutes at 65^{o}C to prime the RNA strands for reverse transcription. Complementary DNA synthesis was initiated through the addition of 1x Reverse Transcriptase Buffer (NEB) and 200U of M-MuLV Reverse transcriptase (NEB). Samples were incubated for 1 hour at 42^{o}C and 10 minutes at 90^{o}C to complete the reaction.

Polymerase Chain Reaction was done to amplify genes of interest from the reverse transcribed cDNA samples. The reaction mixture contained 1x Taq Reaction buffer (BioBasic), 2mM Magnesium Sulfate (BioBasic), and 200 µM dNTP (NEB), along with 1 µM primer solution and 2U Taq DNA Polymerase (BioBasic). The PCR cycle consisted of a 1 minute denaturing step at 94^{o}C, a primer annealing phase for 30 seconds at 55^{o}C, and strand elongation for 30 seconds at 72^{o}C. An Eppendorf 5531 Mastercycler was used to amplify samples for 30 cycles with the final elongation step extended to 5 minutes. PCR products were mixed with 6x Orange G loading dye (Sigma) and electrophoresed through a 1.2% Agarose (Bioshop) gel in 1x TAE (Tris-Acetate-EDTA) buffer. SafeView Classic (Applied Biological Materials) was used to stain the DNA for visualization with the BioDoc-It Imaging System.

Successful reverse transcription was verified by amplifying the cDNA with primers for the housekeeping gene *Gapdh*. Presence of *Gapdh* PCR product confirmed successful cDNA synthesis. The progress of differentiating NE-4C cells was determined by PCR analysis with primers for *Oct4* (Octamer Binding Transcription Factor 4 - early stem marker), and *MapT* (microtubule – associated protein Tau - neuronal differentiation marker). Absence of the astrocyte marker, *Gfap* (glial fibrillary acidic protein), was used to confirm commitment to the neuronal lineage and compared against a mouse whole brain positive control sample. PCR Primer sequences can be found in Table 1.

Table 1: Primers used for PCR amplification.
The target genes were used to determine differentiation progress and cell type.

Target	Forward primer (5'→3')	Reverse primer (5'→3')
Gapdh	TGGAAGGACTCATGACCACA	TTCAGCTCAGGGATGACCTT
Oct4	CTGGCTAAGCTTCCAAGGGC	CCAGGGTCTCCGATTTGCAT
MapT	TGAGATTGCTTGCGTTGTGG	ACAGCAACAGTCAGTGTAGA
Gfap	TCAATCAGTGCTAAGCTTCATA	TGCAGCCAGGAATAGACCTT

2.5 - Quantitative Real-Time PCR

Differences in neurosphere morphology (ie: size) can be affected by cellular proliferation, differentiation, adhesion, or communication. In order to determine the effects of misoprostol on differentiation of neurospheres, quantitative real-time PCR

(qRT-PCR) was done to measure the expression of adhesion related genes *Cdh2* and *NCAM*. *Cadherins2 (Cdh2)* is primarily involved with cell adhesion, but it also has roles in cellular communication and neurodevelopment [99]. *Neural Cell Adhesion Molecule (NCAM)* has been involved with neural differentiation, migration, and synaptic plasticity [80,88,100].

Primers chosen for the aforementioned genes were previously developed by a PhD student (Christine Wong) from the lab and had been verified for qRT-PCR with the NE-4C model system ([24] (Table 2)). For each sample, 1.5 µL of cDNA was added to 18.5 µL of ADVANCED qPCR mastermix with SUPERGREEN dye (LOW ROX; Wisent), prior to being loaded onto custom Taqman Array 96-well FAST plates (Applied Biosystems) in technical triplicates. Equal amounts of RNA from day 0 biological triplicates were pooled and reverse transcribed to use as the calibrator samples between runs. The 7500 Fast RT-PCR system (Applied Biosystems) was used to run the reaction and quantification was done following the ΔΔCt method. The geometric mean from two housekeeping genes, *HPRT (hypoxanthine phosphoribosyl transferase)* and *PGK1 (Phosphoglycerate Kinase 1),* was used as previously established endogenous controls to quantify the expression of the genes of interest [101,102]. Threshold values (Ct) for each gene of interest were compared to the geometric mean of the Ct values for the housekeeping genes ($\Delta Ct = Ct_{target} - GM(Ct_{Ref})$). The relative quantities (RQ) were calculated by comparing the ΔCt values of each sample against the controls. These RQ values represented the fold change difference in gene expression for the sample versus the control. Results were from 3 biological replicates, each run on a separate FAST plate in technical triplicates.

Table 2: Primers used for qRT-PCR.
Primers are written in the 5'-3' direction for the forward (F) and reverse (R) sequences.

Gene	Sequences	Amplicon Length (bp)
HPRT	F - TCCATTCCTATGACTGTAGATTTTAT R - AACTTTTATGTCCCCCGTTGACT	75
PGK1	F - CAGTTGCTGCTGAACTCAAATCTC R - GCCCACACAATCCTTCAAGAA	65
Cdh2	F - CCACTTATGGCCTTTCAAACACA R - CCGTAGAAAGTCATGGCAGTAAACT	93
NCAM	F - TCATGTGCATCGCTGTTAACCT R - CGTTCGGACCTCCACAATG	125

2.6 - NE-4C Migration Timelapses

Timelapses of NE-4C cells were made to analyze cellular migration. Culture plates (35mm, BD Falcon) were seeded with $1.5x10^5$ cells and kept in a chamber (In-Vivo Scientific) which maintained incubation conditions. Within the chamber, cells were imaged with a 10x inverted phase contrast Nikon Eclipse TI-E microscope every ten minutes for a total of 24 hours. Prior to imaging, growth medium was supplemented with either 10 μM or 30 μM of misoprostol (Cayman). For the vehicle condition, growth medium was supplemented with 0.05% dimethylsulfoxide (DMSO, Sigma). Studies have shown that 0.05% DMSO is appropriate and safe to use as a vehicle for *in-vitro* neuron analyses [103]. Analysis using NIS Elements Software (Nikon) was performed to examine migratory characteristics such as displacement, path length, and speed. New daughter cells were tracked until their first division (**Fig 4)**. Cell position was defined as the center of the soma for the purposes of tracking. Time between divisions was recorded as the cell cycle duration. All results are based on 100 cells from 3 independent experiments for each condition. Cell lysates were collected for protein and RNA following completion of each timelapse.

2.7 - Differentiation of NE-4C cells and neurosphere induction

To prepare for differentiation, $1x10^5$ NE-4C cells were seeded on 60mm culture plates (BD Falcon) and left overnight in growth media. Differentiation was induced by replacing the growth media with serum free Neurobasal (Gibco) supplemented with B-27 (Gibco), 2mM L-Glutamine, and 100 U/mL Penicillin/Streptomycin. These supplements have been previously established to promote differentiation and growth in

neuronal cells [24,104,105]. Differentiation medium was supplemented with either 0.05% DMSO for the vehicle condition, or 30 μM misoprostol for the treatment condition. The media was replaced every other day for a total of 8 days of differentiation. Lysates were collected on days 0, 2, 4, 6, and 8 for RNA and protein. Three biological replicates were made for each condition.

2.8 - Measuring neurospheres

Differentiating culture plates were imaged with a 10x inverted phase contrast Nikon Eclipse Ti-E microscope prior to media changes. Each image comprised of 125 fields at 3 different focal lengths. Images were taken every 2 days for the duration of differentiation (days 0, 2, 4, 6, 8). Aggregates of NE-4C cells were seen after two days of differentiation. NIS Elements software (Nikon) was used to trace the perimeter of the neurospheres and determine their areas. Roundness was calculated by using the formula Roundness = $4 \times \pi \times \text{Area} / (\text{Perimeter})^2$. A perfect sphere has a roundness of 1 while a line has a roundness of 0. Therefore, neurospheres whose roundness was closer to 1 had a more spherical shape. The neurosphere analysis protocol was previously established by Wong et al., in 2016 [24].

2.9 - Differentiation of Neuro-2A cells and neurite analysis

To induce differentiation, 1×10^5 Neuro-2A cells were seeded on 60mm culture plates and left overnight in growth media. Differentiation was induced in Neuro-2A cells by culturing them in growth media containing only 0.5% FBS. Serum starvation has previously been shown to induce differentiation in Neuro-2A cells [106]. Differentiation lasted over 72 hours with one media change in between. The vehicle condition had

0.05% DMSO added to the differentiation medium. The misoprostol condition had 30 μM of misoprostol added to the differentiation medium. Cells were imaged with a 10x inverted phase contrast Nikon Eclipse Ti-E microscope twice a day, with each image containing 125 fields. Cells were collected for protein and RNA following the 72 hour differentiation period. Neurites were analyzed using the Fiji distribution of ImageJ with the Simple Neurite Tracer plugin [96–98]. Primary neurites were defined as the longest whole branch extending from the soma of a cell. Branching neurites were defined as extensions coming from the primary neurite (**Fig 13A**). The length ratio was quantified as the cumulative length of all primary neurite extensions divided by the cumulative length of all neurite branches. Branch density was calculated as the number of branches divided by the cumulative length of primary neurites and then multiplied by one hundred. All results were obtained from three biological replicates for each condition and day.

2.10 - Statistical Analysis

Statistical analyses for all experiments were done on Python v3.7 [107] using publicly available libraries (pandas[108], statsmodels [109], numpy[110], matplotlib[111]). A $\log_{10}$ transformation was applied on measures which were skewed in order to satisfy the normality assumption. Criteria for significance was set at $*p < 0.05$, $**p < 0.01$, $***p < 0.001$.

For experiments with undifferentiated NE-4C cells, one-way Analysis of Variance (ANOVA) was done to verify if there were any differences between the groups. Significance for all the pairwise differences were quantified with Tukey's Honestly

Significant Difference (HSD)[112] post hoc test. Protein expression was analyzed with one way ANOVA followed by Holms [113] corrected independent T-tests against the control group.

The differentiating NE-4C neurosphere experiments were measured over time (8 days). Throughout differentiation they undergo a variety of processes. Therefore, there was a possibility that misoprostol could affect some processes differently than others, which would only be seen on specific days rather than a global trend. To account for this, a two-way ANOVA was done to include the possibility of interaction effects between the treatment and the duration of differentiation. All pairwise differences were then compared via Tukey HSD post hoc test. Gene expression was also analyzed with two-way ANOVA and daily pairs were compared by Holm's corrected independent T-tests.

The differentiating neurite experiments were analyzed with two-way ANOVA followed by Tukey HSD post hoc test for the primary and branch measurements, and by Holms corrected pairwise T-tests for the length ratio, branch number, and branch density measurements. The expression of CREB proteins were compared in day three Neuro-2A cells by independent T-tests, as there were only two groups.

3 - RESULTS

3.1 - STUDY 1: The role of misoprostol in the migration of undifferentiated neuroectodermal (NE-4C) stem cells

The cell model used for this study was NE-4C neuroectodermal stem cells. They are derived from E9 mice brains, which corresponds to the most commonly indicated time for misoprostol misuse in reported cases of Moebius syndrome and Autism [75,114]. As the nervous system develops, neuronal precursors will respond to migration signals coming from somites, radial glial cells, and other cells in the immediate environment. These signals include cell adhesion molecules, cadherins, and cytokines[76,115]. Disrupted migration impacts cell fate as well as cell number at the final destination. For example, cortical development is dependent on appropriate responses to signals for proper migration and formation of the functional layers[116]. The following results demonstrate the effect of misoprostol exposure on NE-4C stem cell motility.

3.1.1 - Dose dependent effect of Misoprostol on the migration of undifferentiated NE-4C stem cells

The migration behavior of undifferentiated NE-4C cells was determined via NIS elements time-lapse tracking software as previously done by Wong et al., in 2014 [10]. Cells were treated with 10 μM misoprostol, 30 μM misoprostol, or vehicle prior to the time-lapse. Cells were recorded every 10 minutes for a 24 hour period. They were tracked for their entire cell cycle, starting initially after a daughter cell had split from its mother, and ending right before the daughter cell split again (**Fig 4**). A total of at least 100 cells from three independent experiments were measured for each condition.

Migration was defined as distance travelled, displacement from origin, and overall speed.

The *distance* was defined as the path length travelled by the cell during the duration of a whole cell cycle. One-way ANOVA analyses determined that there was a significant difference between the treatments on the distance travelled by NE-4C cells ($F_{(2,297)} = 24.51$, $p < 0.001$, **Fig 5A**). Vehicle treated cells had travelled an average of 245.08 ± 7.86 μm. The 10 μM misoprostol treatment was not statistically different from the control cells (243.59 ± 8.24 μm, $p > 0.9$). However, when compared to vehicle and 10 μM misoprostol conditions, treatment with 30 μM of misoprostol had significantly decreased the path length travelled to 185.23 ± 6.13 μm. This represents a 24% decrease in total cellular movement vs the control ($p < 0.001$) (**Fig 5A**). The significant difference between 10 μM and 30 μM treatments ($p < 0.001$) suggests that misoprostol induced reduction in distance travelled by NE-4C stem cells is dose dependant.

The *speed* of NE-4C cells was measured by calculating the ratio of distance to cell cycle duration. One-way ANOVA of speed values suggested a significant difference between the treatments ($F_{(2,297)} = 27.18$, $p < 0.001$, **Fig 5B**). On average, NE-4C cells travelled at a speed of 21.51 ± 0.69 μm/hr. Misoprostol's effect on speed was not observed with a 10 μM dose (20.33 ± 0.85 μm/hr, $p = 0.295$). However, when treated with 30 μM misoprostol, the average speed was reduced by 28% to 15.40 ± 0.44 μm/hr ($p < 0.001$). (**Fig 5B**). Additionally, NE-4C stem cells treated with 30 μM misoprostol were significantly slower than cells treated with 10μM misoprostol, adding further support for the dose dependant nature of its effects.

Cell cycle duration was defined as the time between the birth of a new daughter cell and the moment that it divided again (**Fig 4**). There was a significant effect on cell cycle duration based on the One-way ANOVA analysis ($F_{(2,297)} = 3.67$, $p < 0.05$, **Fig 5C**) On average, the NE-4C cell cycle lasted about 11.56 ± 0.19 hrs in the vehicle condition. Misoprostol significantly increased the time between divisions by 6.4% with a 10 μM dose (12.29 ± 0.17 hrs, $p < 0.05$). However, at 30 μM, misoprostol had no effect (12.01 ± 0.21 hrs, $p = 0.226$) (**Fig 5C**).

Misoprostol treatment also significantly reduced the dispersion capability of NE-4C cells, quantified by their displacement. *Displacement* was defined as the straight-line distance of the cell between the start and end of its cycle. One-way ANOVA determined that there was a significant difference between treatments on the displacement of NE-4C cells ($F_{(2,297)} = 3.95$, $p < 0.05$, **Fig 6**). The average displacement of NE-4C cells was 46.67 ± 3.86 μm in the vehicle. The 10 μM misoprostol dose decreased cell displacement to 36.55 ± 2.76 μm, but the difference was not significant ($p = 0.144$). The 30 μM misoprostol dose significantly decreased NE-4C displacement by 30% to 32.68 ± 2.23μm ($p < 0.05$) when compared to the vehicle (**Fig 6A**). Dispersion scatterplots for the vehicle and misoprostol treatments illustrate the dose dependant restraining effect of misoprostol on NE-4C stem cells (**Fig 6C**). When treated with 30 μM misoprostol, NE-4C stem cells were less dispersed than the control ($p < 0.05$) (**Fig 6B**). This effect was only seen at 30 μM, suggesting that it is dose dependant.

In summary, the 30 μM misoprostol treatment caused a significant decrease on all measures of motility (distance, speed, displacement) when compared to the control. This effect was not observed in the 10 μM treatment. Therefore, misoprostol decreased

NE-4C motility in a dose dependant manner. In a similar experiment, PGE_2 also had a dose dependant effect on cell motility [10], but at lower concentrations likely due to its higher affinity to EP receptors [7]. Based on these results, the 30 μM dose of misoprostol was chosen as the primary experimental treatment for studies 2 and 3.

3.1.2 - Misoprostol decreased the expression of CREB protein in NE-4C stem cells

A major downstream regulator of the PGE_2-EP receptor signalling pathway is the activation of PKA. This kinase phosphorylates many effectors, including the key neuronal transcription factor CREB, which typically regulates neuronal survival, migration, and differentiation [13,14,95]. Western blot analysis was done to measure the level of total CREB and phosphorylated pCREB (at Ser-133) proteins in NE-4C stem cells. Fold change values were standardized such that the vehicle = 1. The level of CREB was found to be significantly different amongst the three conditions ($F_{(3,8)} = 5.51$, $p < 0.05$, **Fig 7A**). While 10 μM misoprostol had no effect (Fold Change = 0.931 ± 0.162, $p > 0.900$), treatment with 30 μM misoprostol significantly decreased the level of total CREB (Fold Change = 0.547 ± 0.099, $p < 0.05$) when compared to the control (**Fig 7A**). Misoprostol's effect on pCREB level was similar to its effect on CREB ($F_{(3,8)} = 5.48$, $p < 0.05$, **Fig 7B**). At a 30 μM dose, misoprostol significantly decreased the level of pCREB (Fold Change = 0.639 ± 0.124, $p < 0.05$) when compared to the control (**Fig 7B).** This reduction in pCREB level was not observed with the 10 μM misoprostol treatment (Fold Change = 0.823 ± 0.109, $p = 0.286$). There was no significant difference between 30 μM and 10 μM misoprostol on the levels of CREB and pCREB (CREB: MP10 Fold Change = 0.931 ± 0.162; MP30 Fold Change = 0.547 ± 0.099, $p = 0.07$;

pCREB: MP10 Fold Change = 0.823 ± 0.109; MP30 Fold Change = 0.639 ± 0.124, p = 0.305) (**Fig 7 A, B)**.

Therefore, the results suggest that, in undifferentiated NE-4C cells, the 30 μM misoprostol treatment decreased the level of total CREB protein and reduced the level of Ser-133 phosphorylated CREB.

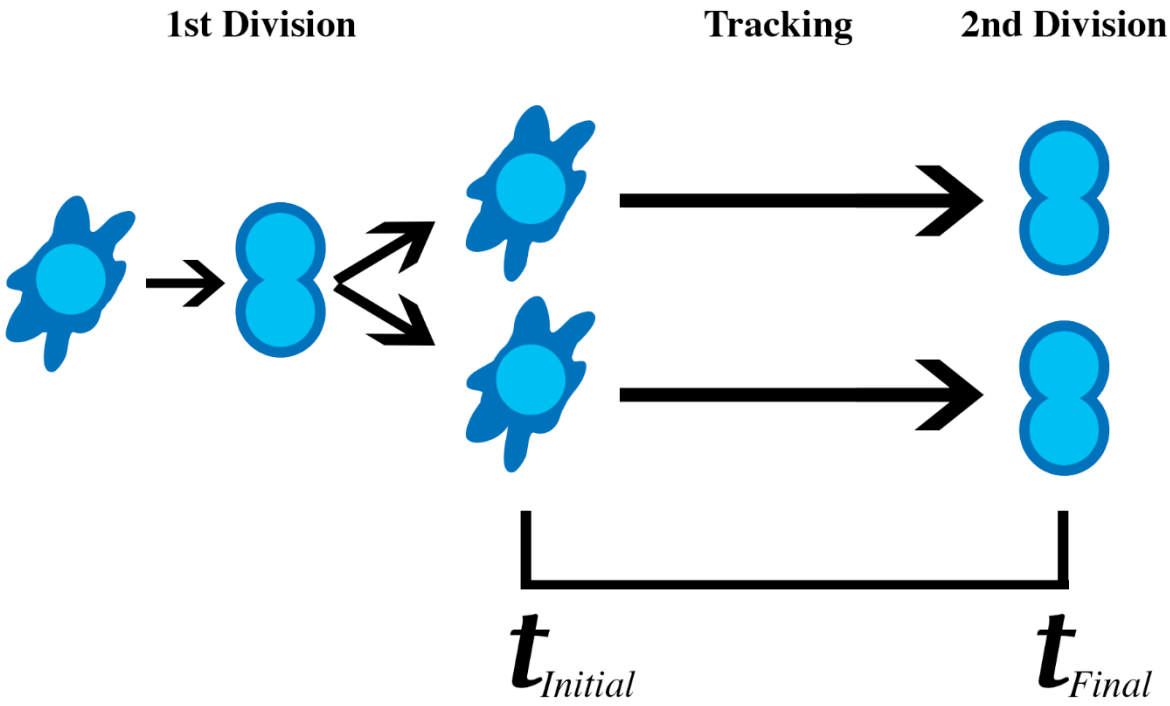

Figure 4: Illustration of the timeline for NE-4C cell tracking.
Tracking began on both daughter cells immediately following the first division. Tracking was stopped for the respective daughter cell when it completed a full cell cycle (reached the second division). Cells were imaged with a 10x inverted phase contrast Nikon Eclipse TI-E microscope. NIS Elements (Nikon) software was used for manual cell tracking. N=100 cells from three independent experiments tracked for each condition.

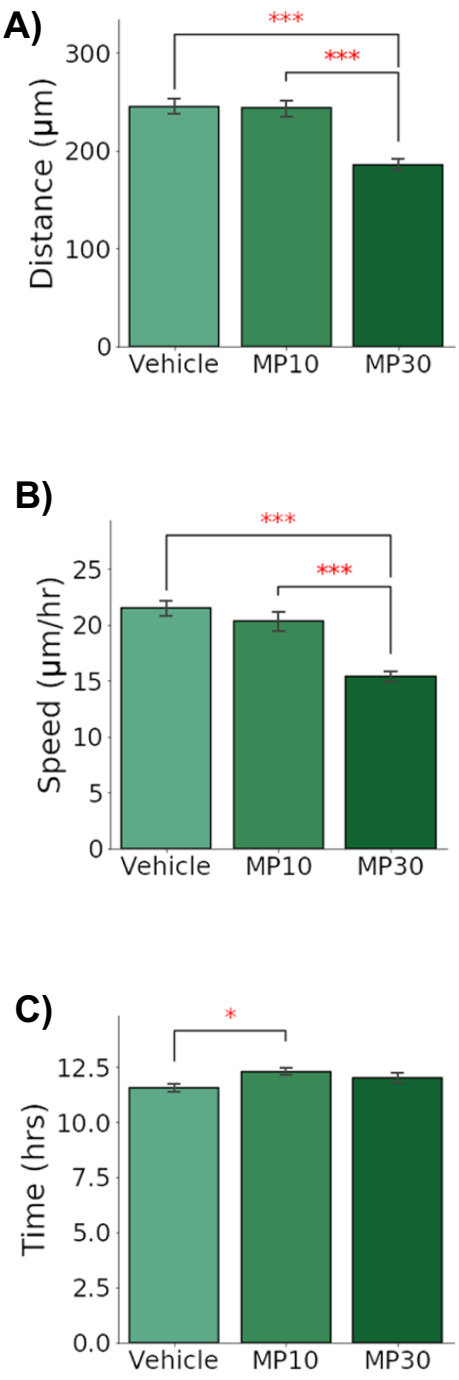

Figure 5: Misoprostol decreased the migration of undifferentiated NE-4C cells.

A) Misoprostol treatment decreased the total path length travelled by NE-4C cells at a 30 µM dose, but not at 10 µM. **B)** Average speed travelled by the cells was significantly decreased only with the 30 µM dose of Misoprostol. **C)** Only the 10 µM misoprostol condition increased the cell cycle duration. The results represent an average of N=100 cells per condition, from three independent experiments. Error bars represent SEM, *p < 0.05, **p < 0.01, ***p < 0.001.

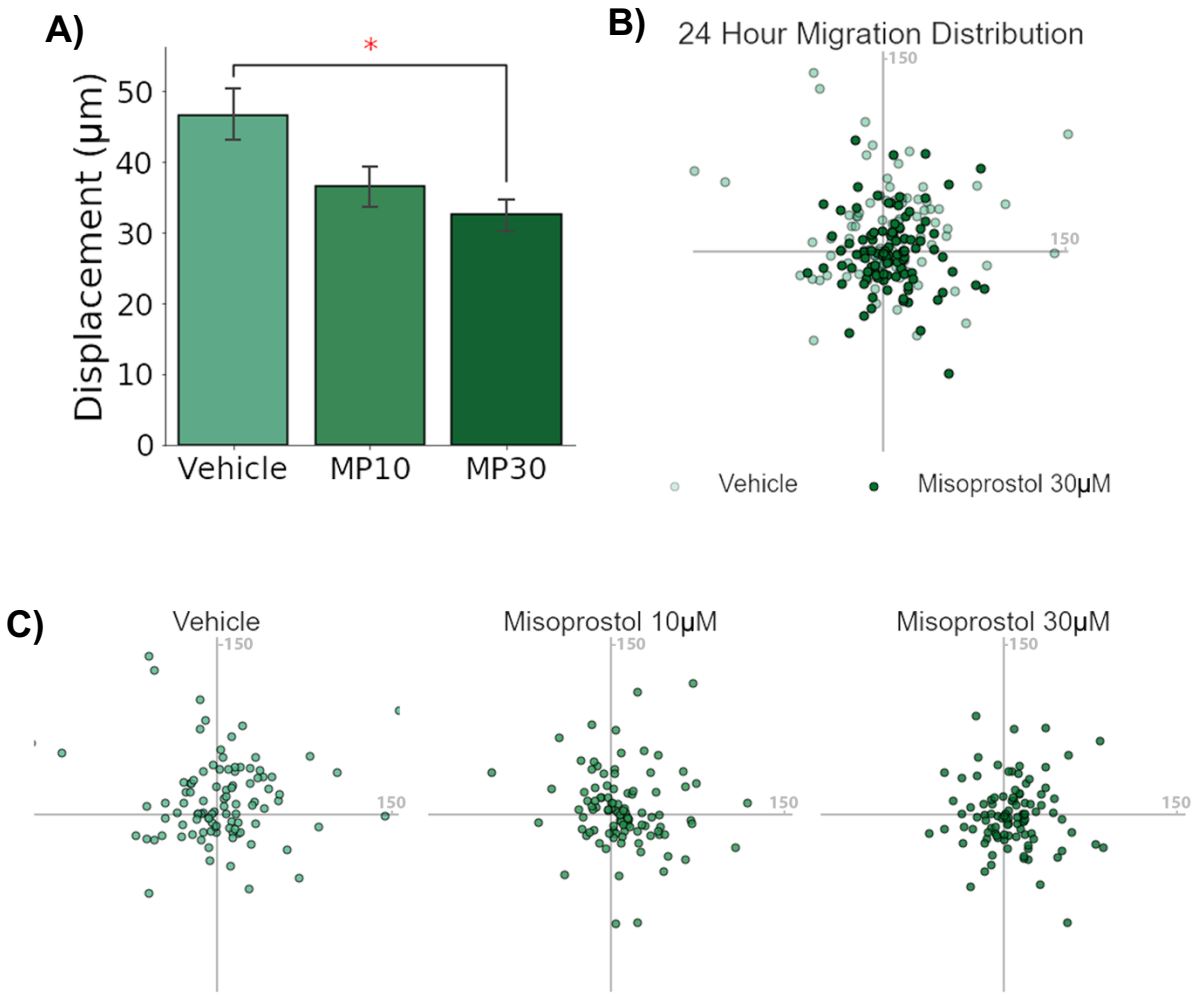

Figure 6: Misoprostol affected the dispersion of undifferentiated NE-4C cells. **A)** Treatment with 30 µM misoprostol decreased the displacement of undifferentiated NE-4C cells. **B)** Overlap of NE-4C cell dispersion comparing the 30 µM misoprostol condition against the vehicle. **C)** Individual dispersion graphs of NE-4C cells for each condition. The edge of each scatterplot is 150µm away from the origin. Treatment with 30 µM misoprostol resulted in less dispersion of cells compared to a 10 µM dose or vehicle. The results represent an average of N=100 cells per condition, from three independent experiments. Error bars represent SEM, *p < 0.05, **p < 0.01, ***p < 0.001.

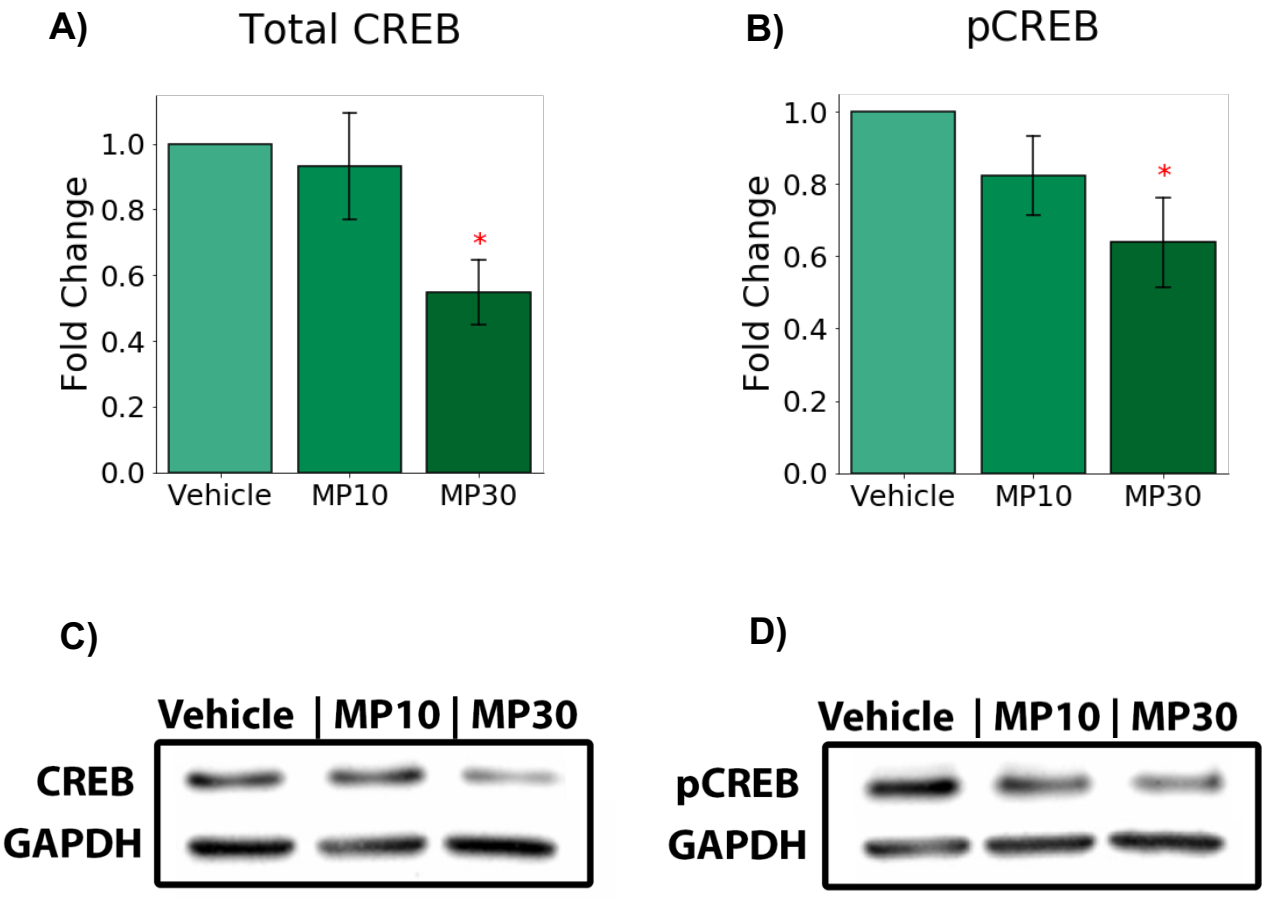

Figure 7: Misoprostol decreased total CREB protein level in NE-4C stem cells. A & B) Treatment with 30 μM misoprostol significantly decreased the expression of CREB and pCREB protein in undifferentiated NE-4C cells. **C & D)** Representative western blots of CREB and Ser-133 pCREB protein for the treatments, including GAPDH controls. The results represent an average of three western blots containing samples from three independent experiments. Statistical analyses were done with one-way ANOVA followed by Holms corrected multiple independent T-tests. Error bars represent SEM, *$p < 0.05$.

3.2 - STUDY 2: Misoprostol increases the growth of NE-4C neurospheres and delays differentiation

In this study NE-4C cells were used due to their characteristic differentiation process (**Fig 3**). Once differentiation is induced, proliferating cells migrate inwards to form aggregates. These aggregates then develop into three dimensional neurospheres in which cells proliferate or commit to neuronal differentiation. After further neurosphere growth, cells proceed to migrate outwards to complete differentiation[24,117]. In the developing nervous system migratory signals like cell adhesion molecules and cadherins regulate the migration and rate of differentiation of neuronal precursors [76,115]. In neurosphere assays, these same signalling molecules regulate cellular communication and cell fate [84,86,87,99]. The morphology of neurospheres throughout differentiation reflect the processes that occur at each step. These processes are analogous to migratory differentiation within the developing nervous system. Previous research has shown that PGE_2 increased the rate of differentiation and altered *Cdh2* expression in NE-4C cells [24]. Therefore, this study aims to determine whether misoprostol has a similar effect on the progression of differentiation and expression of adhesion molecule genes in differentiating NE-4C cells.

3.2.1 - Misoprostol slows the rate of differentiation

As described in **Figure 3**, NE-4C cells differentiate following the characteristic progression of proliferation, aggregation, and neurosphere formation. Neurospheres were imaged every two days for an eight-day period under vehicle or misoprostol conditions. The images in **Figure 8A** demonstrate the growth of neurospheres as the

cells proliferate and aggregate. Cells within the neurospheres express genetic markers which can be analyzed to indicate their stage of development.

PCR analyses was performed using *Oct4* and *MapT* markers which are commonly used to identify the presence of stem cells (early) and neuronal precursor / differentiating cells (late), respectively[24]. In the vehicle treatment, *Oct4* expression lasted up to day 6 coinciding with the appearance of *MapT*. This indicates that at day 6 there was a mixture of stem cells and differentiating neuronal cells. By day 8, the absence of *Oct4* expression suggests that there were few / no more stem cells present in the culture. All or most of the cells were differentiating neurons, evident by the presence of *MapT* (**Fig 8B)**. These results demonstrate a molecular switch from stem cell to neuronal precursor occurring between days 6-8 of differentiation in the vehicle group. In contrast, misoprostol treated cells expressed *Oct4* throughout all the days measured, indicating the presence of NE-4C stem cells on day 8. The differentiation marker, *MapT*, only appeared for misoprostol treated cells at day 8 (**Fig 8B)**. The results showed that, unlike the vehicle, there was no evidence of a complete shift from stem cell to neuronal precursor state by day 8 for the misoprostol treated group. The presence of both stem cells and differentiating neuronal cells at day 8 support the findings of increased neurosphere area and perimeter for the misoprostol condition (**Fig 9 A, B**). These results suggest that there is an overall delay in differentiation due to misoprostol treatment.

Gfap expression was tested to verify the absence of astrocytes in the differentiating neurospheres. *Gfap* exposure was only seen in the positive control

(mouse brain tissue), demonstrating that NE-4C cells only committed to neuronal differentiation in culture (**Fig 8B**).

3.2.2 - Misoprostol's effect on the size of neurospheres

Neurospheres are formed when neuronal stem cells aggregate together to create a microenvironment optimal for differentiation. It was previously found that morphology of the neurospheres indicate the ability of NE-4C cells to differentiate, cluster together, and communicate with adjacent cells[24]. Neurosphere shape is defined by area, perimeter, and roundness. For each measurement, a two-way ANOVA determined that there was a significant interaction between treatment and differentiation day (Area: $F_{(1,1781)} = 12.06$, $p < 0.001$, **Fig 9 A, D** ; Perimeter: $F_{(1,1781)} = 7.88$, $p < 0.001$, **Fig 9 B, E ;** Roundness: $F_{(1,1781)} = 104.37$, $p < 0.001$, **Fig 9 C, F**). Therefore, TukeyHSD post-hoc analysis was done for all comparisons to see the effect of misoprostol for each day that was measured. Approximately 225 neurospheres were measured every two days for each treatment condition, resulting in a total of about 1800 measured neurospheres. The differentiation of NE-4C cells in both conditions followed typical trends, shown in **Figure 8A** and in Wong et al.,[24] (2016), beginning with proliferation between days 0-2, inward migration and aggregation at days 2-4, and neurosphere formation on days 6-8. These behaviours were verified by morphological analysis (**Fig 9 D, E, F**).

The *area* of neurospheres was affected by misoprostol treatment at the start (day 2) and end (day 8) of differentiation. On day 2, misoprostol treated cellular aggregates were smaller compared to the vehicle treatment (Day 2: Vehicle = 9041 ± 595 μm^2; MP = 6289 ± 151 μm^2, $p < 0.01$) **(Fig 9A**). There was no difference between the two

conditions in neurosphere area on days 4 and 6 (Day 4: Vehicle = 19387 ± 1508 μm^2; MP = 15155 ± 710 μm^2, $p = 0.644$; Day 6: Vehicle = 20791 ± 1245 μm^2; MP = 17980 ± 912 μm^2, $p > 0.900$) **(Fig 9A**). However, by day 8, misoprostol treated neurospheres were significantly larger than the control (Day 8: Vehicle = 30922 ± 3470 μm^2; MP = 40427 ± 2852 μm^2, $p < 0.001$) (**Fig 9A**). Based on the area, both conditions demonstrated the typical neurosphere growth pattern of exponential growth (Day 0-2), inward migration (Day 2-4), plateau (Day 4-6), and further growth (Day 6-8), as was previously seen in Wong et al., (2016) [24] (**Fig 9D**). As differentiation progressed, larger neurospheres observed in the misoprostol condition could reflect a greater quantity of proliferating stem cells within the spheres. This would suggest that differentiation was delayed as shown in **Figure 8B**.

The *perimeter* of neurosphere aggregates was approximately 12% greater in the misoprostol condition when compared to the control on day 2 (Day 2: Vehicle = 361 ± 8.61 μm; MP = 403 ± 7.67 μm, $p < 0.01$) (**Fig 9B**). Again, no statistical difference was found between the treatments on days 4 - 6 (Day 4: Vehicle = 502 ± 17.8 μm; MP = 456 ± 10.2 μm, $p = 0.814$; Day 6: Vehicle = 500 ± 13.6 μm; MP = 473 ± 10.9 μm, $p > 0.900$) (**Fig 9B**). By day 8, the perimeter of misoprostol treated neurospheres was significantly greater than the perimeter of neurospheres treated with vehicle (Day 8: Vehicle = 589 ± 27.1 μm; MP = 690 ± 26.4 μm, $p < 0.01$) (**Fig 9B**). The progression of perimeter change per day exhibited the same trend that was seen for the area, starting off with growth (Day 2-4), a plateau (Day 4-6), and further growth (Day 6-8) (**Fig 9E**).

Roundness of neurospheres reflects the migratory and adhesive abilities of the NE-4C stem cells[24,78]. The effect of misoprostol on neurosphere roundness reflected the

decreased area and increased perimeter seen on day 2. Misoprostol treated clusters were significantly less round on day 2 than clusters from the control group (Day 2: Vehicle = 0.786 ± 0.008; MP = 0.547 ± 0.011, $p < 0.001$) (**Fig 9C**). However, by day 4 onwards there was no difference between the two conditions (Day 4: Vehicle = 0.879 ± 0.009; MP = 0.864 ± 0.007, $p < 0.001$, Day 6: Vehicle = 0.874 ± 0.004; MP = 0.886 ± 0.005, $p < 0.001$, Day 8: Vehicle = 0.907 ± 0.007; MP = 0.914 ± 0.006, $p < 0.001$) (**Fig 9F**).

Overall, misoprostol induced reduction in NE-4C stem cell migration may have contributed to the decreased roundness and increased perimeter seen for early, day 2, aggregates. Therefore, misoprostol may delay early differentiation at the inward migration stage.

3.2.3 - Expression of cell adhesion molecules during differentiation

Cell adhesion molecules play an important role in the regulation of cellular differentiation. For example, Cdh2 is responsible for cell-cell adhesion and communication[83,86]. It has many roles in neurodevelopment. Previous research from the Crawford lab has found that PGE_2 increases gene expression of *Cdh2* on day 6 [24]. NCAM is another adhesion molecule that has been shown to affect migration, neurite formation, and differentiation of neuronal cells [87,88,118]. In this study, a qRT-PCR analysis was done to measure the gene expression of *Cdh2* and *NCAM*.

The expression of *Cdh2* was measured across 8 days of differentiation. Results from a two-way ANOVA determined that the main effects of treatment and differentiation progress did not significantly affect the expression of *Cdh2* (differentiation progress:

$F_{(3,16)}$ = 2.89, p = 0.068 ; treatment: $F_{(1,16)}$ = 0.06, p = 0.812) (**Fig 10**). However, there was a significant interaction between the treatment and length of differentiation ($F_{(3,16)}$ = 4.99, p < 0.05) (**Fig 10**). Therefore, *Cdh2* expression was compared on each day. On day 2, vehicle treated aggregates expressed *Cdh2* at a Relative Quantity (RQ) of 6.281 ± 0.996. Treatment with misoprostol trended toward a significant reduction in day 2 *Cdh2* expression as compared to the control (Day 2: MP RQ = 1.996 ± 0.526, p = 0.057) (**Fig 10**). There was no significant difference in *Cdh2* expression between the conditions on days 4 and 6 (Day 4: Vehicle RQ = 8.096 ± 0.725; MP RQ = 7.291 ± 2.715, p > 0.900, Day 6: Vehicle RQ = 6.113 ± 0.998; MP RQ = 6.939 ± 1.024, p > 0.900) (**Fig 10**). On day 8, misoprostol treated neurospheres significantly increased *Cdh2* expression when compared to the control group (Vehicle RQ = 3.394 ± 0.213; MP RQ = 8.503 ± 0.960, p < 0.05) (**Fig 10**). This is opposite to the trend seen on day 2. Overall, misoprostol treatment led to increased expression of *Cdh2* after 8 days of differentiation. These results suggest that misoprostol treatment may alter the regulation of cellular development by affecting the expression of *Cdh2*.

The genetic expression of the cell adhesion molecule, NCAM*,* was also examined. Two-way ANOVA showed that the expression was significantly affected by differentiation progress ($F_{(3,16)}$ = 11.82, p < 0.001), treatment ($F_{(1,16)}$ = 17.55, p < 0.001), and their interaction as well ($F_{(3,16)}$ = 8.14, p < 0.01) (**Fig 11**). Vehicle treated cells expressed *NCAM* at an RQ of 5.248 ± 0.975 on day 2. Misoprostol treatment significantly reduced *NCAM* expression in the day 2 aggregates to an RQ of 0.975 ± 0.096 (p < 0.05) (**Fig 11**). The result was similar to the trend found on day 2 for *Cdh2* expression. *NCAM* expression was not affected by treatment on day 4 (Day 4: Vehicle

RQ = 4.515 ± 0.815; MP RQ = 4.910 ± 1.220, $p > 0.900$) (**Fig 11**). Misoprostol treatment also reduced the expression of *NCAM* in day 6 neurospheres by almost 75% when compared to vehicle (Day 6: Vehicle RQ = 18.341 ± 3.048; MP RQ = 4.937 ± 1.311, $p < 0.05$) (**Fig 11**). By day 8, *NCAM* expression had stabilized for both treatments (Day 8: Vehicle RQ = 8.090 ± 1.189; MP RQ = 7.127 ± 1.852, $p > 0.900$) (**Fig 11**). It was noted in vehicle treated cells that *NCAM* expression increased approximately 4-fold from day 4 to 6 and then decreased to less than half on day 8 (Day 4: Vehicle RQ = 4.515 ± 0.815; Day 6: Vehicle RQ = 18.341 ± 3.048; Day 8: Vehicle RQ = 8.090 ± 1.189) (**Fig 11**). Therefore, on day 6, NE-4C neurospheres experienced a sharp increase in *NCAM* expression, which did not occur in the misoprostol treatment (Day 4: MP RQ = 4.910 ± 1.220; Day 6: MP RQ = 4.937 ± 1.311; Day 8: MP RQ = 7.127 ± 1.852) (**Fig 11**). The upregulation of *NCAM* found in the day 6 vehicle group coincides with the initial appearance of *MapT* expressing neuronal precursors (**Fig 8B).** These results suggest that misoprostol alters the expression of adhesion molecules, such as *Cdh2* and *NCAM*, and disrupts neurodevelopment by affecting the aggregation and differentiation of neuronal precursors.

A)

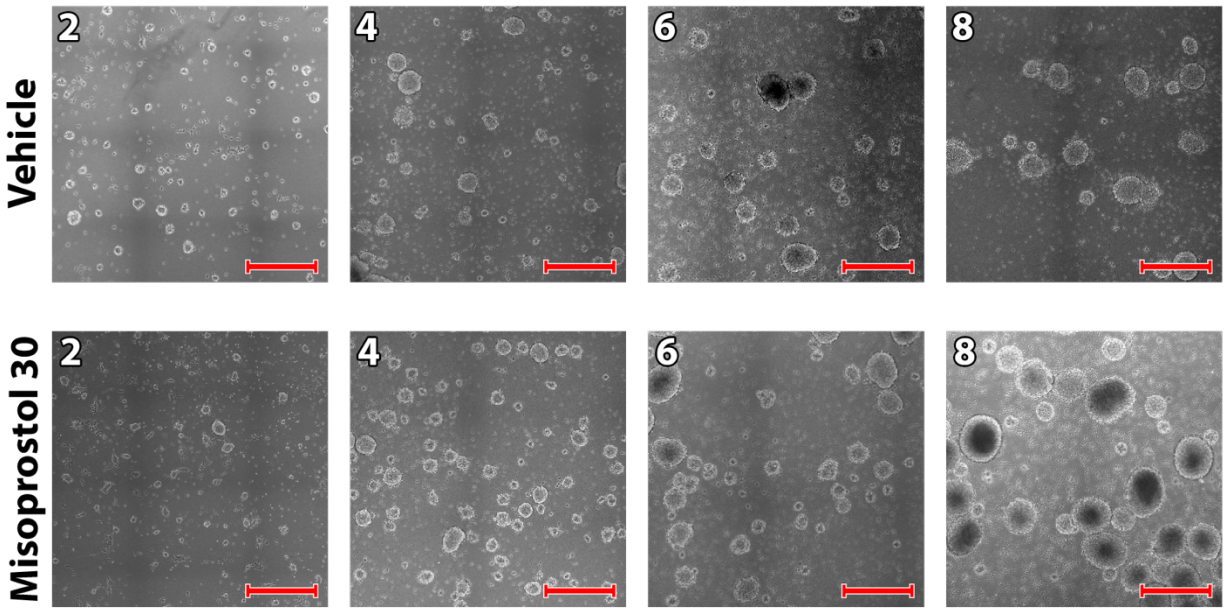

B)

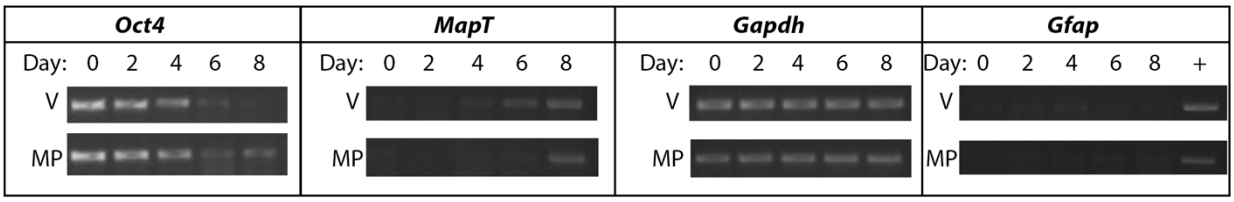

Figure 8: NE-4C neurospheres at different stages of differentiation.
A) Images represent NE-4C neurospheres at day's 2,4,6 and 8 of differentiation. The vehicle condition is on the top, and 30 μM misoprostol condition is below. An average of N= 225 neurospheres were measured every 2 days for each treatment. The scale represents 500 μm. **B)** The PCR results for *Oct4*, *MapT*, and *Gfap* expression from both treatments (V = Vehicle, MP= Misoprostol 30 μM). On day 8 the vehicle group did not express *Oct4* unlike the misoprostol group. *MapT* expression started on day 6 for the vehicle group and on day 8 for the misoprostol treatment. *Gfap* expression was only seen in the positive control mouse brain lane, labelled (+). The PCR was verified against the housekeeping gene *Gapdh*. PCR was run 3 times with 3 biological replicates.

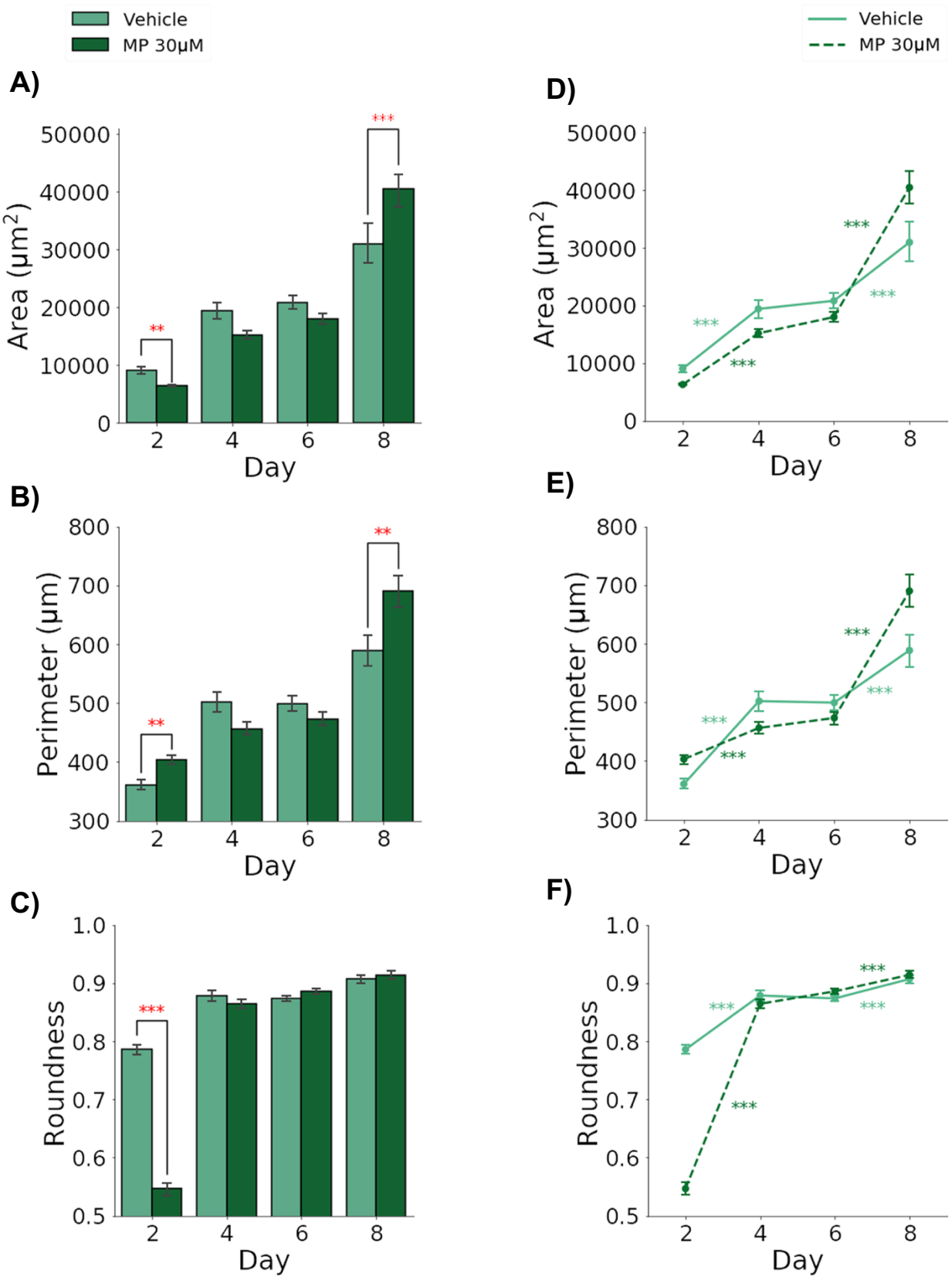
Vehicle
MP 30μM
A)
Area (μm²)
Day
B)
Perimeter (μm)
Day
C)
Roundness
Day
D)
Vehicle
MP 30μM
Area (μm²)
Day
E)
Perimeter (μm)
Day
F)
Roundness
Day

Figure 9: Misoprostol increased neurosphere size during differentiation of NE-4C cells.
A) Misoprostol treatment resulted in a decrease in neurosphere area on day 2 and an increase in area on day 8. **B)** Misoprostol treatment resulted in an increase in neurosphere perimeter on days 2 and 8. **C)** Misoprostol treatment resulted in less round neurospheres on day 2. The line graphs (**D, E, F**) show an increasing trend from days 2-4, with a plateau from days 4-6, and a subsequent increase from days 6-8 on all parameters. Averages for neurosphere area, perimeter, and roundness were determined from approximately N=225 neurosphere measurements for each treatment every two days from a minimum of 3 independent experiments. Statistical significance was determined by a two-way ANOVA with Tukey HSD post hoc analysis; error bars represent SEM. *$p < 0.05$, **$p < 0.01$, ***$p < 0.001$.

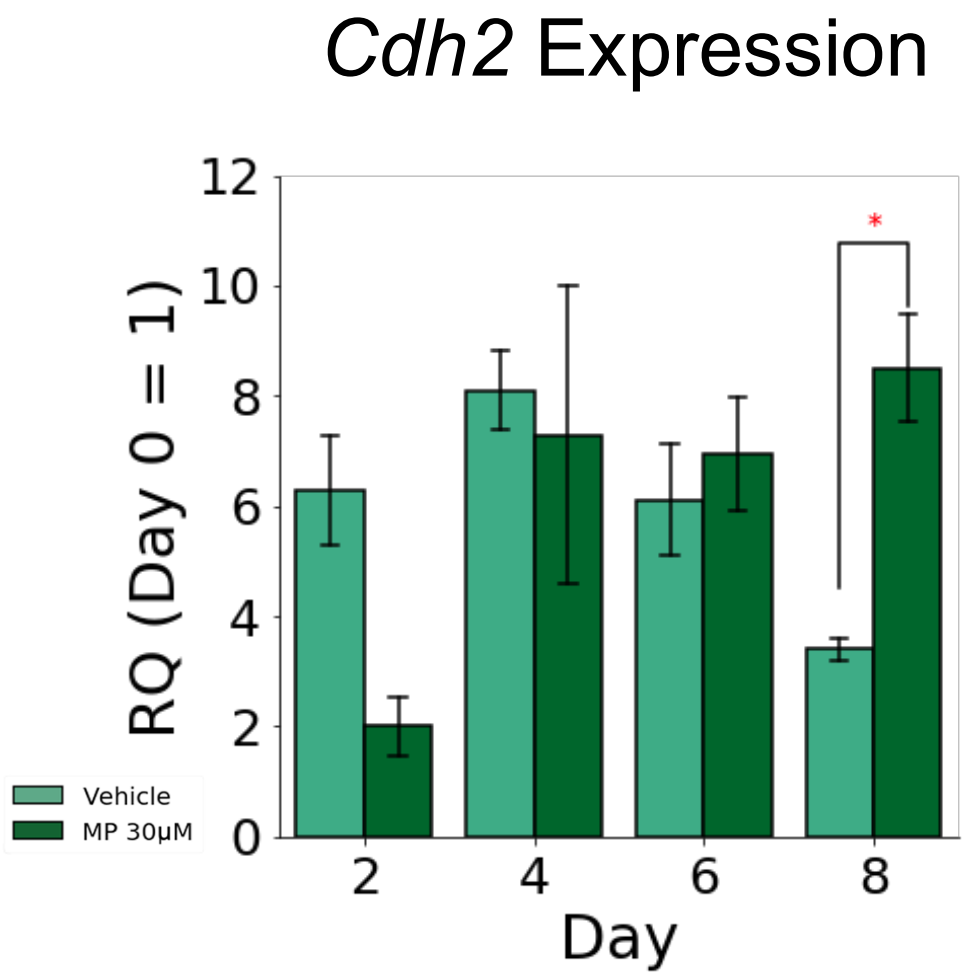

Figure 10: Misoprostol increased *Cdh2* expression of differentiated NE-4C cells. Gene expression is represented as a Relative Quantity (RQ) ratio against day 0 control sample expression. On day 2, misoprostol trended towards a significant decrease in *Cdh2* expression ($p < 0.06$). On day 8, misoprostol treated cells expressed significantly more *Cdh2* than the control. Each sample was run in technical triplicates for each plate. The results represent an average from 3 biological replicates. Statistical significance was determined with two-way ANOVA followed by Holms corrected multiple independent T-tests. Error bars represent SEM.*$p < 0.05$, **$p < 0.01$, ***$p < 0.001$.

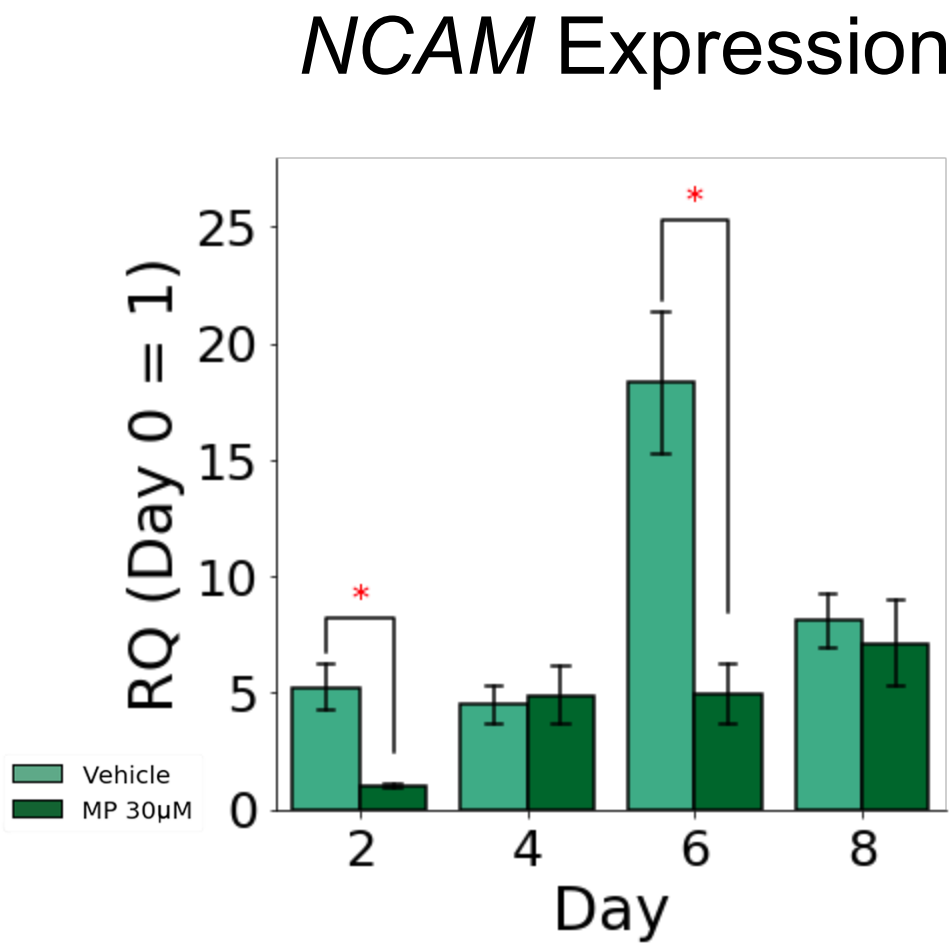

Figure 11: Misoprostol altered *NCAM* expression of differentiating NE-4C cells. Gene expression is represented as a Relative Quantity (RQ) ratio against day 0 control sample expression. Misoprostol treated cells had significantly lower *NCAM* expression on day's 2 and 6 of differentiation. Each sample was run in technical triplicates for each plate. The results represent an average from 3 biological replicates. Statistical significance was determined with two-way ANOVA followed by Holms corrected multiple independent T-tests. Error bars represent SEM.*$p < 0.05$, **$p < 0.01$, ***$p < 0.001$.

3.3 - STUDY 3: The effect of misoprostol on neurite length, CREB phosphorylation, and branch density in Neuro-2A cells

To study the effect of misoprostol on neuronal network formation, Neuro-2A cells were chosen due to their fast rate of differentiation and pronounced neurite extensions. Signalling molecules that guide cellular migration are also known to guide neuronal outgrowths [86,88,118]. Neuritogenesis and elongation occur when differentiation begins. Generally, neurite length corresponds to differentiation progress. Aberrant neuronal extensions may affect the development of the nervous system resulting in altered behaviours. Overactive neuronal signalling has been implicated in neurodevelopmental pathologies such as ASD [35]. The results of this study demonstrate the effects of chronic misoprostol exposure on neurite formation in differentiating Neuro-2A cells.

3.3.1 - Misoprostol affects the length of Neuro-2A neurites

Neurites are the primary form of contact between neuronal cells. Chemicals such as neurotransmitters enable signalling between a network of neurons connected via their dendrites or axons. Neurite measurements represent these extensions. It was previously found that acute PGE_2 and misoprostol induced neurite retraction in differentiated Neuro-2A cells[70,95]. In this experiment I aimed to determine the effect of long-term misoprostol treatment during differentiation, on neurite length. Differentiation was induced for a period of 3 days via the standard technique of serum starvation[106]. Neurites were measured throughout differentiation and classified as primary (the longest extension) or branching (extensions coming off of the primary neurite) (**Fig 12A**). Representative images of the day three Neuro-2A cells can be seen in **Figure 12B**.

A two-way ANOVA analysis determined that there was no interaction between differentiation time and treatment with respect to primary neurite length ($F_{(1,14)} = 1.0$, $p = 0.335$) (**Fig 13 A, B**). However, the main effects of treatment and time were both found to be significant (Treatment: $F_{(1,14)} = 7.91$, $p < 0.05$; Time: $F_{(1,14)} = 69.15$, $p < 0.001$) (**Fig 13 A, B**). At day 1 there was no difference in neurite length between the conditions (Day 1: Vehicle = 34.143 ± 0.614 μm; MP = 37.543 ± 0.801 μm, $p = 0.152$) (**Fig 13A**). On day 2 and 3, treatment with misoprostol significantly elongated primary neurites by approximately 25% when compared to the vehicle on both days (Day 2: Vehicle = 44.740 ± 1.031 μm; MP = 55.265 ± 1.300 μm, $p < 0.001$; Day 3: Vehicle = 60.105 ± 1.235 μm; MP = 76.235 ± 1.739 μm, $p < 0.001$) (**Fig 13A**). Under both conditions, neurites grew significantly longer as differentiation progressed ($p < 0.001$). On individual days, longer neurite extensions were found in the misoprostol treatment (**Fig 13B**). Overall, these results suggest that misoprostol consistently increased the length of primary neurites compared to the vehicle.

Similar to primary neurites, branches are involved in the formation of synapses in the nervous system. Two-way ANOVA determined that treatment ($F_{(1,14)} = 6.48$, $p < 0.05$), differentiation time ($F_{(1,14)} = 19.76$, $p < 0.001$), and their interaction ($F_{(1,14)} = 6.08$, $p < 0.05$), all significantly affected the length of neurite branches) (**Fig 13 C, D**). On the first day, misoprostol had no effect on branch length (Day 1: Vehicle = 13.676 ± 0.522 μm; MP = 13.442 ± 0.596 μm, $p > 0.900$) (**Fig 13C**). However, misoprostol treatment significantly increased the length of neurite branches on days 2 and 3 when compared to the control (Day 2: Vehicle = 14.479 ± 0.562 μm; MP = 18.074 ± 0.882 μm, $p < 0.05$, Day 3: Vehicle = 16.130 ± 0.683 μm; MP = 21.565 ± 1.003 μm, $p < 0.001$) (**Fig 13C**).

The vehicle treated cells did not experience any significant growth in their branching neurites over the course of differentiation (Vehicle: Day 1 = 13.676 ± 0.522 μm; Day 2 = 14.479 ± 0.562 μm; Day 3 = 16.130 ± 0.683 μm, Day 1-2: $p > 0.900$; Day 2-3: $p = 0.736$). On the other hand, misoprostol treated cells had significant neurite branch growth after the first day (MP: Day 1 = 13.442 ± 0.596 μm; Day 2 = 18.074 ± 0.882 μm; Day 3 = 21.565 ± 1.003 μm, Day 1-2: $p < 0.001$, Day 2-3: $p < 0.001$) (**Fig 13D**). These results suggest that misoprostol also increases the length of neurite branches.

The length of primary neurites and branches were compared to each other as a ratio (primary neurite length/ branch length) to determine if misoprostol's effect differs based on the type of neurite. Neurons can be categorized into functional classes based on the morphology of their axons and dendrites. Branching dendrites tend to be involved in divergent connections which send signals to many cells from one neuron[119]. Whereas long axons tend to converge onto a post-synaptic cell which receives signals from multiple other neurons[119]. Therefore, a large length ratio would suggest a preference for convergence, while a small ratio would suggest a preference for divergence. Two-way ANOVA results determined that the neurite length ratio was not affected by differentiation time ($F_{(1,14)} = 1.08$, $p = 0.315$), the treatment ($F_{(1,14)} = 3.92$, $p = 0.068$), or their interaction ($F_{(1,14)} = 0.33$, $p = 0.574$) (**Fig 14)**. Therefore, misoprostol's influence on neurite elongation did not differ for primary neurites or branches.

3.3.2 – Misoprostol affects the density of neurite branches

Neurite branch formation was measured by counting the number of branches for each day. Two-way ANOVA determined that there was no significant effect on the

number of branches during the experiment (Time: $F_{(1,14)} = 2.65$, $p = 0.126$; Treatment: $F_{(1,14)} = 0.54$, $p = 0.475$; Interaction: $F_{(1,14)} = 0.34$, $p = 0.571$) (**Fig 15A**).

The results above showed that misoprostol increased the growth rate of neurites, but did not affect the number of branches. This suggests that misoprostol may affect the density of neurite branches. Density was defined as the number of branches per 100 µm of primary neurite. The two-way ANOVA found that only the treatment affected the branch density ($F_{(1,14)} = 5.19$, $p < 0.05$), while differentiation time ($F_{(1,14)} = 2.68$, $p = 0.124$), and its interaction with the treatment ($F_{(1,14)} = 0.18$, $p = 0.682$), did not (**Fig 15B**). On days 1 and 2, there was no significant difference for branch density between misoprostol and the control (Day 1: Vehicle density = 0.642 ± 0.03 branches/100 µm; MP density = 0.556 ± 0.155 branches/100 µm, $p = 0.613$, Day 2: Vehicle density = 0.571 ± 0.085 branches/100 µm; MP density = 0.386 ± 0.057 branches/100 µm, $p = 0.293$) (**Fig 15B**). However, on day 3, misoprostol treatment significantly decreased branch density by about 27% when compared to the control (Vehicle density = 0.550 ± 0.018 branches/100 µm; MP density = 0.401 ± 0.031 branches/100 µm, $p < 0.05$) (**Fig 15B**). Therefore, after three days of differentiation, misoprostol decreased the density of branches in Neuro-2A cells, which may affect their ability to form synapses.

3.3.4 - Misoprostol regulates CREB phosphorylation

PKA is the major kinase activated in the PGE_2-EP2/EP4 signalling pathway. One of the targets of PKA is the transcription factor CREB. It was previously found that acute PGE_2 or misoprostol treatment caused neurite retraction and a short-term increase in CREB phosphorylation for differentiated Neuro-2A cells [70,95]. Other work from the

Crawford lab found that PGE_2 induced neurite growth in differentiating NE-4C cells was PKA dependant [42]. The goal of this experiment was to determine if chronic exposure would result in CREB phosphorylation after 3 days of differentiation. Protein levels of total CREB and Ser-133 phosphorylated CREB were analyzed from the lysates of Neuro-2A cells which differentiated under vehicle or misoprostol conditions. Total CREB level did not differ between conditions (Vehicle Fold Change = 1; MP Fold Change = 0.979 ± 0.141, $T_{(1,4)} = 0.15$, $p = 0.888$) (**Fig 16A**). However, the level of phosphorylated CREB (active) was significantly increased in misoprostol treated Neuro-2A cells compared to the vehicle (Vehicle Fold Change = 1.0; MP Fold Change = 1.2 ± 0.035, $T_{(1,4)} = 5.73$, $p < 0.01$) (**Fig 16B**). The trend suggests that misoprostol treatment increased CREB phosphorylation. These results suggest that chronic exposure does increase the amount of Ser-133 phosphorylated CREB, likely due to increased PGE_2-PKA activity.

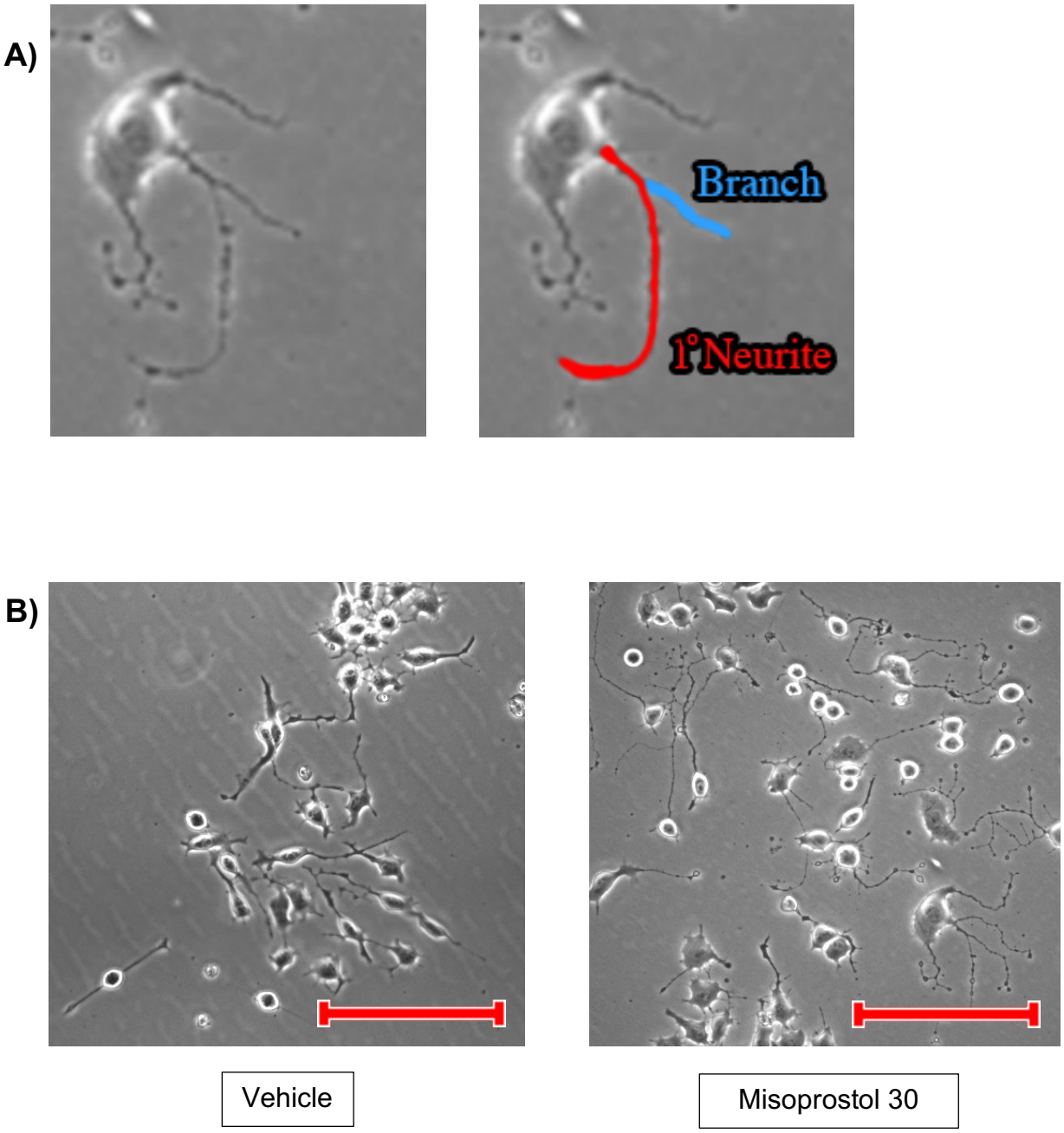

Figure 12: Representative images of differentiating Neuro-2A cells and neurites.
Images are from Neuro-2A cells which have been differentiating for 3 days in serum free medium. **A)** Unedited image on the left. Image on the right shows the primary neurite highlighted in red and the branch highlighted in blue. **B)** Vehicle cells are on the left and 30 μM misoprostol treated cells are on the right. The scale represents 200μm.

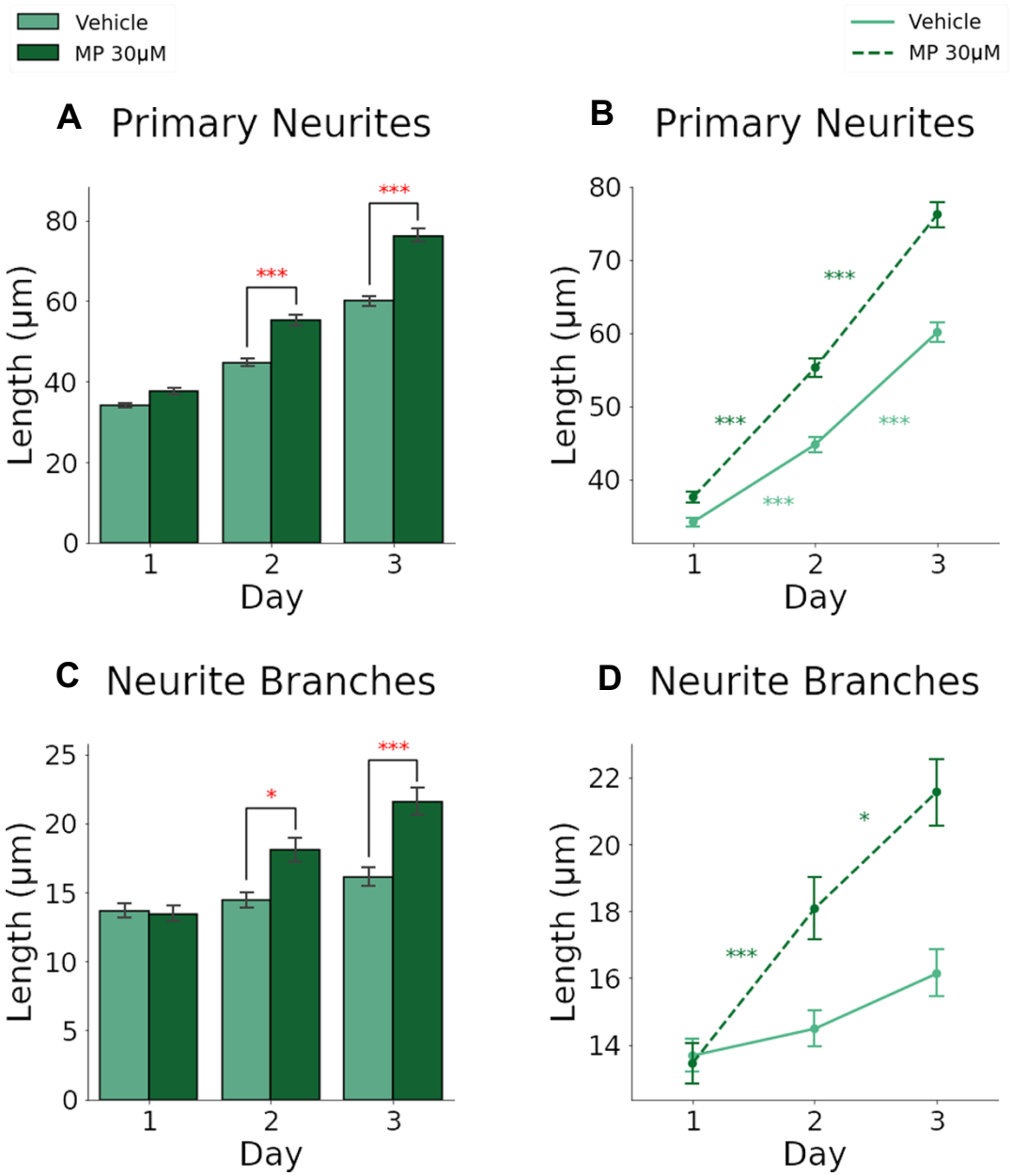

Figure 13: Growth of Neuro-2A neurites during differentiation.
Cell cultures treated with vehicle or 30 μM misoprostol were imaged every 24 hours and neurite extensions were measured on a Log_{10} scale for statistical analyses. **A,C)** After 1 day of differentiation, neurites from both conditions were similar in length. By day 2 and 3, misoprostol treated cells had significantly longer primary neurites and branches than the vehicle control. **B)** Primary neurites from both treatments grew significantly on a daily basis. **D)** Branches grew daily only from the misoprostol condition. Measurements were taken from an average of approximately N=750 primary neurites and N=200 branches per condition per day. Statistical analysis was done via Two-way ANOVA, followed by Tukey HSD post-hoc tests. Error bars represent SEM. *p < 0.05, **p < 0.01, ***p < 0.001.

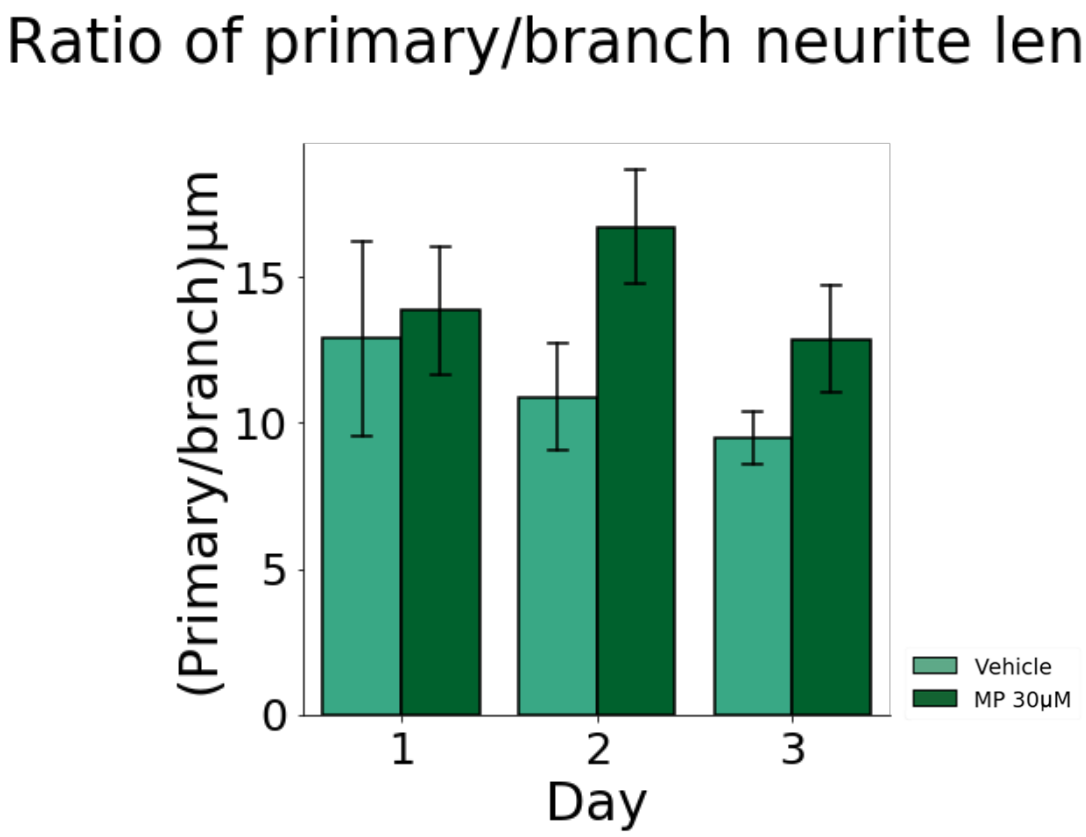

Figure 14: Length ratio of primary neurites compared to branches
The length ratio of primary neurites compared to neurite branches in Neuro-2A cells treated with vehicle or 30 µM misoprostol. Throughout differentiation, misoprostol treatment did not significantly affect the ratio of primary/branch neurite length. Therefore, the effect of misoprostol does not differ between the type of neurite. Measurements were taken from an average of approximately N=750 primary neurites and N=200 branches per condition per day. Statistical analysis was done via Two-way ANOVA, followed by Holm's corrected multiple T-tests. Error bars represent SEM. *p < 0.05, **p < 0.01, ***p < 0.001.

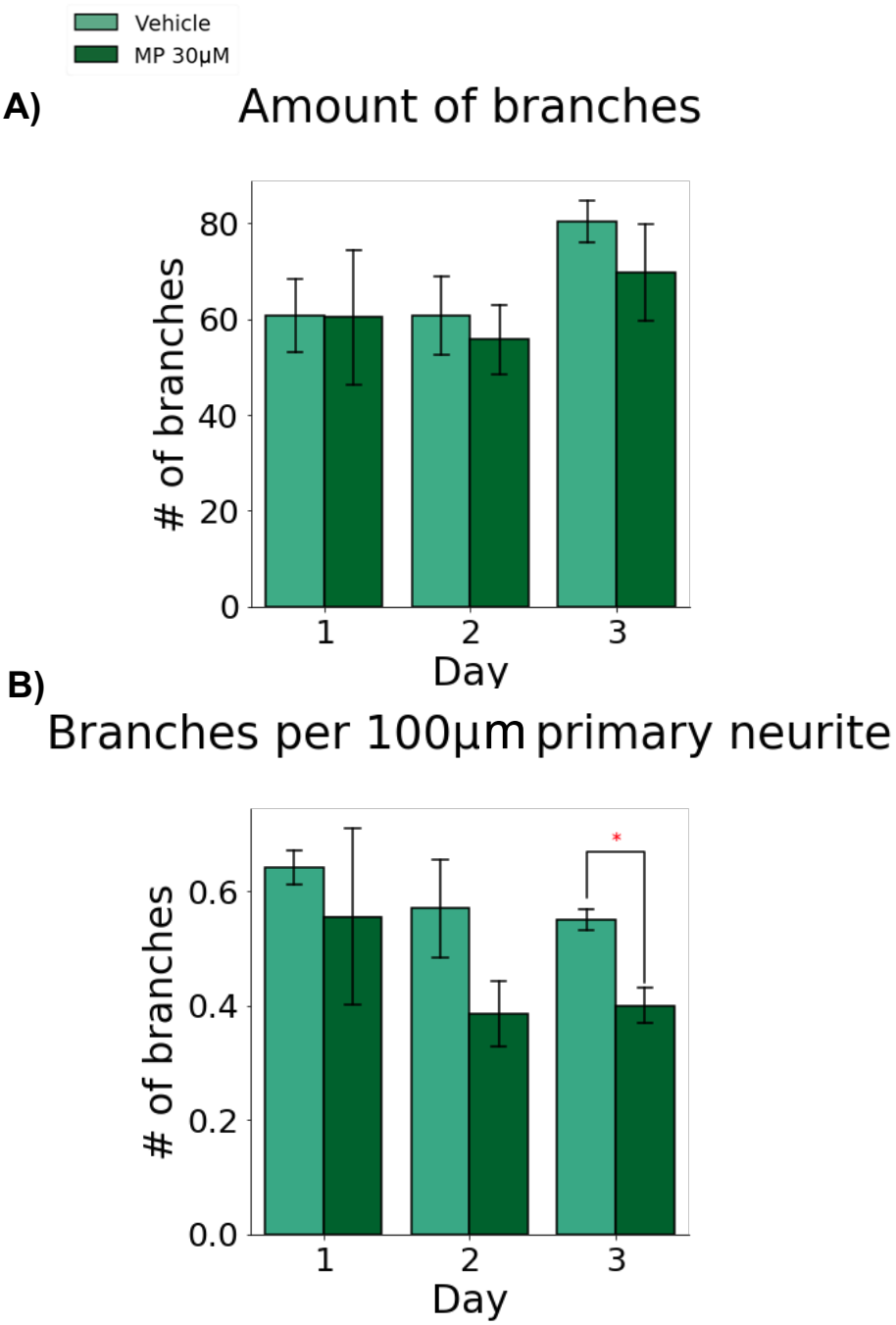

Figure 15: Neurite branch formation and density in Neuro-2A cells treated with Vehicle or 30 µM Misoprostol.

A) The number of neurite branches did not differ between condition or day for Neuro-2A cells. **B)** The density of branches was quantified as the number of branches per 100µm of primary neurite. By day three, the density of branches was significantly lower for misoprostol treated Neuro-2A cells. Statistical analyses were done with two-way ANOVA followed by Holm's corrected pairwise T-tests. Error bars represent SEM. *p < 0.05, **p < 0.01, ***p < 0.001.

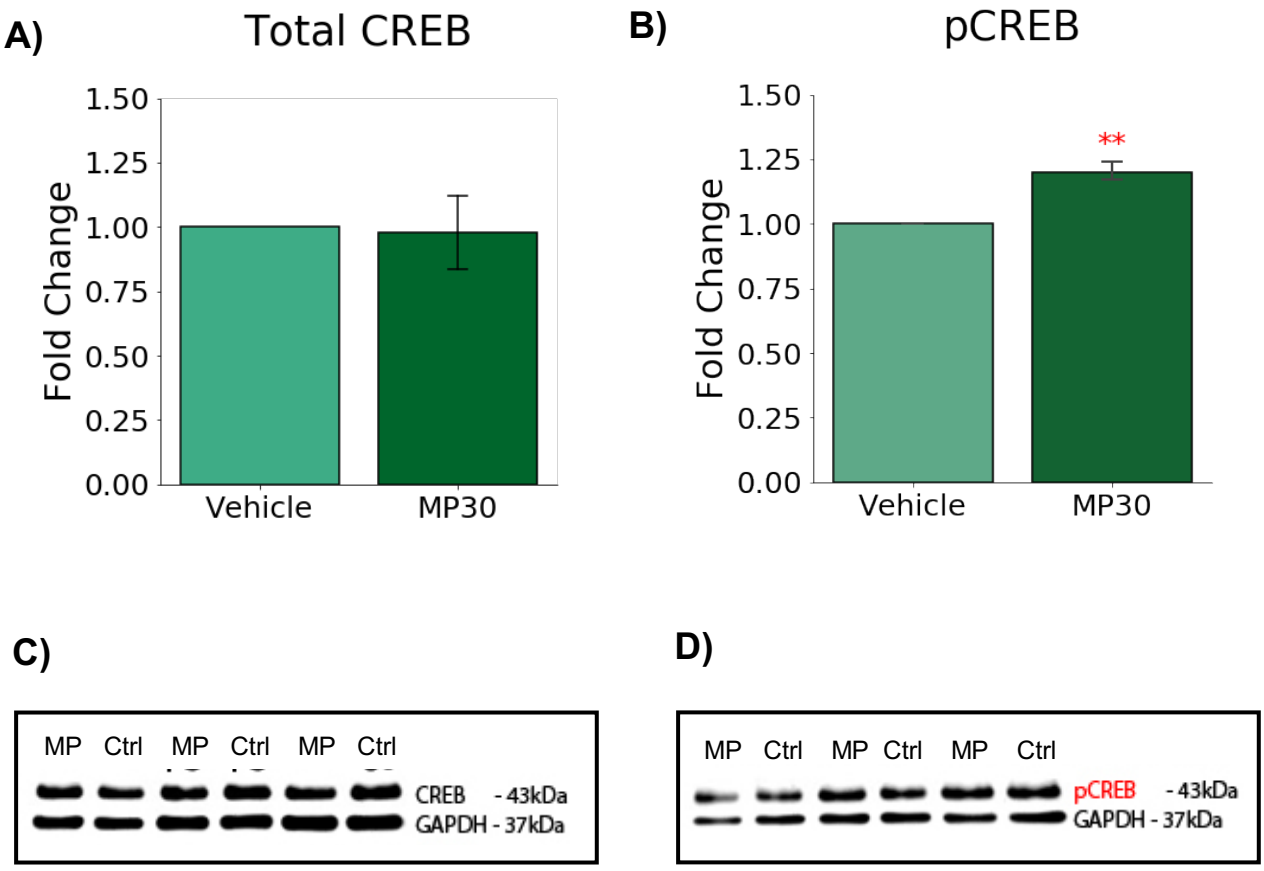

Figure 16: Level of CREB and pCREB proteins in Neuro-2A cells after 3 days of differentiation.
CREB proteins were quantified via western blot. Fold Change of protein level is relative to the vehicle control. **A)** Level of CREB protein was unaffected by misoprostol treatment. **B)** Level of Ser-133 phosphorylated CREB protein was significantly increased with misoprostol treatment compared to vehicle.
C & D) Representative western blots for the protein level of CREB and Ser-133 pCREB in the cell treatments, including GAPDH controls. Three biological replicates were analyzed. Independent T-tests were done for the statistical analysis. Error bars represent SEM. *$p < 0.05$, **$p < 0.01$, ***$p < 0.001$.

4 - Discussion

Previous findings in the literature and from the Crawford lab suggest that alterations in COX/PGE_2 signalling can disrupt neurodevelopment and contribute to pathologies such as ASD [20,21,30]. The present study provides evidence that misoprostol alters processes crucial to neurodevelopment, such as migration and differentiation of neuronal cells. I found that misoprostol reduced the migratory ability of NE-4C stem cells (**Fig 5, 6**) and decreased CREB protein levels (**Fig 7**). Moreover, misoprostol delayed the differentiation of NE-4C neurospheres (**Fig 8**), resulting in morphological changes (**Fig 9**) that were associated with altered expression of cell adhesion molecule genes *Cdh2* and *NCAM* (**Fig 10, 11**). In differentiating Neuro-2A cells, chronic misoprostol exposure enhanced neurite elongation (**Fig 13**), reduced neurite density (**Fig 15**), and increased the level of pCREB (**Fig 16**). The objective of this work was to determine misoprostol's influence on cellular behavior *in-vitro*, and its relation to neurodevelopment.

In many conservative countries, such as those found in Latin America, misoprostol is often used off-label to induce medical termination of pregnancy [67]. However, due to the conservative nature of those areas, follow-up care and education is very poor, which radically reduces the efficacy of the drug [63,68]. In this study I hypothesized that misoprostol would have similar effects as PGE_2 based on (1) previous studies from the Crawford lab, (2) its structural similarity to PGE_2, and (3) its affinity to the EP 1-4 receptors. In the subsequent sections I discuss possible explanations for the outcomes of this study, and how misoprostol exposure may contribute to brain pathology.

4.1 - Misoprostol reduces the migration ability of NE-4C stem cells

In the first study I investigated the effects of misoprostol on NE-4C stem cell migration. Previous research from the Crawford lab showed that PGE_2 rescued migration in NE-4C cells that were suppressed by WNT treatment [10]. Comparisons between the two studies are difficult due to the addition of WNT. Although PGE_2 had no effect on its own, I hypothesized that misoprostol would affect motility in NE-4C cells due to its different affinity to EP receptors. The results showed that at low concentrations misoprostol had no effect on migratory traits (cell speed, distance travelled, and final displacement). At higher concentrations misoprostol decreased the motility of the cells, opposite to the effect of PGE_2 on WNT-treated NE-4C cells. I determined that misoprostol decreased the cellular migration ability of NE-4C stem cells, evident by their reduced speed, distance and displacement, in a dose dependant manner. Decreased motility was only seen in the 30 μM misoprostol group. The 10 μM treatment had no effect on the cell's motility.

Reduced cellular motility can have severe implications on the organization of cells in the developing nervous system. Within the first month of gestation the neural tube is formed. Cells from the neural tube then migrate throughout the embryo to form the peripheral and central nervous systems. Misoprostol exposure during these critical periods may disrupt the ability of these cells to reach their targets, resulting in disrupted formation of neuronal networks. A recent study from the Crawford lab looked at the brains of P8 mice whose mothers were injected with PGE_2 at E11 or E16 [43]. They found that PGE_2 injection on either day caused a decrease in cerebellar cell density by P8 [43]. This reduction affected both males and females [43]. Additionally, prenatal PGE_2 injection

altered the expression of growth and motility genes (*Spn* and *Actb*) and affected cellular migration in the neocortex [43]. Genes that regulate the cytoskeleton and cellular migration, such as *DCX*, have been previously associated with ASD [120]. Furthermore, Impaired cytoskeletal dynamics have been observed in a subset of ASD patients [121]. It is well known that cortical organization of cells is impacted in individuals with ASD. For example, it was found that patients with ASD had significant alterations in the cytoarchitecture of the cerebellum, amygdala, and striatum regions of the brain [122]. Typically, neuronal migration occurs during the 2nd trimester in humans. Therefore, early misoprostol exposure may disturb neuronal migration leading to developmental pathologies.

My findings demonstrated that misoprostol treatment significantly reduced the level of total CREB and phosphorylated CREB in NE-4C cells. Traditionally, PKA phosphorylates CREB to regulate genes such as *c-fos, BDNF*, and *TH* (tyrosine hydroxylase), which are known to coordinate cellular proliferation, migration, survival, and tumorigenicity [123–125]. Misoprostol induced reduction of Ser-133 phosphorylated CREB and total CREB protein in NE-4C stem cells may have implications on neurodevelopment by altering CREB mediated gene expression. A major role of CREB is to potentiate synapses associated with long term memory [126]. CREB is considered to be necessary for learned behaviours, such as social norms, which are often impaired in ASD [126]. Disruptions in CREB signalling have been implicated in several cognitive disorders such as Alzheimer's Disease and Huntington's [127]. In fact, CREB was found to be downregulated in post-mortem brain samples of Alzheimer's disease [128]. Other studies have demonstrated that CREB signalling plays an important role in regulating

cellular migration during development. It was found that in mice a CNS specific CREB knockout altered the migration of neuronal precursors causing abnormal architecture in the hippocampus and cerebral cortex [129]. One study in zebrafish found that embryos treated with a functional knockdown of CREB showed altered somite morphology [130]. Neural crest cells rely on somites to guide them as they migrate away from the notochord. Based on this data, it is likely that misoprostol induced reduction of cellular motility in NE-4C cells is due to a reduction in total CREB protein, which may affect the synaptic plasticity and organization of highly structured brain regions during development.

4.2 – Reduced motility delays early differentiation in misoprostol treated NE-4C stem cells

When differentiation is induced *in-vitro*, cells start to release chemotropic signals in order to aggregate, forming neurospheres. My results showed that in NE-4C stem cells, misoprostol caused a reduction in speed, distance travelled, and displacement. Therefore, the ability to aggregate and form neurospheres may be inhibited by misoprostol. During the aggregation phase of differentiation, misoprostol treated cells were not as quick to form complete spherical clusters as the control. This is corroborated by the fact that on differentiation day 2, misoprostol treated clusters were less round, had larger perimeters (due to cells that were not completely integrated into the neurosphere), and smaller areas than clusters from the vehicle condition. Research has shown that neurosphere formation may also be affected by CREB. A study found that neuronal stem cells cultured from E14 $CREB^{-/-}$ mice formed less neurospheres that were also smaller in size than those from the control [131]. Therefore, misoprostol delayed the initial phase of differentiation by decreasing the level of total CREB protein and reducing the motility of NE-4C stem cells, resulting in neurospheres that were initially smaller and irregular in shape when compared to the control. This delay is further supported by the expression of differentiation markers, *Oct4* and *MapT*, which showed that misoprostol treated neurospheres were less differentiated than the control by day 6. Therefore, by suppressing the movement of stem cells during the inward migration, and by reducing the level of CREB, misoprostol delayed the early phase of NE-4C differentiation.

4.3 – Misoprostol affects neurosphere morphology and delays differentiation of NE-4C cells by altering the expression of *Cdh2* and *NCAM* at different phases

For the second study, I examined the effect of misoprostol on NE-4C differentiation, neurosphere formation, and genetic expression of two cell adhesion molecules, *Cdh2* and *NCAM*. Both genes have been implicated in neuronal differentiation and embryonic development. The results showed that misoprostol treated cells formed smaller aggregates than the controls on differentiation day 2, suggesting that it affected inward migration and early cluster formation. This was associated with a significant reduction in *NCAM* expression and was mirrored by a decreasing trend in *Cdh2* expression. Additionally, the expression of differentiation markers, *Oct4* (stem cell) and *MapT* (committed neuron), on days 6 and 8, indicated that misoprostol delayed the differentiation of NE-4C cells when compared to the control. The effects of misoprostol on early differentiation were reversed on day 8, evident by the formation of larger neurospheres that expressed more *Cdh2* than the controls. These results suggest that misoprostol causes a reduction in the expression of cellular adhesion genes, *NCAM* and *Cdh2,* during early stages of differentiation, but an increase in expression of these genes during later stages, resulting in altered neurosphere morphology and differentiation progress. The data warrants further consideration of the roles of these genes in neurodevelopment and the possible repercussions of misoprostol exposure.

4.3.1 - *Cdh2* expression is associated with decreased migration and delayed differentiation

During embryonic development, neural crest cells undergo an epithelial-mesenchymal transformation (EMT) before they migrate from the neural tube to form the peripheral nervous system [76]. The process of EMT enables neural crest cells to migrate and has been associated with upregulation of *Cdh2* [132]. This is in line with the previous finding that misoprostol reduces the migration ability of NE-4C stem cells by demonstrating that early misoprostol treated neurospheres have reduced *Cdh2* expression, similar to non-migrating neural crest cells. Moreover, *Cdh2* is known to regulate the start of neuronal differentiation. Early *Cdh2* expression was found to be essential for neuronal differentiation of mouse derived induced pluripotent stem cells (iPSC's), with differentiation being completely blocked by *Cdh2* knockdown [133]. These data supplement the current findings which suggest that misoprostol delays the start of neuronal differentiation by showing that it decreases the expression of *Cdh2,* a gene required for differentiation. Additionally, *Cdh2* expression was greatest for misoprostol treated neurospheres on day 8, and was significantly higher than the corresponding controls. This was concurrent with the advent of *MapT* differentiation marker expression, indicating that committed neuronal cells first appeared during high expression of *Cdh2*. These findings add evidence that *Cdh2* expression supports neuronal differentiation in NE-4C cells.

Previous research from the Crawford lab found that PGE_2 treated NE-4C cells had greater expression of *Cdh2* than controls at earlier stages of differentiation (Day 6) [24]. Moreover, the PGE_2 treated cells initiated differentiation earlier than their controls [24].

In the present study, misoprostol treatment resulted in greater *Cdh2* expression than controls only on the last day (Day 8). This effect coincided with the appearance of committed neuronal precursors in the misoprostol treatment, based on the expression of *MapT* differentiation marker. Therefore, PGE_2 and misoprostol both increase *Cdh2* expression, but at different stages of development, resulting in seemingly opposite effects on the rate of NE-4C differentiation. The difference in timing is most likely due to the difference in EP receptor affinity between the two treatments. It is possible that misoprostol's lower affinity for EP receptors resulted in a slower *Cdh2* response than PGE_2 treatment, leading to an overall delay in differentiation, although this relationship has not yet been tested.

4.3.2 - *NCAM* expression affects early neurosphere formation and commitment to neuronal differentiation.

Neurospheres, aggregates, and migrating cells all respond to a specific balance of signals that regulate cell fate and differentiation. In the present study, misoprostol treated neurospheres had a smaller area and expressed less *NCAM* than the control on day 2. One study on mouse neural progenitor stem cells found that acrylamide treatment inhibited the formation of neurospheres, which was associated with a decrease in NCAM protein, supporting the current finding that NCAM is associated with early formation of neurospheres [134]. Furthermore, the results suggest that commitment to neuronal differentiation is regulated by the timed expression of *NCAM*. Differentiating neurospheres in vehicle demonstrated a notable increase in *NCAM* expression on day 6, about 4 times greater than what was seen on day 4. This event coincided with the expression of *MapT* differentiation marker, suggesting that *NCAM* upregulation was associated with the appearance of committed differentiating neuronal cells. By day 8, *NCAM* expression returned to normal and *Oct4* stem cell marker expression was absent, indicating that all cells became committed to neuronal differentiation. The timing of *NCAM* upregulation in this study suggests that it may be associated with the switch from neuronal stem cells to committed differentiating neurons. Minamino et al. (2015) found that *NCAM* expression was also upregulated on day 6 for neurospheres derived from murine embryonic stem cells (ESC) treated with neural induction medium [135]. Moreover, day 6 upregulation of *NCAM* in the ESC derived neurospheres coincided with the absence of *Oct4* stem cell marker expression [135]. Therefore, the current results, along with findings from the literature, suggest that *NCAM* may function as a signal to

induce the differentiation of stem cells into committed neurons. This theory of *NCAM* induced neuronal commitment is further supported by research that showed *NCAM* binding inhibited proliferation and induced differentiation of neurons in rat and mouse hippocampal progenitor cells [100]. There was not a similar upregulation event for *Cdh2*, suggesting that this role may be specific to *NCAM*.

4.3.3 - Misoprostol affects neurosphere morphology by delaying differentiation

Misoprostol treatment suppressed the upregulation of *NCAM* seen in the controls, and resulted in neurospheres that were larger (greater area and perimeter) on day 8. A model for neurosphere growth found that the size of spheres was correlated to the proliferative potential of cells within the sphere [136]. Neurospheres containing a larger proportion of committed neuronal precursors were smaller in size than neurospheres mostly comprised of neural stem cells [137]. Generally, as stem cells progress towards a differentiated state, their capacity for proliferation decreases [138]. This supports the finding that misoprostol treatment delayed differentiation, evident by the delayed expression of differentiation marker *MapT*, and retained expression of stem cell marker *Oct4* on day 8. The markers indicated that misoprostol treated neurospheres were comprised of a mixed population of NE-4C stem cells and differentiating neurons, unlike vehicle treated neurospheres which were mostly comprised of committed neuronal cells. These results support the current finding that misoprostol increased the size of neurospheres due to its effects on differentiation. The suppression of *NCAM* upregulation suggests that misoprostol disturbed the commitment of neural stem cells into neurons, resulting in a larger proportion of proliferative stem cells which led to the increase in neurosphere size.

A previous study from the Crawford lab found that PGE_2 treatment on differentiating NE-4C cells resulted in larger neurospheres than the controls on day 8, similar to the present findings with misoprostol [24] . Moreover, there was a simultaneous increase in the expression and protein level of Cyclin D1 [24]. Research has shown that

Cyclin D1 shortens the G1 phase of the cell cycle, which is characteristic of proliferative stem cells [139]. A study found that Cyclin D1 overexpression inhibited neurogenesis and promoted proliferation in mouse cortical progenitor cells [140]. Although the effect of misoprostol on Cyclin D1 has not been examined in this study, I suspect that, like PGE_2, misoprostol may also increase the expression and level of Cyclin D1, enhancing the proliferative potential of cells within the neurospheres causing it to increase in size. However, unlike misoprostol, PGE_2 increased the rate of differentiation[24]. The opposing effects are likely due to differences in the downstream effectors induced by PGE_2 and misoprostol. For example, misoprostol treatment alone affected migration in NE-4C stem cells, whereas PGE_2 treatment alone did not [10]. Furthermore, the Crawford lab has shown that PGE_2 treatment on differentiating NE-4C cells increased the expression of *WNT*, a gene known to regulate neuronal migration and cell fate [24,33,34]. Therefore, Cyclin D1 enhancement of proliferative cells may have contributed to increased neurosphere size from both PGE_2 and misoprostol, whereas earlier differentiation in PGE_2 treated cells might have occurred due to the action of other developmental factors induced specifically by PGE_2.

Additional research is required to determine differences between the effects of misoprostol and PGE_2 on downstream signalling as they have different affinities and sensitization tolerances for the EP receptors. However, results from this study and findings from the literature suggest that misoprostol treatment delays differentiation of NE-4C cells and alters neurosphere morphology by affecting the expression of adhesion molecule genes, *NCAM* and *Cdh2*, which are factors associated with cellular proliferation, migration, and induction of differentiation and neuronal commitment.

4.5 – Comparing the effects of misoprostol and other teratogens in the neurosphere model of development

Studies in neuronal models of development demonstrate shared effects caused by misoprostol and other well-known teratogens such as valproic Acid (VPA), thalidomide, and ethanol. Interestingly, research shows that these drugs can all interact with the prostaglandin signalling pathway. Valproic acid was found to decrease the levels of COX enzymes and PGE_2 in the rat brain [141]. Prenatal ethanol exposure altered prostaglandin E levels in fetal sheep brains [142]. COX activity was inhibited by thalidomide and its analogues [143]. On the molecular level, these drugs disrupt mechanisms involved with cellular adhesion, differentiation, and migration. Phenotypically, deformities of facial regions and speech are affected. Neurospheres have been previously described as a useful model for studying neurotoxic effects on early neurodevelopment *in-vitro* [144,145]. They have been compared to endogenous processes such as neural tube formation [144,145]. Therefore, the neurotoxicity of misoprostol can be examined by looking at its effects on neurosphere development. Possible developmental outcomes of misoprostol exposure may be inferred by comparing misoprostol to better known teratogens that affect similar molecular processes.

The present findings showed that misoprostol affected the differentiation and formation of NE-4C neurospheres by disturbing the expression of adhesion molecules, resulting in altered neurosphere morphology and delayed differentiation. Similar studies have looked at the neurosphere model of development to demonstrate neurotoxicity of known teratogens such as ethanol and VPA [64,144,146,116,117]. Embryonic exposure to

these drugs led to common symptoms such as craniofacial abnormalities, limb malformation, and intellectual impairment [63,148–150]. Ethanol treatment on differentiating fetal neural progenitor cells resulted in larger neurospheres and altered gene expression of laminin and integrin adhesion molecules [78]. VPA treatment altered the morphology of human induced pluripotent stem cell (hIPSC) neurospheres and delayed their commitment to neural differentiation [144]. Results from this study, along with findings from the literature, suggest that misoprostol disrupts neuronal development in a manner similar to VPA and ethanol, altering neurosphere morphology, differentiation, and expression of adhesion molecules. It is well known that ethanol and VPA interfere with prenatal neurodevelopment, resulting in postnatal cognitive and behavioural defects. Rats exposed to VPA during E9 exhibited ASD behaviours such as decreased socialism and hyper-activity[146]. Research from the Crawford lab in COX-2 deficient mice and PGE_2 injected offspring found similar deficits including anxiety-linked and repetitive behaviours, supporting the involvement of prostaglandin signalling in ASD neuropathy [20,45]. Furthermore, VPA and thalidomide have both been shown to cause cranial nerve damage, which is a common pathology of misoprostol associated Moebius syndrome [64,147,148]. The effects of misoprostol found in this study parallel findings from other teratogens on *in-vitro* neurodevelopment, suggesting that prenatal misoprostol exposure may lead to similar postnatal cognitive behavioural defects.

The results from this study warrant further research on the neurotoxic effects that misoprostol may have on a developing embryo. Misoprostol should only be used for medical termination of pregnancy if taken concomitantly with mifepristone, so as not to reduce efficacy. Countries with poor access to treatment, like those in Latin America,

should consider the danger they pose to their citizens by prohibiting proper medical management options.

4.6 - Misoprostol induces neurite elongation

Neurite morphology in differentiated NE-4C cells and Neuro-2A cells has been previously studied by the Crawford lab [18,70,71,95]. They found that acute PGE_2 or misoprostol treatment caused neurite retraction in differentiated Neuro-2A cells, suggesting that misoprostol has the same effect on neurite growth as PGE_2 [70]. The hypothesis was that chronic misoprostol treatment would reduce neurite length in differentiating Neuro-2A cells, similar to what was shown in differentiated cells from Tamiji's studies (2010) [70,71,95]. However, unlike that study, cells were differentiated in serum free medium instead of H7 (a PKC inhibitor), and treatment was applied over 3 days instead of one day [70,71,95]. Results from the current study show that chronic misoprostol treatment increased the length of primary neurites and branches in Neuro-2A cells after the first day of differentiation. The contradicting outcome is likely because H7 was used to induce differentiation. H7 is an inhibitor of PKC that is known to induce differentiation in Neuro-2A cells [151]. Other studies from the Crawford lab looked at neurites in NE-4C cells and found that PGE_2 increased neurite length, similar to the findings in the present study [18,42]. In the present study, serum starvation was chosen as a well established alternative method for differentiation of Neuro-2A cells [106]. Neurites were defined as primary for the longest extension, and all extensions attached to it were defined as branches.

Chronic misoprostol exposure significantly increased the length of primary neurites and branches compared to controls on days 2 and 3. This was associated with an increase in the level of Ser-133 pCREB, indicating increased activity and phosphorylation of CREB. Several studies have shown that CREB activation promotes

the growth of neurites [152–154] . Prostaglandin signalling through EP2 and EP4 receptors regulate the activity of PKA which phosphorylates CREB [8]. Unpublished research from the Crawford lab found that PGE_2 induces neurite elongation in differentiated NE-4C cells through a PKA dependant mechanism [42]. In cultured mouse Dorsal Root Ganglia (DRG) cells, PGE_2 treatment increased neurite length specifically through the EP2-cAMP-PKA pathway [155]. PGE_2 was also found to increase neuritogenesis in NSC-34 motor neuron-like cells via cAMP activity [156]. Therefore, I propose that chronic misoprostol exposure activated downstream EP2 and EP4 receptor pathways which led to increased CREB phosphorylation via PKA, promoting CREB mediated transcription of genes responsible for neurite elongation.

Neurite growth and morphology are valuable indicators of neurite dynamics which occur during development. Disturbing these processes could result in neurodevelopmental defects. One study did whole exome analysis of blood samples from 30 patients with ASD [157]. They found that out of 14 candidate genes with novel mutations, 8 of them regulated neurite growth in Neuro-2A cells [157]. The study suggests that neurite analysis in Neuro-2A cells is a powerful tool to study genes and chemicals which can alter the formation of neuronal networks [157]. Another study looked at neurite formation in induced pluripotent stem cell (iPSC) derived neurons from ASD patients with a mutation in *SHANK3*, a scaffold protein which connects membrane proteins (i.e. receptors) to the actin cytoskeleton, regulates synapses, and is highly correlated with ASD [158]. They found that during early neurodevelopment, the *SHANK3* cells had elongated primary neurites compared to controls [158]. Post-mortem ASD brains were found to have increased expression of *SLC25A12* in the prefrontal cortex [159].

Overexpression of *SLCA25A12* induced elongated neurites in mouse embryonic cortical neurons [159]. Data from the literature shows that altered neurite dynamics is a common pathology associated with ASD. The present finding of misoprostol induced neurite elongation suggests that misoprostol also affects neurite dynamics. Therefore, prenatal misoprostol exposure may disturb processes associated with neural network formation, a pathology common to many neurodevelopmental disorders.

4.7 - Misoprostol decreases the density of neurite branches in differentiating Neuro-2A cells

The development of neuronal networks is dependent on many factors, such as the length of neuronal extensions and arborization of the branches. To examine the effects of misoprostol on the arborization of neurites, extensions were classified as primary or branches. The length of primary neurites was compared to the length of branches by calculating their ratio for each day. Neurite length ratio did not change throughout differentiation and was unaffected by misoprostol treatment. This suggests that misoprostol affected neurite elongation the same way for primary and secondary neurites. The results showed that the quantity of branches unaffected by misoprostol. However, because misoprostol increased the length of neurites without affecting the number of branches, I decided to measure branch density by calculating the number of branches per 100 μm of primary neurite. Compared to vehicle, misoprostol treatment decreased the density of branches by day 3. Therefore, misoprostol treatment reduced the arborization of differentiated Neuro-2A cells. One study examined neurite growth of cerebellar primary Purkinje cell cultures from E17 and postnatal day 0 mice[160]. They found that embryonic Purkinje cells had greater axonal elongation, whereas postnatal Purkinje cells had greater branch arborization[160]. The different neurite characteristics of embryonic and postnatal Perkinje cells suggests that misoprostol treatment alters the morphology of Neuro-2A neurites towards an embryonic state, evident by the increase in neurite length and decrease in branch density [160]. This is supported by the current finding that misoprostol delayed the differentiation of NE-4C cells. However, differentiation progress was not measured for Neuro-2A cells in this study. Therefore,

prenatal misoprostol exposure may affect the arborization of neuronal cells, like Purkinje cells, altering the formation of neuronal networks which may contribute to developmental neuropathy.

ASD is associated with a variety of symptoms stemming from defects in neurodevelopmental processes. For example, microcephaly and macrocephaly were both found in ASD afflicted adolescents[161]. Brain volume is a function of neuronal migration and dendritic arborization [161]. It is well established that ASD neuropathy involves cerebellar deficiencies such as altered neural circuitry and Purkinje cell defects [162,163]. Cerebellar Purkinje cells were found to have decreased branch density in mice lacking neurotrophin receptor, a common model system for autism research [164]. Defects in neural circuitry may result in neuronal death due to decreased trophic signalling [164,165]. Research has shown that withdrawal of trophic factors *in-vitro* causes cerebellar Purkinje neuron death through similar processes seen in neurodegenerative disorders [166]. A study found that chemogenetic inhibition of Purkinje neuron activity induced social and repetitive ASD like behaviours [167]. Moreover, stimulation of Purkinje neurons rescued social impairment in a mouse model of ASD [167]. VPA has been shown to induce ASD behaviours in rats, and was associated with decreased Purkinje Cells and atypical cerebrocerebellar circuitry [168]. In the present study, misoprostol increased the level of pCREB and altered neurite morphology and branch density in differentiating Neuro-2A cells. Therefore, its plausible that prenatal misoprostol exposure could disrupt the arborization of neurons, like Purkinje cells, leading to neural circuitry defects and ASD like behaviours.

4.8 – Limitations

Several limitations of this study must be considered when interpreting the results. Firstly, two neuronal cell lines were used as experimental models: mouse neuroectodermal stem cells (NE-4C) and mouse neuroblastoma cells (Neuro-2A). Cell lines enable effective study of neuronal differentiation. However, they may not accurately represent the effects of misoprostol exposure on the cells *in-vivo*. For *in-vitro* studies, primary cell cultures would better predict the effects of misoprostol exposure on neuronal migration and differentiation. Furthermore, cells within a monoculture are limited in the extracellular signals that they receive. Prenatal development involves the release of trophic factors from many different cell types in order to guide cellular processes of proliferation, migration, differentiation, and apoptosis. Therefore, *in-vivo* studies in mice would provide the best representation for the effects of prenatal misoprostol exposure. In fact, the effect on cellular migration in the brain was already demonstrated by the Crawford lab with their PGE_2 injected mouse model [43]. Future studies in mice will be able to demonstrate if misoprostol has a similar effect.

The current results showed that misoprostol induced the expression of *Cdh2* and *NCAM*, and affected CREB protein level and phosphorylation. These measurements were made via qRT-PCR and Western Blot analyses. However, measurements of mRNA based gene transcription do not always correlate with protein translation, and vice versa. Other factors may regulate the level of specific proteins, such as ubiquitin degradation complexes, resulting in protein degradation. The prostaglandin signalling pathway imparts physiological changes by altering the expression of a variety of genes via the regulation of downstream transcription factors like CREB and β-Catenin.

Therefore, misoprostol may affect neurodevelopment through indirect pathways that were not measured in this study. A microarray study would be effective at determining the set of genes most affected by misoprostol exposure. Selected candidates should then be measured for transcription and translation in order to accurately describe the molecular response to misoprostol.

Lastly, research from the literature allows us to speculate about the pathways involved in misoprostol induced reduction of motility and delay in differentiation. However, the addition of kinase blockers, such as H-89 (PKA inhibitor), would enable us to determine causal relationships and better deduce the prostaglandin signalling cascades that are involved in misoprostol induced changes in cellular behaviour. Future research should expand on these findings by determining additional ways in which prostaglandin signalling can affect neurodevelopment.

4.9 - Conclusion

The research presented contributes novel findings of cellular processes that are vulnerable to misoprostol exposure. Misoprostol reduced neuronal migration in NE-4C stem cells in a dose dependant manner. It also delayed the differentiation of NE-4C cells, affecting neurosphere formation and morphology. I propose this was due to misoprostol induced changes in *Cdh2* and *NCAM* expression, disrupting early migration and aggregation, and suppressing the commitment of stem cells into neurons. Lastly, in differentiating Neuro-2A cells misoprostol increased the length of primary neurites and branches, most likely via EP2 and EP4 receptor mediated signalling which activated CREB. This led to a reduction in neurite branch density, which has implications for the effect of misoprostol on neuronal network formation.

The results of this study, along with previous research from the Crawford lab, demonstrated similar effects of PGE_2 and misoprostol. Differing outcomes were most likely due to different receptor affinities and sensitization tolerances that cause changes in downstream signalling. Findings from the literature support the results of this study by demonstrating similar involvement of CREB, *Cdh2*, and *NCAM* as regulators of cellular migration, differentiation, and neurite extension. Neurotoxicity studies with other teratogens mirrored the current findings with misoprostol, suggesting that prenatal exposure may cause similar postnatal cognitive behavioural deficits. The current study has demonstrated that misoprostol exposure affects molecular mechanisms involved in neurodevelopmental processes such as cellular migration, formation of neuronal circuitry, and cortical organization, all of which have been implicated in the etiology of ASD. Prenatal exposure to environmental factors, like misoprostol, could disturb

neurodevelopment during critical periods leading to adverse outcomes. Knowledge of the molecular mechanisms affected by misoprostol enable further understanding of its involvement in the occurrence of neurodevelopmental disorders. Future research should be done in animal studies to determine misoprostol's effects on brain physiology.

Bibliography

1. Harizi, H., Corcuff, J.-B. B. & Gualde, N. Arachidonic-acid-derived eicosanoids: roles in biology and immunopathology. *Trends Mol. Med.* **14**, 461–469 (2008).
2. El-Ansary, A. & Al-Ayadhi, L. Lipid mediators in plasma of autism spectrum disorders. *Lipids Health Dis.* (2012). doi:10.1186/1476-511X-11-160
3. Gunaydin, C. & Bilge, S. S. Effects of nonsteroidal anti-inflammatory drugs at the molecular level. *Eurasian Journal of Medicine* **50**, 116–121 (2018).
4. Yagami, T., Koma, H. & Yamamoto, Y. Pathophysiological Roles of Cyclooxygenases and Prostaglandins in the Central Nervous System. *Molecular Neurobiology* **53**, 4754–4771 (2016).
5. Yang, H. & Chen, C. Cyclooxygenase-2 in synaptic signaling. *Curr. Pharm. Des.* **14**, 1443–1451 (2008).
6. Das, U. N. Essential Fatty acids - a review. *Curr. Pharm. Biotechnol.* (2006). doi:10.2174/138920106779116856
7. Abramovitz, M. *et al.* The utilization of recombinant prostanoid receptors to determine the affinities and selectivities of prostaglandins and related analogs. *Biochim. Biophys. Acta - Mol. Cell Biol. Lipids* **1483**, 285–293 (2000).
8. O'Callaghan, G. & Houston, A. Prostaglandin E2 and the EP receptors in malignancy: possible therapeutic targets? *Br. J. Pharmacol.* **172**, 5239–50 (2015).
9. Sachs, D., Villarreal, C., Cunha, F., Parada, C. & Ferreira, S. The role of PKA and PKCepsilon pathways in prostaglandin E2-mediated hypernociception. *Br. J. Pharmacol.* **156**, 826–34 (2009).

10. Wong, C. T., Ahmad, E., Li, H. & Crawford, D. A. Prostaglandin E2 alters Wnt-dependent migration and proliferation in neuroectodermal stem cells: Implications for autism spectrum disorders. *Cell Commun. Signal.* (2014). doi:10.1186/1478-811X-12-19

11. Davidson, J. M., Wong, C. T., Li, H. & Crawford, D. A. Prostaglandin E2 facilitates subcellular translocation of the EP4 receptor in neuroectodermal NE-4C stem cells. *Biochem. Biophys. reports* **7**, 173–179 (2016).

12. Wong, C. & Crawford, D. A. Lipid Signalling in the Pathology of Autism Spectrum Disorders. in *Comprehensive Guide to Autism* 1259–1283 (Springer New York, 2014). doi:10.1007/978-1-4614-4788-7_68

13. Landeira, B. S. *et al.* Activity-Independent Effects of CREB on Neuronal Survival and Differentiation during Mouse Cerebral Cortex Development. *Cereb. Cortex* (2016). doi:10.1093/cercor/bhw387

14. Fujino, H., Salvi, S. & Regan, J. W. Differential Regulation of Phosphorylation of the cAMP Response Element-Binding Protein after Activation of EP 2 and EP 4 Prostanoid Receptors by Prostaglandin E 2. *Mol. Pharmacol.* (2005). doi:10.1124/mol.105.011833.to

15. Neeb, L. *et al.* IL-1β stimulates COX-2 dependent PGE2 synthesis and CGRP release in rat trigeminal ganglia cells. *PLoS One* **6**, e17360 (2011).

16. Kawahara, K., Hohjoh, H., Inazumi, T., Tsuchiya, S. & Sugimoto, Y. Prostaglandin E2-induced inflammation: Relevance of prostaglandin E receptors. *Biochim. Biophys. Acta - Mol. Cell Biol. Lipids* **1851**, 414–421 (2015).

17. Sang, N., Zhang, J., Marcheselli, V., Bazan, N. G. & Chen, C. Postsynaptically

synthesized prostaglandin E2 (PGE2) modulates hippocampal synaptic transmission via a presynaptic PGE2 EP2 receptor. *J. Neurosci.* **25**, 9858–9870 (2005).

18. Davidson, J. M., Wong, C. T., Rai-Bhogal, R., Li, H. & Crawford, D. A. Prostaglandin E2 elevates calcium in differentiated neuroectodermal stem cells. *Mol. Cell. Neurosci.* (2016). doi:10.1016/j.mcn.2016.03.010
19. Akaneya, Y. & Tsumoto, T. Bidirectional trafficking of prostaglandin E2 receptors involved in long-term potentiation in visual cortex. *J. Neurosci.* **26**, 10209–10221 (2006).
20. Wong, C. T., Bestard-Lorigados, I. & Crawford, D. A. Autism-related behaviors in the cyclooxygenase-2-deficient mouse model. *Genes, Brain Behav.* e12506 (2018). doi:10.1111/gbb.12506
21. Rai-Bhogal, R., Ahmad, E., Li, H. & Crawford, D. A. Microarray analysis of gene expression in the cyclooxygenase knockout mice - a connection to autism spectrum disorder. *Eur. J. Neurosci.* **47**, 750–766 (2018).
22. Chen, C., Bazan, N. G. & Pge, E. Endogenous PGE 2 Regulates Membrane Excitability and Synaptic Transmission in Hippocampal CA1 Pyramidal Neurons. *J. Neurophysiol.* (2005). doi:10.1152/jn.00696.2004.
23. Dean, S. L. *et al.* Prostaglandin E2 stimulates estradiol synthesis in the cerebellum postnatally with associated effects on purkinje neuron dendritic arbor and electrophysiological properties. *Endocrinology* (2012). doi:10.1210/en.2012-1350
24. Wong, C. T. *et al.* Prostaglandin E2 promotes neural proliferation and

differentiation and regulates Wnt target gene expression. *J. Neurosci. Res.* (2016). doi:10.1002/jnr.23759

25. Kawano, T. *et al.* Prostaglandin E2 EP1 receptors: downstream effectors of COX-2 neurotoxicity. *Nat. Med.* **12**, 225–229 (2006).
26. Ricciotti, E. & FitzGerald, G. A. Prostaglandins and inflammation. *Arterioscler. Thromb. Vasc. Biol.* **31**, 986–1000 (2011).
27. Lin, C.-R. *et al.* Prostaglandin E 2 Receptor EP4 Contributes to Inflammatory Pain Hypersensitivity. (2006). doi:10.1124/jpet.106.105569
28. Niringiyumukiza, J. D., Cai, H. & Xiang, W. Prostaglandin E2 involvement in mammalian female fertility: ovulation, fertilization, embryo development and early implantation. *Reprod. Biol. Endocrinol.* **16**, 43 (2018).
29. Bauer, A. Z., Kriebel, D., Herbert, M. R., Bornehag, C. G. & Swan, S. H. Prenatal paracetamol exposure and child neurodevelopment: A review. *Hormones and Behavior* (2018). doi:10.1016/j.yhbeh.2018.01.003
30. Rai-Bhogal, R. *et al.* Maternal exposure to prostaglandin E2modifies expression of Wnt genes in mouse brain – An autism connection. *Biochem. Biophys. Reports* (2018). doi:10.1016/j.bbrep.2018.03.012
31. James, S. J. *et al.* Metabolic biomarkers of increased oxidative stress and impaired methylation capacity in children with autism. *Am. J. Clin. Nutr.* **80**, 1611–1617 (2004).
32. Majewska, M. D. *et al.* Marked elevation of adrenal steroids, especially androgens, in saliva of prepubertal autistic children. *Eur. Child Adolesc. Psychiatry* **23**, 485–498 (2014).

33. Komiya, Y. & Habas, R. Wnt signal transduction pathways. *Organogenesis* (2008). doi:10.4161/org.4.2.5851

34. Zhang, Y., Yuan, X., Wang, Z. & Li, R. The canonical Wnt signaling pathway in autism. *CNS Neurol. Disord. Drug Targets* (2014). doi:10.2174/18715273126661312231141 49

35. Kennedy, D. P., Redcay, E. & Courchesne, E. Failing to deactivate: Resting functional abnormalities in autism. *Proc. Natl. Acad. Sci. U. S. A.* **103**, 8275–8280 (2006).

36. Robertson, C. E., Ratai, E. M. & Kanwisher, N. Reduced GABAergic Action in the Autistic Brain. *Curr. Biol.* **26**, 80–85 (2016).

37. Khazaeipool, Z., Wiederman, M. & Inoue, W. Prostaglandin E2 depresses GABA release onto parvocellular neuroendocrine neurones in the paraventricular nucleus of the hypothalamus via presynaptic receptors. *J. Neuroendocrinol.* **30**, e12638 (2018).

38. Yang, G., Dong, W.-H., Hu, C.-L. & Mei, Y.-A. PGE_2 Modulates $GABA_A$ Receptors via an EP1 Receptor-Mediated Signaling Pathway. *Cell. Physiol. Biochem.* **36**, 1699–1711 (2015).

39. Saliba, S. W. *et al.* AM404, paracetamol metabolite, prevents prostaglandin synthesis in activated microglia by inhibiting COX activity. *J. Neuroinflammation* **14**, 246 (2017).

40. Liew, Z., Ritz, B., Virk, J. & Olsen, J. Maternal use of acetaminophen during pregnancy and risk of autism spectrum disorders in childhood: A Danish national birth cohort study. *Autism Res.* **9**, 951–958 (2016).

41. Bagasra, O., Golkar, Z., Garcia, M., Rice, L. N. & Pace, D. G. Role of perfumes in pathogenesis of Autism. *Med. Hypotheses* **80**, 795–803 (2013).

42. Kissoondoyal, A. & Crawford, D. A. Prostaglandin E2 regulates phosphorylation of Spinophilin and growth cone morphology via PKA. in Poster (Society for Neuroscience, 2018).

43. Wong, C. T., Bestard-Lorigados, I. & Crawford, D. A. *Prenatal exposure to prostaglandin E2 leads to abnormal cell density and migration in the mouse brain*.

44. Angers, S. & Moon, R. T. Proximal events in Wnt signal transduction. (2009). doi:10.1038/nrm2717

45. Wong, C. T., Bestard-Lorigados, I. & Crawford, D. A. Maternal exposure to prostaglandin E2 leads to autism-like behaviours in C57bl/6 mouse offspring. *Genes, Brain Behav.* **In Review**, 32

46. Matson, J. L., Rieske, R. D. & Williams, L. W. The relationship between autism spectrum disorders and attention-deficit/hyperactivity disorder: An overview. *Res. Dev. Disabil.* **34**, 2475–2484 (2013).

47. Wong, C. T., Smith, J. & Crawford, D. A. *Abnormal microglial density and morphology in mice with defective cyclooxygenase-2/prostaglandin E2 signalling*.

48. Eyo, U. B. & Wu, L. J. Bidirectional microglia-neuron communication in the healthy brain. *Neural Plasticity* **2013**, (2013).

49. Smith, P. L. P., Hagberg, H., Naylor, A. S. & Mallard, C. Neonatal Peripheral Immune Challenge Activates Microglia and Inhibits Neurogenesis in the Developing Murine Hippocampus. *Dev. Neurosci.* **36**, 119–131 (2014).

50. Appel, J. R. *et al.* Increased microglial activity, impaired adult hippocampal

neurogenesis, and depressive-like behavior in microglial VPS35-depleted mice. *J. Neurosci.* **38**, 5949–5968 (2018).

51. Laine, L. Gastrointestinal effects of NSAIDs and coxibs. *Journal of Pain and Symptom Management* **25**, 32–40 (2003).

52. Gonzalez, C. H. *et al.* Limb deficiency with or without Mobius sequence in seven Brazilian children associated with misoprostol use in the first trimester of pregnancy. *Am. J. Med. Genet.* (1993). doi:10.1002/ajmg.1320470113

53. Escumalha, M., Gouveia, C., Cunha, M., Vale, F. & Machado, M. C. Neonatal morbidity and outcome of live born premature babies after attempted illegal abortion with misoprostol. *Pediatr Nurs* (2005).

54. Vauzelle, C., Beghin, D., Cournot, M. P. & Elefant, E. Birth defects after exposure to misoprostol in the first trimester of pregnancy: Prospective follow-up study. *Reprod. Toxicol.* **36**, 98–103 (2013).

55. Ornoy, A., Weinstein- Fudim, L. & Ergaz, Z. Genetic Syndromes, Maternal Diseases and Antenatal Factors Associated with Autism Spectrum Disorders (ASD). *Front. Neurosci.* (2016). doi:10.3389/fnins.2016.00316

56. Auffret, M. *et al.* Misoprostol exposure during the first trimester of pregnancy: Is the malformation risk varying depending on the indication? *Eur. J. Obstet. Gynecol.* **207**, 188–192 (2016).

57. *Safe Abortion*. *Safe Abortion: Technical and Policy Guidance for Health Systems* (World Health Organization, 2012).

58. Gemzell-Danielsson, K., Bygdeman, M. & Aronsson, A. Studies on uterine contractility following mifepristone and various routes of misoprostol.

Contraception **74**, 31–35 (2006).

59. Zamberlin, N., Romero, M. & Ramos, S. Latin American women's experiences with medical abortion in settings where abortion is legally restricted. *Reprod. Health* **9**, 34 (2012).

60. Ngoc, N. T. N. *et al.* Comparing two early medical abortion regimens: mifepristone+misoprostol vs. misoprostol alone. *Contraception* **83**, 410–417 (2011).

61. Dahiya, K., Ahuja, K., Dhingra, A., Duhan, N. & Nanda, S. Efficacy and safety of mifepristone and buccal misoprostol versus buccal misoprostol alone for medical abortion. *Arch. Gynecol. Obstet.* **285**, 1055–1058 (2012).

62. *EUROCAT Guide 1.4 Section 3.2 3.2 Minor Anomalies and other conditions for Exclusion*.

63. Bandim, J. M., Ventura, L. O., Miller, M. T., Almeida, H. C. & Costa, A. E. Autism and Mobius sequence: an exploratory study of children in northeastern Brazil. *Arq. Neuropsiquiatr.* (2003). doi:10.1590/S0004-282X2003000200004

64. Pirmez, R., Freitas, M. E. T., Gasparetto, E. L. & Araújo, A. P. Q. C. Moebius syndrome and holoprosencephaly following exposure to misoprostol. *Pediatr. Neurol.* **43**, 371–373 (2010).

65. Rice, D. & Barone, S. Critical periods of vulnerability for the developing nervous system: Evidence from humans and animal models. *Environ. Health Perspect.* **108**, 511–533 (2000).

66. Marret, H. *et al.* Overview and expert assessment of off-label use of misoprostol in obstetrics and gynaecology: review and report by the Collège national des

gynécologues obstétriciens français. *Eur. J. Obstet. Gynecol. Reprod. Biol.* **187**, 80–84 (2015).

67. Ganatra, B. *et al.* Global, regional, and subregional classification of abortions by safety, 2010-14: estimates from a Bayesian hierarchical model. *Lancet (London, England)* **390**, 2372–2381 (2017).

68. Zordo, S. De & Zordo, S. De. The biomedicalisation of illegal abortion: the double life of misoprostol in Brazil. *História, Ciências, Saúde-Manguinhos* **23**, 19–36 (2016).

69. Turner, J. V, Agatonovic-Kustrn, S. & Ward, H. Off-label use of misoprostol in gynaecology. *Facts, views Vis. ObGyn* **7**, 261–264 (2015).

70. Tamiji, J. & Crawford, D. A. Prostaglandin E2and misoprostol induce neurite retraction in Neuro-2a cells. *Biochem. Biophys. Res. Commun.* (2010). doi:10.1016/j.bbrc.2010.06.098

71. Tamiji, J. & Crawford, D. A. Misoprostol elevates intracellular calcium in Neuro-2a cells via protein kinase A. *Biochem. Biophys. Res. Commun.* (2010). doi:10.1016/j.bbrc.2010.07.112

72. Koenig, C. M., Walker, C. K., Qi, L., Pessah, I. N. & Berman, R. F. Lack of Evidence for Neonatal Misoprostol Neurodevelopmental Toxicity in C57BL6/J Mice. *PLoS One* **7**, e38911 (2012).

73. Audet, M. *et al.* Crystal structure of misoprostol bound to the labor inducer prostaglandin E 2 receptor. *Nat. Chem. Biol.* **15**, 11–17 (2019).

74. Ungrin, M. D. *et al.* Key structural features of prostaglandin E2 and prostanoid analogs involved in binding and activation of the human EP1 prostanoid receptor.

Mol. Pharmacol. **59**, 1446–1456 (2001).

75. Schlett, K. & Madarász, E. Retinoic acid induced neural differentiation in a neuroectodermal cell line immortalized by p53 deficiency. *J. Neurosci. Res.* **47**, 405–415 (1997).

76. Krull, C. E. Segmental organization of neural crest migration. *Mech. Dev.* **105**, 37–45 (2001).

77. Mori, H. *et al.* Effect of neurosphere size on the growth rate of human neural stem/progenitor cells. *J. Neurosci. Res.* (2006). doi:10.1002/jnr.21082

78. Vangipuram, S. D., Grever, W. E., Parker, G. C. & Lyman, W. D. Ethanol increases fetal human neurosphere size and alters adhesion molecule gene expression. *Alcohol. Clin. Exp. Res.* (2008). doi:10.1111/j.1530-0277.2007.00568.x

79. Hayon, Y., Dashevsky, O., Shai, E., Varon, D. & Leker, R. R. Platelet microparticles promote neural stem cell proliferation, survival and differentiation. *J. Mol. Neurosci.* (2012). doi:10.1007/s12031-012-9711-y

80. Prodromidou, K., Papastefanaki, F., Sklaviadis, T. & Matsas, R. Functional Cross-Talk Between the Cellular Prion Protein and the Neural Cell Adhesion Molecule is Critical for Neuronal Differentiation of Neural Stem/Precursor Cells. *Stem Cells* **32**, 1674–1687 (2014).

81. Varga, B. V *et al.* Generation of diverse neuronal subtypes in cloned populations of stem-like cells. *BMC Dev. Biol.* **8**, 89 (2008).

82. Kwon, C. *et al.* Notch post-translationally regulates β-catenin protein in stem and progenitor cells. *Nat. Cell Biol.* (2011). doi:10.1038/ncb2313

83. Takeichi, M. The cadherins: cell-cell adhesion molecules controlling animal morphogenesis. *Development* (1988). doi:10.1016/j.pain.2009.04.011.The

84. Cremer, H. & Durbec, P. Revisiting the Function of PSA-NCAM in the Nervous System. *Mol. Neurobiol.* **24**, 053–064 (2001).

85. Takeichi, M. & Abe, K. Synaptic contact dynamics controlled by cadherin and catenins. *Trends in Cell Biology* **15**, 216–221 (2005).

86. Yamagata, M., Duan, X. & Sanes, J. R. Cadherins Interact With Synaptic Organizers to Promote Synaptic Differentiation. *Front. Mol. Neurosci.* **11**, 142 (2018).

87. Angata, K. *et al.* Polysialic acid-directed migration and differentiation of neural precursors are essential for mouse brain development. *Mol. Cell. Biol.* **27**, 6659–68 (2007).

88. Seidenfaden, R., Krauter, A. & Hildebrandt, H. The neural cell adhesion molecule NCAM regulates neuritogenesis by multiple mechanisms of interaction. *Neurochem. Int.* **49**, 1–11 (2006).

89. Maestrini, E. *et al.* High-density SNP association study and copy number variation analysis of the AUTS1 and AUTS5 loci implicate the IMMP2L-DOCK4 gene region in autism susceptibility. *Mol. Psychiatry* **15**, 954–68 (2010).

90. Xiao, Y. *et al.* The atypical guanine nucleotide exchange factor Dock4 regulates neurite differentiation through modulation of Rac1 GTPase and actin dynamics. *J. Biol. Chem.* **288**, 20034–20045 (2013).

91. Villarroel-Campos, D. & Gonzalez-Billault, C. The MAP1B case: An old MAP that is new again. *Dev. Neurobiol.* **74**, 953–971 (2014).

92. Ma, X. X. *et al.* PiT2 regulates neuronal outgrowth through interaction with microtubule-associated protein. *Sci. Rep.* **7**, 17850 (2017).

93. Wong, C. T., Wais, J. & Crawford, D. A. Prenatal exposure to common environmental factors affects brain lipids and increases risk of developing autism spectrum disorders. *European Journal of Neuroscience* **42**, 2742–2760 (2015).

94. Tamiji, J. & Crawford, D. A. The Neurobiology of Lipid Metabolism in Autism Spectrum Disorders. *Neurosignals* **18**, 98–112 (2010).

95. Tamiji, J. EFFECTS OF MISOPROSTOL AND PROSTAGLANDIN E2 ON NEURO-2A CELLS: A POSSIBLE LINK TO AUTISM. (York University, 2010).

96. Longair, M. H., Baker, D. A. & Armstrong, J. D. Simple Neurite Tracer: open source software for reconstruction, visualization and analysis of neuronal processes. *Bioinformatics* **27**, 2453–2454 (2011).

97. Schindelin, J. *et al.* Fiji: an open-source platform for biological-image analysis. *Nat. Methods* **9**, 676–682 (2012).

98. Schindelin, J., Rueden, C. T., Hiner, M. C. & Eliceiri, K. W. The ImageJ ecosystem: An open platform for biomedical image analysis. *Molecular Reproduction and Development* **82**, 518–529 (2015).

99. Miyamoto, Y., Sakane, F. & Hashimoto, K. N-cadherin-based adherens junction regulates the maintenance, proliferation, and differentiation of neural progenitor cells during development. *Cell Adh. Migr.* **9**, 183–92 (2015).

100. Amoureux, M.-C., Cunningham, B. A., Edelman, G. M. & Crossin, K. L. *N-CAM Binding Inhibits the Proliferation of Hippocampal Progenitor Cells and Promotes Their Differentiation to a Neuronal Phenotype*. (2000).

101. Carnahan, M. N. *et al.* Identification of cell-specific patterns of reference gene stability in quantitative reverse-transcriptase polymerase chain reaction studies of embryonic, placental and neural stem models of prenatal ethanol exposure. *Alcohol* **47**, 109–120 (2013).

102. Karge, W. H., Schaefer, E. J. & Ordovas, J. M. Quantification of mRNA by polymerase chain reaction (PCR) using an internal standard and a nonradioactive detection method. *Methods in molecular biology (Clifton, N.J.)* **110**, 43–61 (1998).

103. Zhang, C. *et al.* Effects of dimethyl sulfoxide on the morphology and viability of primary cultured neurons and astrocytes. *Brain Res. Bull.* (2017). doi:10.1016/j.brainresbull.2016.11.004

104. Chen, Y. *et al.* NS21: Re-defined and modified supplement B27 for neuronal cultures. *J. Neurosci. Methods* (2008). doi:10.1016/j.jneumeth.2008.03.013

105. Yan, Y. *et al.* Efficient and rapid derivation of primitive neural stem cells and generation of brain subtype neurons from human pluripotent stem cells. *Stem Cells Transl. Med.* **2**, 862–70 (2013).

106. Evangelopoulos, M. E., Weis, J. & Krüttgen, A. Signalling pathways leading to neuroblastoma differentiation after serum withdrawal: HDL blocks neuroblastoma differentiation by inhibition of EGFR. *Oncogene* (2005). doi:10.1038/sj.onc.1208494

107. van Rossum, G. & de Boer, J. Interactively testing remote servers using the Python programming language. *CWI Q.* (1991).

108. Mckinney, W. *Data Structures for Statistical Computing in Python*. *PROC. OF THE 9th PYTHON IN SCIENCE CONF* (2010).

109. Seabold, S. & Perktold, J. *Statsmodels: Econometric and Statistical Modeling with Python*. *PROC. OF THE 9th PYTHON IN SCIENCE CONF* (2010).

110. Oliphant, T. E. (19. .-. . . .). *Guide to NumPy*. (Continuum Press, 2015).

111. Hunter, J. D. Matplotlib: A 2D Graphics Environment. *Comput. Sci. Eng.* **9**, 90–95 (2007).

112. Tukey, J. W. (John W. *The collected works of John W. Tukey.* (Chapman & Hall, 1990).

113. Holm, S. A Simple Sequentially Rejective Multiple Test Procedure. *Scand. J. Stat.* (1979). doi:10.2307/4615733

114. Ngo, T. D., Park, M. H., Shakur, H. & Free, C. Comparative effectiveness, safety and acceptability of medical abortion at home and in a clinic: a systematic review. *Bull. World Health Organ.* **89**, 360–370 (2011).

115. Kriegstein, A. R. & Noctor, S. C. Patterns of neuronal migration in the embryonic cortex. *Trends Neurosci.* **27**, 392–399 (2004).

116. Huang, Z. Molecular regulation of neuronal migration during neocortical development. *Mol. Cell. Neurosci.* **42**, 11–22 (2009).

117. Madarász, E. Diversity of Neural Stem/Progenitor Populations: Varieties by Age, Regional Origin and Environment. in *Neural Stem Cells* (ed. Bonfanti, L.) (IntechOpen, 2013). doi:10.5772/55678

118. Gnanapavan, S. & Giovannoni, G. Neural cell adhesion molecules in brain plasticity and disease. *Multiple Sclerosis and Related Disorders* (2013). doi:10.1016/j.msard.2012.08.002

119. Chklovskii, D. B. Synaptic connectivity and neuronal morphology: Two sides of

the same coin. *Neuron* (2004). doi:10.1016/j.neuron.2004.08.012

120. An, J. Y. *et al.* Towards a molecular characterization of autism spectrum disorders: an exome sequencing and systems approach. *Transl. Psychiatry* **4**, e394–e394 (2014).
121. Griesi-Oliveira, K. *et al.* Actin cytoskeleton dynamics in stem cells from autistic individuals. *Sci. Rep.* **8**, (2018).
122. Wegiel, J. *et al.* Stereological study of the neuronal number and volume of 38 brain subdivisions of subjects diagnosed with autism reveals significant alterations restricted to the striatum, amygdala and cerebellum. *Acta Neuropathol. Commun.* **2**, (2014).
123. Steven, A. & Seliger, B. Control of CREB expression in tumors: from molecular mechanisms and signal transduction pathways to therapeutic target. *Oncotarget* **7**, 35454–65 (2016).
124. Dworkin, S. & Mantamadiotis, T. Targeting CREB signalling in neurogenesis. *Expert Opinion on Therapeutic Targets* **14**, 869–879 (2010).
125. Purves, D. *et al. Neuroscience 3rd Ed*. *Neuroscience* (2004). doi:978-0878937257
126. Silva, A. J., Kogan, J. H., Frankland, P. W. & Kida, S. CREB AND MEMORY. *Annu. Rev. Neurosci.* **21**, 127–148 (1998).
127. Saura, C. A. & Valero, J. The role of CREB signaling in Alzheimer's disease and other cognitive disorders. *Rev. Neurosci.* **22**, 153–169 (2011).
128. Pugazhenthi, S., Wang, M., Pham, S., Sze, C. I. & Eckman, C. B. Downregulation of CREB expression in Alzheimer's brain and in Aβ-treated rat hippocampal neurons. *Mol. Neurodegener.* **6**, (2011).

129. Díaz-Ruiz, C. *et al.* Regulation of neural migration by the CREB/CREM transcription factors and altered Dab1 levels in CREB/CREM mutants. *Mol. Cell. Neurosci.* **39**, 519–528 (2008).

130. Dworkin, S. *et al.* CREB activity modulates neural cell proliferation, midbrain-hindbrain organization and patterning in zebrafish. *Dev. Biol.* **307**, 127–141 (2007).

131. Dworkin, S. *et al.* cAMP Response Element Binding Protein Is Required for Mouse Neural Progenitor Cell Survival and Expansion. *Stem Cells* **27**, 1347–1357 (2009).

132. Alimperti, S. & Andreadis, S. T. CDH2 and CDH11 act as regulators of stem cell fate decisions. *Stem Cell Research* **14**, 270–282 (2015).

133. Su, H. *et al.* Immediate expression of Cdh2 is essential for efficient neural differentiation of mouse induced pluripotent stem cells. *Stem Cell Res.* **10**, 338–348 (2013).

134. Chen, J.-H., Lee, D.-C., Chen, M.-S., Ko, Y.-C. & Chiu, I.-M. Inhibition of Neurosphere Formation in Neural Stem/Progenitor Cells by Acrylamide. *Cell Transplant.* **24**, 779–796 (2015).

135. Minamino, Y., Ohnishi, Y., Kakudo, K. & Nozaki, M. Isolation and propagation of neural crest stem cells from mouse embryonic stem cells via cranial neurospheres. *Stem Cells Dev.* **24**, 172–181 (2015).

136. Sipahi, R. & Zupanc, G. K. H. Stochastic cellular automata model of neurosphere growth: Roles of proliferative potential, contact inhibition, cell death, and phagocytosis. *J. Theor. Biol.* **445**, 151–165 (2018).

137. Shaker, M. R., Kim, J. Y., Kim, H. & Sun, W. Identification and characterization of secondary neural tube-derived embryonic neural stem cells in vitro. *Stem Cells Dev.* **24**, 1171–1181 (2015).

138. Ruijtenberg, S. & van den Heuvel, S. Coordinating cell proliferation and differentiation: Antagonism between cell cycle regulators and cell type-specific gene expression. *Cell Cycle* **15**, 196–212 (2016).

139. Calegari, F., Haubensak, W., Haffher, C. & Huttner, W. B. Selective lengthening of the cell cycle in the neurogenic subpopulation of neural progenitor cells during mouse brain development. *J. Neurosci.* **25**, 6533–6538 (2005).

140. Lange, C., Huttner, W. B. & Calegari, F. Cdk4/CyclinD1 Overexpression in Neural Stem Cells Shortens G1, Delays Neurogenesis, and Promotes the Generation and Expansion of Basal Progenitors. *Cell Stem Cell* **5**, 320–331 (2009).

141. Bosetti, F., Weerasinghe, G. R., Rosenberger, T. A. & Rapoport, S. I. Valproic acid down-regulates the conversion of arachidonic acid to eicosanoids via cyclooxygenase-1 and -2 in rat brain. *J. Neurochem.* **85**, 690–696 (2003).

142. Reynolds, J. D. *et al.* Ethanol-induced changes in prostaglandin E concentration in the intact cerebral cortex of preterm and near-term fetal sheep. *Alcohol. Clin. Exp. Res.* **21**, 997–1004 (1997).

143. Noguchi, T., Shimazawa, R., Nagasawa, K. & Hashimoto, Y. Thalidomide and its analogues as cyclooxygenase inhibitors. *Bioorganic Med. Chem. Lett.* **12**, 1043–1046 (2002).

144. Miranda, C. C. *et al.* A scale out approach towards neural induction of human induced pluripotent stem cells for neurodevelopmental toxicity studies. *Toxicol.*

Lett. **294**, 51–60 (2018).

145. Zhang, S. C., Wernig, M., Duncan, I. D., Brüstle, O. & Thomson, J. A. In vitro differentiation of transplantable neural precursors from human embryonic stem cells. *Nat. Biotechnol.* **19**, 1129–1133 (2001).
146. Dufour-Rainfray, D. *et al.* Behavior and serotonergic disorders in rats exposed prenatally to valproate: A model for autism. *Neurosci. Lett.* **470**, 55–59 (2010).
147. Rodier, P. M., Ingram, J. L., Tisdale, B., Nelson, S. & Romano, J. Embryological origin for autism: Developmental anomalies of the cranial nerve motor nuclei. *J. Comp. Neurol.* **370**, 247–261 (1996).
148. Strömland, K., Nordin, V., Miller, M., Akerström, B. & Gillberg, C. AUTISM IN THALIDOMIDE EMBRYOPATHY: A POPULATION STUDY. *Dev. Med. Child Neurol.* **36**, 351–356 (1994).
149. Landgren, M., Svensson, L., Stromland, K. & Andersson Gronlund, M. Prenatal Alcohol Exposure and Neurodevelopmental Disorders in Children Adopted From Eastern Europe. *Pediatrics* (2010). doi:10.1542/peds.2009-0712
150. Harris, S. R., MacKay, L. L. J. & Osborn, J. A. Autistic Behaviors in Offspring of Mothers Abusing Alcohol and Other Drugs: A Series of Case Reports. *Alcohol. Clin. Exp. Res.* (1995). doi:10.1111/j.1530-0277.1995.tb01564.x
151. Miñana, M. D., Felipo, V. & Grisolia, S. Inhibition of protein kinase C induces differentiation of neuroblastoma cells. *FEBS Lett.* **255**, 184–186 (1989).
152. Jessen, U. *et al.* The transcription factors CREB and c-Fos play key roles in NCAM-mediated neuritogenesis in PC12-E2 cells. *J. Neurochem.* **79**, 1149–1160 (2001).

153. Ghil, S.-H., Kim, B.-J., Lee, Y.-D. & Suh-Kim, H. Neurite Outgrowth Induced by Cyclic AMP Can Be Modulated by the α Subunit of Go. *J. Neurochem.* **74**, 151–158 (2001).

154. Shmueli, O. DCX in PC12 cells: CREB-mediated transcription and neurite outgrowth. *Hum. Mol. Genet.* **10**, 1061–1070 (2001).

155. Hiruma, H. *et al.* Prostaglandin E(2) enhances axonal transport and neuritogenesis in cultured mouse dorsal root ganglion neurons. *Neuroscience* **100**, (2000).

156. Nango, H. *et al.* Prostaglandin E2 facilitates neurite outgrowth in a motor neuron-like cell line, NSC-34. *J. Pharmacol. Sci.* **135**, 64–71 (2017).

157. Hashimoto, R. *et al.* Whole-exome sequencing and neurite outgrowth analysis in autism spectrum disorder. *J. Hum. Genet.* **61**, 199–206 (2016).

158. Kathuria, A. *et al.* Stem cell-derived neurons from autistic individuals with SHANK3 mutation show morphogenetic abnormalities during early development. *Mol. Psychiatry* **23**, 735–746 (2018).

159. Lepagnol-Bestel, A. M. *et al.* SLC25A12 expression is associated with neurite outgrowth and is upregulated in the prefrontal cortex of autistic subjects. *Mol. Psychiatry* **13**, 385–397 (2008).

160. de Luca, A. *et al.* Distinct modes of neuritic growth in purkinje neurons at different developmental stages: axonal morphogenesis and cellular regulatory mechanisms. *PLoS One* **4**, e6848 (2009).

161. Fombonne, E., Rogé, B., Claverie, J., Courty, S. & Frémolle, J. Microcephaly and macrocephaly in autism. *J. Autism Dev. Disord.* **29**, 113–9 (1999).

162. Skefos, J. *et al.* Regional alterations in Purkinje cell density in patients with autism. *PLoS One* **9**, (2014).

163. Bruchhage, M. M. K., Bucci, M. P. & Becker, E. B. E. Cerebellar involvement in autism and ADHD. in *Handbook of Clinical Neurology* **155**, 61–72 (2018).

164. Lotta, L. T., Conrad, K., Cory-Slechta, D. & Schor, N. F. Cerebellar purkinje cell p75 neurotrophin receptor and autistic behavior. *Transl. Psychiatry* **4**, (2014).

165. Lo, D. C. Neurotrophic factors and synaptic plasticity. *Neuron* **15**, 979–981 (1995).

166. Florez-McClure, M. L. *et al.* The p75 neurotrophin receptor can induce autophagy and death of cerebellar Purkinje neurons. *J. Neurosci.* **24**, 4498–4509 (2004).

167. Stoodley, C. J. *et al.* Altered cerebellar connectivity in autism and cerebellar-mediated rescue of autism-related behaviors in mice. *Nat. Neurosci.* **20**, 1744–1751 (2017).

168. Spisák, T. *et al.* Purkinje cell number-correlated cerebrocerebellar circuit anomaly in the valproate model of autism. *Sci. Rep.* **9**, 1–15 (2019).

Appendix A: Copyright Permission

JOHN WILEY AND SONS LICENSE TERMS AND CONDITIONS

Nov 24, 2019

This Agreement between 252 brighton ave ("You") and John Wiley and Sons ("John Wiley and Sons") consists of your license details and the terms and conditions provided by John Wiley and Sons and Copyright Clearance Center.

License Number	4715700108023
License date	Nov 24, 2019
Licensed Content Publisher	John Wiley and Sons
Licensed Content Publication	British Journal of Pharmacology
Licensed Content Title	Prostaglandin E2 and the EP receptors in malignancy: possible therapeutic targets?
Licensed Content Author	G O'Callaghan, A Houston
Licensed Content Date	Oct 26, 2015
Licensed Content Pages	10
Type of Use	Dissertation/Thesis
Requestor type	University/Academic
Format	Print and electronic
Portion	Figure/table
Number of figures/tables	1
Original Wiley figure/table number(s)	Figure 2
Will you be translating?	No
Title of your thesis / dissertation	THE EFFECT OF MISOPROSTOL ON NEURONAL STEM CELL MIGRATION AND DIFFERENTIATION
Expected completion date	Jan 2020
Expected size (number of pages)	120
Requestor Location	Denis Adigamov [redacted] [redacted] Attn: Denis Adigamov
Publisher Tax ID	EU826007151
Total	**0.00 CAD**
Terms and Conditions	

TERMS AND CONDITIONS

This copyrighted material is owned by or exclusively licensed to John Wiley & Sons, Inc. or one of its group companies (each a"Wiley Company") or handled on behalf of a society with which a Wiley Company has exclusive publishing rights in relation to a particular work (collectively "WILEY"). By clicking "accept" in connection with completing this licensing transaction, you agree that the following terms and conditions apply to this transaction (along with the billing and payment terms and conditions established by the Copyright Clearance Center Inc., ("CCC's Billing and Payment terms and conditions"), at the time that you opened your RightsLink account (these are available at any time at http://myaccount.copyright.com).

Terms and Conditions

- The materials you have requested permission to reproduce or reuse (the "Wiley Materials") are protected by copyright.

- You are hereby granted a personal, non-exclusive, non-sub licensable (on a stand-alone basis), non-transferable, worldwide, limited license to reproduce the Wiley Materials for the purpose specified in the licensing process. This license, **and any CONTENT (PDF or image file) purchased as part of your order,** is for a one-time use only and limited to any maximum distribution number specified in the license. The first instance of republication or reuse granted by this license must be completed within two years of the date of the grant of this license (although copies prepared before the end date may be distributed thereafter). The Wiley Materials shall not be used in any other manner or for any other purpose, beyond what is granted in the license. Permission is granted subject to an appropriate acknowledgement given to the author, title of the material/book/journal and the publisher. You shall also duplicate the copyright notice that appears in the Wiley publication in your use of the Wiley Material. Permission is also granted on the understanding that nowhere in the text is a previously published source acknowledged for all or part of this Wiley Material. Any third party content is expressly excluded from this permission.

- With respect to the Wiley Materials, all rights are reserved. Except as expressly granted by the terms of the license, no part of the Wiley Materials may be copied, modified, adapted (except for minor reformatting required by the new Publication), translated, reproduced, transferred or distributed, in any form or by any means, and no derivative works may be made based on the Wiley Materials without the prior permission of the respective copyright owner.**For STM Signatory Publishers clearing permission under the terms of the STM Permissions Guidelines only, the terms of the license are extended to include subsequent editions and for editions in other languages, provided such editions are for the work as a whole in situ and does not involve the separate exploitation of the permitted figures or extracts,** You may not alter, remove or suppress in any manner any copyright, trademark or other notices displayed by the Wiley Materials. You may not license, rent, sell, loan, lease, pledge, offer as security, transfer or assign the Wiley Materials on a stand-alone basis, or any of the rights granted to you hereunder to any other person.

- The Wiley Materials and all of the intellectual property rights therein shall at all times remain the exclusive property of John Wiley & Sons Inc, the Wiley Companies, or their respective licensors, and your interest therein is only that of having possession of and the right to reproduce the Wiley Materials pursuant to Section 2 herein during the continuance of this Agreement. You agree that you own no right, title or interest in or to the Wiley Materials or any of the intellectual property rights therein. You shall have no rights hereunder other than the license as provided for above in Section 2. No right, license or interest to any trademark, trade name, service mark or other branding ("Marks") of WILEY or its licensors is granted hereunder, and you agree that you shall not assert any such right, license or interest with respect thereto

- NEITHER WILEY NOR ITS LICENSORS MAKES ANY WARRANTY OR REPRESENTATION OF ANY KIND TO YOU OR ANY THIRD PARTY, EXPRESS, IMPLIED OR STATUTORY, WITH RESPECT TO THE MATERIALS OR THE ACCURACY OF ANY INFORMATION CONTAINED IN THE MATERIALS, INCLUDING, WITHOUT LIMITATION, ANY IMPLIED WARRANTY OF MERCHANTABILITY, ACCURACY, SATISFACTORY QUALITY, FITNESS FOR A PARTICULAR PURPOSE, USABILITY, INTEGRATION OR NON-INFRINGEMENT AND ALL SUCH WARRANTIES ARE HEREBY EXCLUDED BY WILEY AND ITS LICENSORS AND WAIVED BY YOU.

- WILEY shall have the right to terminate this Agreement immediately upon breach of this Agreement by you.

- You shall indemnify, defend and hold harmless WILEY, its Licensors and their respective directors, officers, agents and employees, from and against any actual or threatened claims, demands, causes of action or proceedings arising from any breach of this Agreement by you.

- IN NO EVENT SHALL WILEY OR ITS LICENSORS BE LIABLE TO YOU OR ANY OTHER PARTY OR ANY OTHER PERSON OR ENTITY FOR ANY SPECIAL, CONSEQUENTIAL, INCIDENTAL, INDIRECT, EXEMPLARY OR PUNITIVE DAMAGES, HOWEVER CAUSED, ARISING OUT OF OR IN CONNECTION WITH THE DOWNLOADING, PROVISIONING, VIEWING OR USE OF THE MATERIALS REGARDLESS OF THE FORM OF ACTION, WHETHER FOR BREACH OF CONTRACT, BREACH OF WARRANTY, TORT, NEGLIGENCE, INFRINGEMENT OR OTHERWISE (INCLUDING, WITHOUT LIMITATION, DAMAGES BASED ON LOSS OF PROFITS, DATA, FILES, USE, BUSINESS OPPORTUNITY OR CLAIMS OF THIRD PARTIES), AND WHETHER OR NOT THE PARTY HAS BEEN ADVISED OF THE POSSIBILITY OF SUCH DAMAGES. THIS LIMITATION SHALL APPLY NOTWITHSTANDING ANY FAILURE OF ESSENTIAL PURPOSE OF ANY LIMITED REMEDY PROVIDED HEREIN.

- Should any provision of this Agreement be held by a court of competent jurisdiction to be illegal, invalid, or unenforceable, that provision shall be deemed amended to achieve as nearly as possible the same economic effect as the original provision, and the legality, validity and enforceability of the remaining provisions of this Agreement shall not be affected or impaired thereby.

- The failure of either party to enforce any term or condition of this Agreement shall not constitute a waiver of either party's right to enforce each and every term and condition of this Agreement. No breach under this agreement shall be deemed waived or excused by either party unless such waiver or consent is in writing signed by the party granting such waiver or consent. The

waiver by or consent of a party to a breach of any provision of this Agreement shall not operate or be construed as a waiver of or consent to any other or subsequent breach by such other party.

- This Agreement may not be assigned (including by operation of law or otherwise) by you without WILEY's prior written consent.
- Any fee required for this permission shall be non-refundable after thirty (30) days from receipt by the CCC.
- These terms and conditions together with CCC's Billing and Payment terms and conditions (which are incorporated herein) form the entire agreement between you and WILEY concerning this licensing transaction and (in the absence of fraud) supersedes all prior agreements and representations of the parties, oral or written. This Agreement may not be amended except in writing signed by both parties. This Agreement shall be binding upon and inure to the benefit of the parties' successors, legal representatives, and authorized assigns.
- In the event of any conflict between your obligations established by these terms and conditions and those established by CCC's Billing and Payment terms and conditions, these terms and conditions shall prevail.
- WILEY expressly reserves all rights not specifically granted in the combination of (i) the license details provided by you and accepted in the course of this licensing transaction, (ii) these terms and conditions and (iii) CCC's Billing and Payment terms and conditions.
- This Agreement will be void if the Type of Use, Format, Circulation, or Requestor Type was misrepresented during the licensing process.
- This Agreement shall be governed by and construed in accordance with the laws of the State of New York, USA, without regards to such state's conflict of law rules. Any legal action, suit or proceeding arising out of or relating to these Terms and Conditions or the breach thereof shall be instituted in a court of competent jurisdiction in New York County in the State of New York in the United States of America and each party hereby consents and submits to the personal jurisdiction of such court, waives any objection to venue in such court and consents to service of process by registered or certified mail, return receipt requested, at the last known address of such party.

WILEY OPEN ACCESS TERMS AND CONDITIONS

Wiley Publishes Open Access Articles in fully Open Access Journals and in Subscription journals offering Online Open. Although most of the fully Open Access journals publish open access articles under the terms of the Creative Commons Attribution (CC BY) License only, the subscription journals and a few of the Open Access Journals offer a choice of Creative Commons Licenses. The license type is clearly identified on the article.

The Creative Commons Attribution License

The Creative Commons Attribution License (CC-BY) allows users to copy, distribute and transmit an article, adapt the article and make commercial use of the article. The CC-BY license permits commercial and non-

Creative Commons Attribution Non-Commercial License

The Creative Commons Attribution Non-Commercial (CC-BY-NC)License permits use, distribution and reproduction in any medium, provided the original work is properly cited and is not used for commercial purposes.(see below)

Creative Commons Attribution-Non-Commercial-NoDerivs License

The Creative Commons Attribution Non-Commercial-NoDerivs License (CC-BY-NC-ND) permits use, distribution and reproduction in any medium, provided the original work is properly cited, is not used for commercial purposes and no modifications or adaptations are made. (see below)

Use by commercial "for-profit" organizations

Use of Wiley Open Access articles for commercial, promotional, or marketing purposes requires further explicit permission from Wiley and will be subject to a fee.

Further details can be found on Wiley Online Library http://olabout.wiley.com/WileyCDA/Section/id-410895.html

Other Terms and Conditions:

v1.10 Last updated September 2015

Questions? customercare@copyright.com or +1-855-239-3415 (toll free in the US) or +1-978-646-2777.